SNAKE-LIKE ROBOT
(ELECTRONICS PART)

YEOH CHERN YI

A project report submitted in partial fulfilment of the requirements for the award of the degree of Bachelor (Hons.) of Mechanical Engineering

Faculty of Engineering and Science
Universiti Tunku Abdul Rahman

April 2011

DECLARATION

I hereby declare that this project report is based on my original work except for citations and quotations which have been duly acknowledged. I also declare that it has not been previously and concurrently submitted for any other degree or award at UTAR or other institutions.

Signature : ____________________________

Name : Yeoh Chern Yi

ID No. : 07UEB06218

Date : 26th April 2011

APPROVAL FOR SUBMISSION

I certify that this project report entitled **"SNAKE-LIKE ROBOT DESIGN"** was prepared by **YEOH CHERN YI** has met the required standard for submission in partial fulfilment of the requirements for the award of Bachelor of Engineering (Hons.) Mechatronics at Universiti Tunku Abdul Rahman.

Approved by,

Signature : ____________________________

Supervisor : Dr. Wang Xin

Date : ____________________________

Specially dedicated to

my beloved grandmother, mother and father, and families

SNAKE-LIKE ROBOT DESIGN

ABSTRACT

Snake robot is a well known hyper-redundant robot which mimics the biological snake locomotion. The snake-like robot has various uses in various industries. The hyper-redundant movements allow the robot to move into tight spaces and makes irregular movement patterns.

This project focuses on the design of snake-like robot. Mechanical wise, the robot must have multiple body segments and joints which allow each body segment to move unrestricted relative to the other body segments. The robot will be able to flex, reach, and slither through narrow workspaces with its infinite number of joints configurations. Electronic wise, the robot also must have a good power management which allows the robot to wander freely for long period of time without any cables and travel to farther locations. Another important criteria that mobile robot must have is good control actuations. Good control actuations enable the robot to move efficiently and safely through difficult various obstacles. Programming wise, the robot must have the locomotion of the real biological snake. The robot also must possess the ability to overcome obstacles of certain height limit, or find another alternative routes if it cannot climb over the obstacles.

The main focus of this report would be on the electronics part. This report discusses and proposes suitable solutions to the robot’s power management and control actuations. The power management in this report refers to the power usage and losses occur in the robot. It covers the voltage regulator, voltage ripple filter, and current-limiting circuits. The control actuations in this report refer to the installation of the motors on the robot. It covers the motor controllers which allow multiple motor controls.

At the end of this project, the implementation of efficient and effective power management and control actuations would give the mobile snake-like robot better advantages of realizing its operations. It would also increase the interests of mobile robot exploration into remote operations.

TABLE OF CONTENTS

DECLARATION	**ii**
APPROVAL FOR SUBMISSION	**iii**
ABSTRACT	**vi**
TABLE OF CONTENTS	**viii**
LIST OF TABLES	**xi**
LIST OF FIGURES	**xii**
LIST OF SYMBOLS / ABBREVIATIONS	**xvii**
LIST OF APPENDICES	**xviii**

CHAPTER

1	**INTRODUCTION**			**1**
	1.1	Background		1
	1.2	Applications of snake-like robot		2
	1.3	Aims and Objectives		5
2	**LITERATURE REVIEW**			**7**
	2.1	Power Management: Voltage Regulator		7
	2.2	Different Topologies of Switching Regulator		8
	2.3	Issues Concerning Usage of Switching Regulator		10
	2.4	Solution to the Power Management of the Snake-Like Robot		11
		2.4.1	Buck Converter	11
		2.4.2	Synchronous Buck Converter	14
		2.4.3	Multi-Phase Buck Converter	16
	2.5	Solution to EMI Problem in DC-DC Converter Using Fourth Generation Converter		18
	2.6	Switched-component Converter		19

2.7 Converters with Isolation Features 21
2.8 Actuators of Snake Robot 22
2.9 Summary of Literature Review 23

3 METHODOLOGY 26
3.1 Project Overview 26
3.2 Identify the Potential Circuit for Power Management 28
3.3 Calculations 29
3.3.1 Planning of the Converter Circuit 30
3.3.2 Calculations of Buck Converter 31
3.3.2.1 Operating Mode of Converter 31
3.3.2.2 Output Capacitor 32
3.3.2.3 Input Capacitor 35
3.3.2.4 Diode 36
3.3.2.5 MOSFET 37
3.3.2.6 Buck Converter Efficiency and Power Loss 39
3.3.2.7 Summary of Calculations 41
3.3.2.8 Duty Cycle of Buck Converter 42
3.3.2.9 MOSFET Gate Signal 42
3.3.2.10 MOSFET Gate Signal Amplifier 44
3.3.2.11 Voltage Feedback to the Converter 47
3.4 Circuit Construction and Simulation 49
3.4.1 Transient Load Simulation on the Buck Converter 50
3.4.2 Transient Input Simulation on the Buck Converter 53
3.4.3 Startup Simulation on the Buck Converter 55
3.4.4 Steady State Simulation on the Buck Converter 58
3.5 Buck Converter in a Single Chip 61
3.5.1 Simulation of Transient Input for LM2678 62
3.5.2 Simulation of Transient Load for LM2678 64
3.5.3 Simulation of Steady State for LM2678 66
3.5.4 Simulation of Startup for LM2678 68
3.6 Wiring of Components 70

4	**RESULTS AND DISCUSSION**		**72**
	4.1	Results Overview	72
	4.2	Circuit Construction	73
	4.3	Experimental Results	78
	4.4	Discussion	84
		4.4.1 Discussions on the Simulations	85
		4.4.2 Discussions on the Experimental Results	86
5	**CONCLUSION**		**89**
	5.1	Conclusion	89
6	**RECOMMENDATIONS AND FUTURE IMPROVEMENTS**		**91**
	6.1	Recommendations and Future Improvements	91
REFERENCES			**93**
APPENDICES			**97**

LIST OF TABLES

TABLE	TITLE	PAGE
2.1	Classification of various different converters and topologies	9
2.2	A summary of the reviews	23
3.1	Summary of Operating Specification for the Regulator Circuit	29
3.2	Summary of Estimated Specification for the Output Load	30
3.3	Summary of ESR Value for Capacitors	34
3.4	List of Power Loss Associated to the Converter	39
3.5	Resistance Value for the Capacitor and Inductor in the Circuit	40
3.6	Power Loss in Components in the Circuit	40
3.7	Summary of Calculation and Measured Results	41
4.1	Bill of Material for DC-DC Converter Circuit	75
4.2	Bill of Material for PWM Signal	75
4.3	Bill of Material for Signal Amplifier	76
4.4	Bill of Material for Feedback Voltage	76
4.5	Bill of Material for LM2678T-ADJ Circuit	76
4.6	Experimental Results for No-Load	78
4.7	Experimental Results for Resistive Load	78

LIST OF FIGURES

FIGURE	TITLE	PAGE
2.1	An example of adjustable linear voltage regulator	8
2.2(a)	Buck Converter Circuit Diagram	11
2.2(b)	Typical Waveforms For Buck Converter	12
2.2(c)	First-Order Switching Cell	13
2.2(d)	Operating Region of Buck Converter	14
2.3	Typical Waveforms for Buck Converter	15
2.4	Multi-Phase Buck Converter	16
2.5	Multi-Phase Synchronous Buck Converter	16
2.6	Switching Rule	17
2.7	ZVS Topologies: a) ZVS-QR Switching Cell; b) ZVS-QR Buck Converter	19
2.8	A Highly Efficient Inductorless Voltage Regulator	20

2.9	Waveform of Regulator Input and Output Voltages and Schmitt-Trigger State	20
3.1	The flow graph for the snake-like robot design project overview	27
3.2	Basic Connection Diagram for Timer 555	43
3.3	Push-Pull Amplifier	45
3.4	Push-Pull Amplifier as MOSFET Gate Driver	45
3.5	Constructed Push-Pull Amplifier	46
3.6	Optocoupler as Voltage Feedback	48
3.7	An Example of the Optocoupler Connected to the Timer 555 CONTROL Pin	49
3.8	Constructed Buck Converter Circuit	49
3.9	Voltage Responses of V_{in} and V_{out} for Transient Load	51
3.10	Current Responses of I_{in} and I_{out} for Transient Load	51
3.11	Signal MOSFET Gate Responses of V_{gate} and V_{gs}	52

3.12	Voltage Responses of V_{in} and V_{out} for Transient Input	53
3.13	Current Responses of I_{in} and I_{out} for Transient Input	54
3.14	Signal MOSFET Gate Responses of V_{gate} and V_{gs} for Transient Input	55
3.15	Voltage Responses of V_{in} and V_{out} for Startup Stage	56
3.16	Current Responses of I_{in} and I_{out} for Startup Stage	56
3.17	Signal MOSFET Gate Responses of V_{gate} and V_{gs} for Startup Stage	57
3.18	Voltage responses of V_{in} and V_{out} for Steady State	58
3.19	Voltage Responses of V_{in} and V_{out} for Steady State (Zoomed In)	58
3.20	Current Responses of I_{in} and I_{out} for Startup Stage	59
3.21	Signal MOSFET Gate Responses of V_{gate} and V_{gs} for Steady State (Zoomed In)	60
3.22	Signal MOSFET Gate Responses of V_{gate} and V_{gs} for Steady State	60
3.23	The Model Circuit for LM2678	61

3.24	The Simulation Chart of V_{in} and V_{out} at Transient Input	63
3.25	The Simulation Chart of I_{load} and I_{in} at Transient Input	63
3.26	The Simulation Chart of I_{load} and I_{in} at Transient Load	65
3.27	The Simulation Chart of V_{in} and V_{out} of the Circuit at Transient Load	66
3.28	The simulation chart of V_{out} and V_{in} at Steady State	67
3.29	The simulation chart of I_{in} and I_{out} at Steady State	67
3.30	The simulation chart of V_{in} and V_{out} of the circuit at Startup	69
3.31	simulation chart of I_{load} and I_{in} at Startup	69
3.32	A Layout of PCB for a Part of Constructed Buck Converter	71
4.1	The Constructed Buck Converter on Breadboard	74
4.2	The Constructed Circuit of LM2678T-ADJ	77
4.3	The Waveform of Output Voltage for 3.3 Ω	79
4.4	The Waveform of Output Voltage for 5.1 Ω	79
4.5	The Waveform of Output Voltage for 33 Ω	80

4.6	The Waveform of Output Voltage for 51 Ω	80
4.7	The Waveform of Output Voltage for 1.682 Ω	81
4.8	The Waveform of Output Voltage for 33 Ω (LM2678)	81
4.9	The Waveform of Output Voltage for 51 Ω (LM2678)	82
4.10	The Waveform of Output Current for 3.3 Ω	82
4.11	The Waveform of Output Current for 1.682 Ω	83
4.12	The Waveform of Output Current for 1.682 Ω (LM2678)	83
4.13	The Waveform of Gate Voltage for IRF540N MOSFET	84
4.14	The Waveform of Gate-to-Source Voltage for IRF540N MOSFET	84
4.15	Simulation Result Showing the Current Flow from Input to Output	85

LIST OF SYMBOLS / ABBREVIATIONS

t	total time period, s
T	time, s
V, v	voltage, V
I, i	current, A
L	inductor, H
C	capacitor, C
k	conduction cycle
f	switching frequency, Hz
R	resistance, Ω
α	angular position, rad
ε	variation ratio

ZVS	Zero Voltage Switching
ZCS	Zero Current Switching
MOSFET	Metal-Oxide-Semiconductor Field-Effect-Transistor
IGBT	Insulated Gate Bipolar Transistor
LiPo	Lithium-Polymer

LIST OF APPENDICES

APPENDIX	TITLE	PAGE
A	Journal of Non-Inverting Buck-Boost Converter	97
B	LM2678S/T-ADJ Design Documentation	102
C	Pictures of Components	105
D	Construction of Snake Robot	106
E	Layout of the PCBs for the circuits	108
F	Tests for Constructed Buck Converter	110
G	Tests for LM2678T-ADJ	114
H	Calculations for the Buck Converter	117

CHAPTER 1

INTRODUCTION

1.1 Background

Snake robot is also known as serpentine robot. This type of robot is made up of multiple actuated joints. Thus, the robots possess multiple degrees of freedom from the construction of its joints. This gives the snake robot will their ability to flex, reach, and approach a huge volume in its workspace with infinite number of configurations. (Dowling, 1997)

It is known that biological snake is capable of moving and adapt in wide variety of terrains. By implementing such features in machines, a snake-like device could be made to slide, glide, and slither. The device could be used for exploration, hazardous environments, inspection, and medical intervention. (Dowling, 1997)

1.2 Application of Snake-like robot

Potential applications of snake robot can be found in army, industries, robotic surgery, and search and rescue operations. The current and future use of snake robots or snake-like robots whether in industries or any sectors proves to be rewarding. It could change the view of current operation of automation has been done. The robot could reach small and restricted areas with less effort, bend into any angles and shapes without breaking. Also, the robot could move in rhythmic locomotion; however is non-linear direction, as compared to wheeled and legged robots.

In army application, the development of snake-like autonomous systems (called as Robotic Tentacle Manipulator) will likely to take on the task of soldiers in search and rescue missions especially in dangerous mission area. The snake-robot can be made scalable where it can be made large or small as a subsystem to a larger platform. It will be several snakes (or tentacles) arranged in a circular array and linked to a base. They will function as a team using multiple parts of their bodies to manipulate an object, scan a room or handle improvised explosive devices. The number of snakes determines the breadth or scope of its search capabilities. The number of joints (or links) on each snake supports each snake's length or reach into an area, as well as its ability to crawl, climb or shimmy through narrow spaces while transmitting images to the operator operating the system remotely. With the increasing manipulator dexterity, soldiers can offload more tasks to the robotic platform. (Gibson, 2010)

In industries application, snake-like robots are preferable in manufacturing and assembly, particularly in aerospace aircraft assembly. A noted application of snake robot is in nuclear industry, where it is used in decommissioning operation and repair and maintenance nuclear reactor operation. As found in a study case involving a single pipe repair of a boiling water reactor, on a nuclear plant, owned by Ringhals AB, located on the west coast of Sweden in year 2003. The leak was discovered in a strategic section of pipe located in narrowly packed section with more pipe systems surrounding it. There was no direct line of sight of the leak and the access to the leak was limited to only two routes; descending from above or crawling from below. When Ringhals AB asked companies to tender to conduct the repair, two of three bidding companies proposed to cut down the other pipe systems serving as obstacles so as to create a man-sized access path in order to conduct a manual repair. It was recognized that cutting down the obstacles would have proved impossible to replace them to the required tolerances and would result in reactor shutdown. The only remaining bidding company, Uddcomb Engineering, won the contract when they proposed the novel solution of using OC Robotics' snake-arm robots to remotely access the pipe and repair the leaking section, without much tempering with the structure of the pipe systems. The single pipe repair was successfully completed in three days. In case of repair and maintenance in restricted areas, snake-arm robot nonetheless offers a flexible and versatile solution to numerous maintenance and repair issues across the industry. (Anscombe, Buckingham, Graham, Parry, Lichon, Ferguson, 2006)

As for application in aircraft assembly, a study case involved the co-operation between OC Robotics and Airbus in development of snake-arm robot technology that is suitable for conducting automated inspection and assembly tasks within wing boxes. The aerospace industry needed to adapt to automation as a means to increase throughput and standardize processes. However, the demand and emphasis on high and relative accuracy over large structure hindered the use of standard industrial robot. Furthermore, tasks within low access areas such as the found throughout the aircraft structures, such as the rib bays and wing boxes, have remained inaccessible to a conventional robot-arm. Operating within the rib bay requires the robot to be able to place tools precisely and also to have a structure that does not have prominent 'elbow' joints. Thus, a suitable structure is one with low profile elbows or continuous curvature that is able to snake into confined structures. Such example is the snake-arm robot. (Anscombe et al., 2006)

As for the medical application, snake-like robot can be designed to increase the efficiency of surgical tasks without compromising much of the patient's safety. One such case study pointed out that such technology could allow surgeons to perform surgical tasks safely and effectively. As highlighted by Science Daily on John Hopkins University research, the snake-like robot could enable surgeons to operate in the narrow throat region, to make incisions and tie sutures with greater dexterity and precision. Such technology intervention came because of the situation where a surgeon's fingers are too large to work in a small confined space within the human body. Currently, a surgeon performing throat surgery must insert and manually manipulate long inflexible tools and camera into the narrow throat passageways. The alternative solution to this problem would be the snake-like robot capable of moving with six degrees of freedom. If directed, the robot can easily bend into an S-curve. The robot would be controlled remotely by the surgeon, from a robotic workstation. The surgeon will have three-dimensional view of the operating site, and so would be able to manoeuvre the movement of the robot. The robot's movement can be made nimble by using sophisticated software that makes up to 100 adjustments per second. The robot must be made of non-magnetic metals so that it can be safely used around or near magnetic imaging equipments. Such technology would push the partnership of automation with surgeons to help the surgeons do their works more effectively. (Science Daily, 2006)

The application of snake-like robot in search and rescue operation will increase the effort of the operation as the robot could be adaptable and flexible moving through difficult workspaces of rescue mission. With higher number of degrees of freedom, the robot could move through an environment of unstructured and technically challenged area shaped by natural forces with less effort. Equipped with multiple sensing modules, the robot will have higher chances of success in finding and reaching its objectives (victims) than using only detection devices mainly based on human voices and sniffing dogs, and manpower to find a passageway to the victims. The robot with multiple bodies could be equipped with first-aid and monitoring devices to provide supports to isolated victims which could take long time for rescuers to reach the victims. (Thomas K. K., 2008)

1.3 Aims and Objectives

The aim of this project is to design a snake-like robot which could be used in search operations. The robot will be operated remotely, thus, it must have a proper power supply which could allow the robot to run for a long time and able to supply adequate power to the running devices on the robot. It also must have efficient motor drives that could manage multiple motors on the robot to ensure the robot could fully utilize the motors to run through various obstacles.

Thus the objectives of the project would cover the design of the power supply and the motor drives. As such, the completion of the objective would ensure the robot could fully operate in the tasks below:

i. The mechanical part

– The robot has 2 axis motions, which it can move in x-y plane. The robot must be robust to overcome obstacles like stones and branches, and uneven surfaces.

ii. The electronics part

– The robot also must have sufficient power for self sustain in remote environment. The power management on the robot must achieve high efficiency for low-voltage high-current applications such as driving multiple motors.

iii. The programming part

– The robot must perform snake-like locomotion, and with the vision assist of the camera, the snake-like robot will able to decide the possible solutions to overcome the obstacle that it face, and also able to respond to the feedback of the controlling sensors like angle sensor.

Highlighting the point (ii) above, the further requirements for the objectives of the electronics part are:

a. Investigate types of regulators that could achieve high efficiency for low-voltage high-current conditions. Switching regulators are recommended.
b. Further improvement to the switching regulator by reducing ripple on the output voltage.
c. Provide multiple motor controls using motor controllers.
d. Provide controllers for sensors that would be attached to the robot.
e. Construct wiring for the motors and circuits on the robot.

CHAPTER 2

LITERATURE REVIEW

2.1 Power Management: Voltage Regulator

There are few types of voltage regulators; zener diode voltage regulator, linear voltage regulator, and switching voltage regulator. Switching voltage regulator is considered more efficient when dealing with power distribution from power supply to motors and microcontroller.

Supporting this fact is from the learned cases of one major problem with linear regulator is the power dissipated as heat (power loss) by the regulator as shown by the relationship $P_{loss} = I_{out}(V_{in} – V_{out})$. However, it also pointed out that by using linear voltage regulator with a smaller dropout voltage. Linear regulator is only a good choice if the power requirement of the regulated circuit is only a small fraction of the total power the robot consumes. Typically, if an output voltage is required to be higher than the input voltage or an output voltage is to have polarity opposite to that of the input voltage, dc-dc converter must be used. (Joseph L. Jones, Anita M. Flynn, Bruce A. Seiger, 1999)

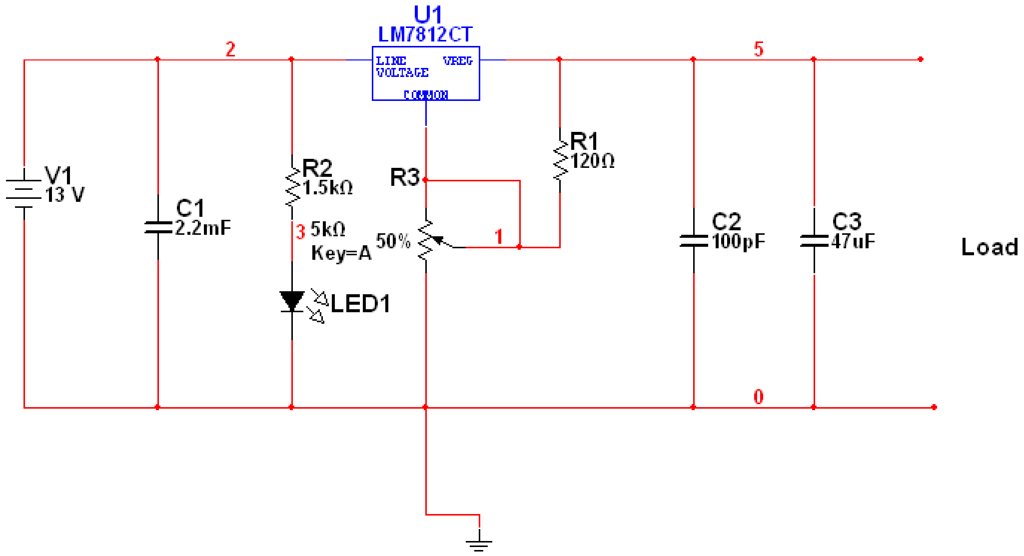

Figure 2.1: An Example of Adjustable Linear Voltage Regulator.

As noted, switching regulator has the control transistor to operate as a switch, either in cutoff or saturation region. Regulation is achieved by adjusting the *on* time of the control transistor. Thus, the control transistor does not dissipate as much power as seen in linear type regulators. Therefore, switching regulators have a much higher efficiency and can provide greater load currents at low voltage than linear type regulators. (Y. M. Lai, 2001)

2.2 Different Topologies of Switching Regulator

Switching regulators can be implemented by many topologies. Each of the topology has their advantages and disadvantages. However, most of them can work for various applications. Suitable topology is determined from the factors such as the cost, performances, and application that make one topology more desirable than the others. (Y. M. Lai, 2001)

Tabulating the available topologies of switching regulator, in dc-to-dc mode

Table 2.1: Classification of Various Different Converters and Topologies

Classification	Topologies	Performance
First Generation (Classical Converters)	Buck converter Boost converter Buck-boost converter	Single-quadrant mode; low power range (up to 100W)
Second Generation (Multi-quadrant Converters)		Available in two- or four-quadrant mode; medium output power range (hundred watts or higher)
Third Generation (Switched-component Converters)	Switched Inductors Converter Switched Capacitors Converter	Available in two- or four-quadrant mode; high output power range (thousands of watts)
Fourth Generation (Soft-switching Converters)	Zero-current-switching (ZCS) Converters Zero-voltage-switching (ZVS) Converters	Single-, two-, or four-quadrant mode; high output power range (thousands of watts)
Fifth Generation (Synchronous Rectifier Converters)		Possess technical features of very low voltage, strong current, high power transfer efficiency (up to 95 %) and high power density (22 – 25 W/in^3)

(Source: Fang Lin Luo, Hong Ye, and Muhammad H. Rashid, 2001)

2.3 Issues Concerning Usage of Switching Regulator

One disadvantage of a switching regulator is identified which must be taken into account when designing switching regulators. A drawback of using switch-mode power supply (SMPS) resides in the fact that due to its switching nature, electromagnetic noise will be radiated. This electromagnetic interference (EMI) emission may affect the SMPS itself and also interfere with other electronics equipment. This issue becomes especially relevant at high switching frequencies, which is necessary to achieve low ripple in output voltage. (Quevedo, Goodwin, 2004)

One way, using hardware added to the circuit, to mitigate the EMI problem resides in improving shielding, input filters and isolation of signal coupling paths. However, it may be more convenient to reduce EMI emission directly at the source. This can be accomplished by careful design of the switching methods of the SMPS. (Quevedo et al., 2004)

A major issue of using dc-dc converters is that they have inherited parasitic elements effects (due to losses from capacitors, inductors, switches and diodes) which would limit their output voltage and transfer efficiency. A sharp performance drop of the output voltage can be seen when the conduction duty is towards unity. (Fang Lin Luo et al., 2001)

2.4 Solution to the Power Management of the Snake-Like Robot

Linear regulators are used effectively at low power levels. This is because they provide a very high-quality output voltage. At higher power levels, switching regulators are used. (Darius Czarkowski, 2001)

Various electronic applications demand different topologies of switching regulators. In this snake-like robot project, the power supply used will be dc batteries and the output voltage is to be dc output. Therefore, dc-dc converters would be recommended. Some of the switching regulators selected for the project are

- Buck converter
- Synchronous Buck converter
- Multi-phase Buck converter

2.4.1 Buck Converter

The circuit diagram is shown in Figure 2.2(a). Typical waveforms in the converter are shown in Figure 2.2(b) under the assumption that the inductor current is always positive.

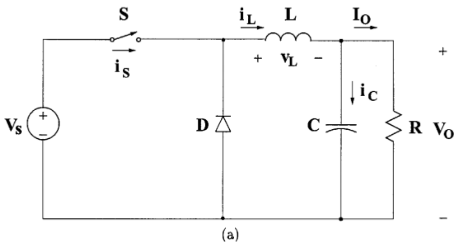

Figure 2.2(a): Buck Converter Circuit Diagram. (Source: Darius Czarkowski, 2001)

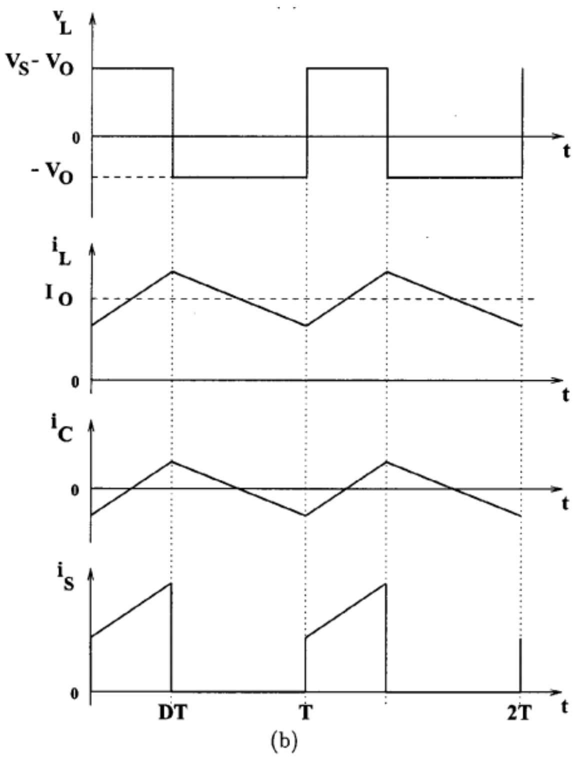

Figure 2.2(b): Typical Waveforms for Buck Converter. (Source: Darius Czarkowski, 2001)

If the converter operates in Continuous Conduction Mode (CCM), the relationship between the input voltage (V_s) and output voltage (V_o) is given by

$$d = \frac{V_o}{V_s} = \frac{T_{ON}}{T_S} \tag{2.1}$$

where *d* is the duty cycle

T_{ON} is the conducting time of the switch

T_S is the switching period

(Shulin Liu, et al., 2005)

The boundary condition of Continuous Conduction Mode (CCM) and Discontinuous Conduction Mode (DCM) is

$$L_K = \frac{R_L(V_S - V_O)}{2fV_S} \tag{2.2}$$

where R_L is the load resistance

f is the switching frequency

When L > L_K, the converter is in CCM. Otherwise, it is in DCM.

(Shulin Liu, et al., 2005)

The first-order switching cell is shown in Figure 2.2(c). The active switch S is controlled by an external control input. Practically, the switch would be implemented by Metal-Oxide-Semiconductor Field-Effect Transistor (MOSFET), Insulated Gate Bipolar Transistor (IGBT), or other switching device. The state of second switch, the diode D, is indirectly controlled by the state of active switch and other circuit conditions. The switching cell also contains a storage element which is inductor L.

(Grigore V., 2001)

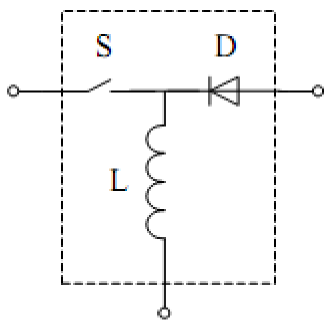

Figure 2.2(c): First-Order Switching Cell. (Source: Grigore V.)

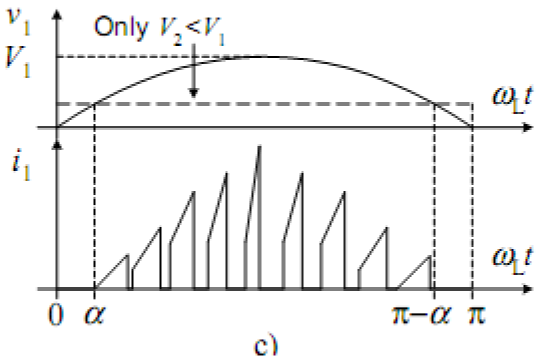

Figure 2.2(d): Operating Region of Buck Converter. (Source: Grigore V.)

Buck converter is a second-order circuit, considering the output filtering capacitor. The output filtering capacitor can be assimilated to a voltage source. Thus, all the switching ports are connected to voltage sources, a fact which explains why the storage element of the switching cell is an inductor and not capacitor. Buck converter operates with a discontinuous input current, as shown in Figure 2.2(d). Since the input current of the buck converter is discontinuous, the input current has a significant high-frequency component that has to be filtered out. The converter can only operate when the instantaneous input voltage is higher than the output voltage.

(Grigore V., 2001)

2.4.2 Synchronous Buck Converter

To reduce the conduction losses in the diode of the buck converter, a low on-resistance switch can be added in parallel as shown in Figure 2.3. The input switch and the switch parallel to the diode must be turned on and off alternately. A synchronous converter may exhibit higher efficiency than a conventional one at output currents as large as tens of amperes. The efficiency is increased at the expense of a more complicated driving circuitry for the switches. A special care must be exercised to avoid having both switches *on* at the same time as this would short the input voltage source.

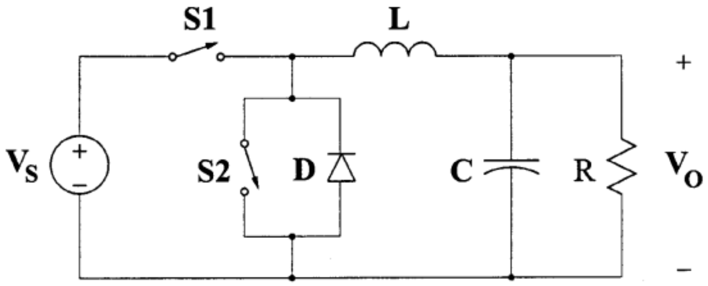

Figure 2.3: Typical Waveforms for Buck Converter. (Source: Darius Czarkowski, 2001)

The inductor value for desired operating ripple current (converter operates in CCM) can be determined using the following relationship:

$$L_{min} \geq \frac{(1-d)R}{2f} \tag{2.3}$$

where R is the load resistance

f is the switching frequency

d is the duty cycle

The output capacitor must have a large value to decrease the output voltage ripple, and is calculated as:

$$\frac{\Delta V_O}{V_O} = \frac{(1-d)}{8LCf^2} \tag{2.4}$$

where L is the inductor value

C is the capacitor value

2.4.3 Multi-Phase Buck Converter

Parallel connection of switching converters allows the converters to share the output current. The sharing is suitable for lower voltages with higher current applications. The sharing is also effective to improve reliability and fault tolerance. The ripple reduction of the output current is also possible. It is convenient to reduce the size and losses of the filtering stages (inductor and capacitor) and to decrease switching and conduction losses and EMI levels. (Toshimichi Saito et al, 2005)

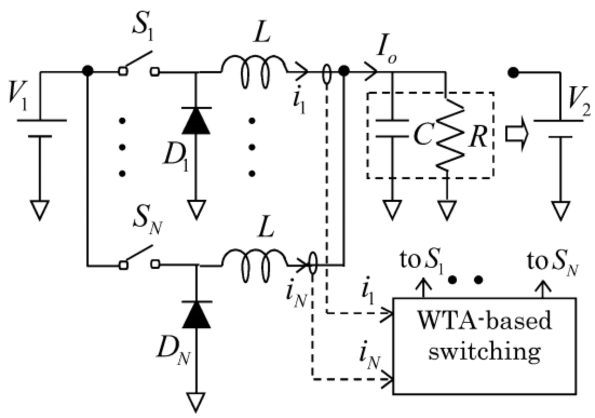

Figure 2.4: Multi-Phase Buck Converter. (Source: Toshimichi Saito et al, 2003)

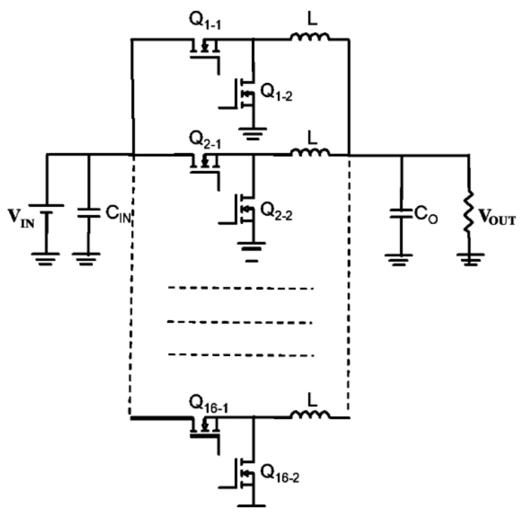

Figure 2.5: Multi-Phase Synchronous Buck Converter. (Source: Oscar García et al, 2006)

From Figure 2.4, N identical buck converters are interleaved between voltage source V_1 and the load is represented by an RC circuit. The jth converter, $j \in \{1... N\}$, includes a current-controlled switch S_j and an ideal diode D_j. The switch S_j is controlled based on a periodically sampled current i_j (nT), where T is a sampling period and n is a positive integer. To define the switching rule, let jth converter be one of the following states:

State 1: S_j conducting, D_j blocking and $0 < i_j < J$

State 2: S_j blocking, D_j conducting and $0 < i_j < J$

State 3: S_j and D_j both blocking and $i_j = 0$,

where J is the threshold for i_j. (Toshimichi Saito et al, 2003)

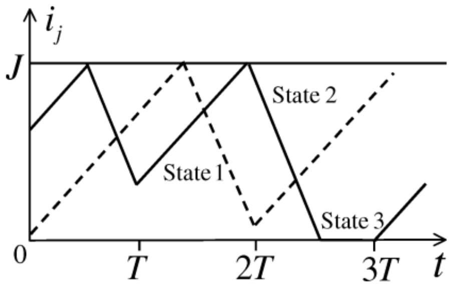

Figure 2.6: Switching Rule. (Source: Toshimichi Saito et al, 2003)

The switching rule can be summarized as the following:

- State 1 → State 2, if $i_j = J$
- State 2 → State 1, if t = nT and i_j = min
- State 2 → State 3, $i_j = 0$
- State 3 → State 1, if t = nT.

If the system operates to include State 3, the system operates in DCM. Without State 3 in the system, the system operates in CCM. The output current is given by $I_o = \sum_{j=1}^{N} i_j$. (Toshimichi Saito et al, 2003)

2.5 Solution to First Generation DC-DC Converter Using Fourth Generation Converter

The input current of buck converter is discontinuous. This would put a high current stress on the MOSFET switch. As such, in fourth-order switching converters it is possible to associate continuous input current with a step-down conversion ratio. This is not possible for buck converter. (Grigore V., 2001)

Fourth-order converter applies a technique called soft-switching technique. It is a zero-ripple technique which a coupled inductor technique can be applied in a DC circuit in order to reduce the current ripple in an inductor. It can be used, for example, to reduce the ripple of the input/output current of a switching converter. Switching losses in a switching converter can be reduced with soft switching techniques. (Grigore V., 2001)

The capacitive turn-on losses can be theoretically eliminated and the overlap of non-negligible active switch voltage and current be avoided at turn-on, by using Zero Voltage Switching – ZVS technique. This technique consists of forcing to zero the active switch voltage, prior to its turn-on, by creating a resonance between an inductor and capacitor. The inductor also limits the rate of variation of diode current, so losses due to reverse recovery are reduced as well. The ZVS technique has been applied in a variety of topologies, such as resonant and quasi-resonant (QR). (Grigore V., 2001)

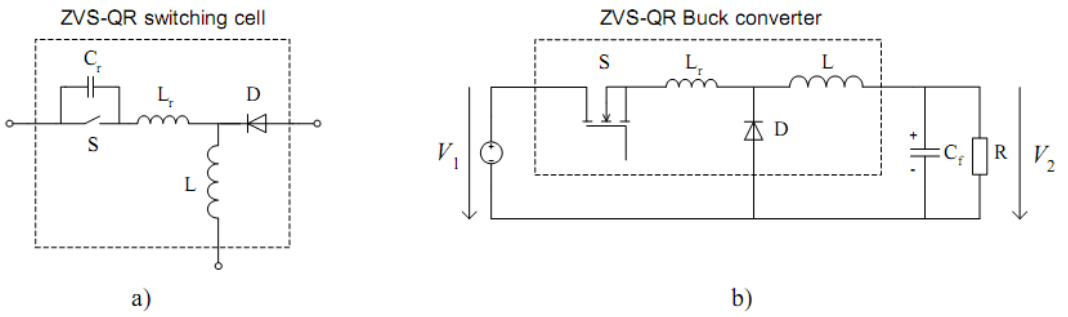

Figure 2.7: ZVS Topologies: a) ZVS-QR Switching Cell; b) ZVS-QR Buck Converter (Source: Grigore V., 2001)

2.6 Switched-component Converter

A voltage regulator which uses solid-state switching techniques and requires no inductor for filtering represents a significant improvement over standard series and switching regulators because of its increased efficiency and peak-current capabilities. The circuit achieves good regulation and high power output with relatively small physical size as compared to a series regulator designed for the same purpose. The advantages of this inductorless regulator are 1) with ideal devices the regulator is dissipationless; 2) no series inductor is required; 3) energy storage in the capacitor is done at the lowest voltage level, which is the load voltage, and therefore the capacitor physical size is reduced; and 4) transient changes in output voltage are restored completely during the following half cycle of the line frequency. (Keeney, McWhorter, 1969)

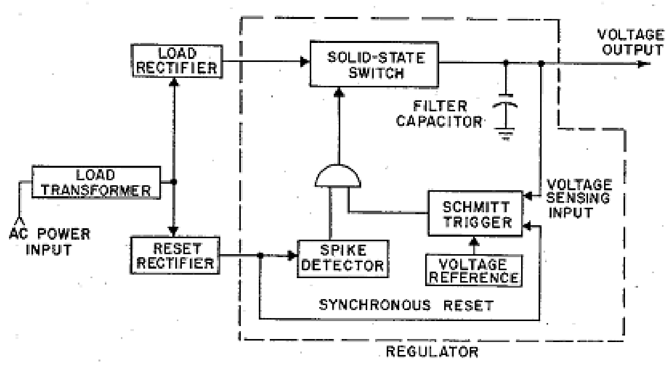

Figure 2.8: A Highly Efficient Inductorless Voltage Regulator. (Source: Keeney, McWhorter, 1969)

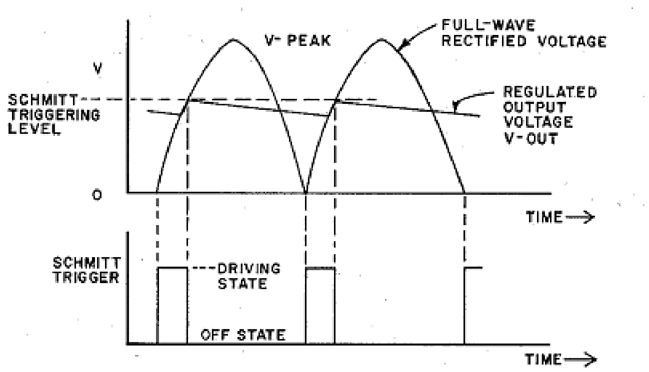

Figure 2.9: Waveform of Regulator Input and Output Voltages and Schmitt-Trigger State. (Source: Keeney, McWhorter, 1969)

2.7 Converters with Isolation Features

Another method opinioned that active-clamped flyback converter is one of the most well known converters which can reduce the switching losses and EMI noises. However, this converter is more than conventional flyback converter with respect to power consumption in the no-load condition. This is due to high conduction current of resonant converter. To reduce conduction loss at no-load condition, the converter turns off the auxiliary switch and operates only flyback mode. This is the active-clamped ZVS flyback converter. The active-clamped circuit provides the benefits of recycling the transformer leakage energy while minimizing turn-off voltage stress and a means of zero-voltage-switching for the power switch. (Jong Hyun Kim, Myung Hyo Ryu, Byung Duk Min, Eui Ho Sang, 2006)

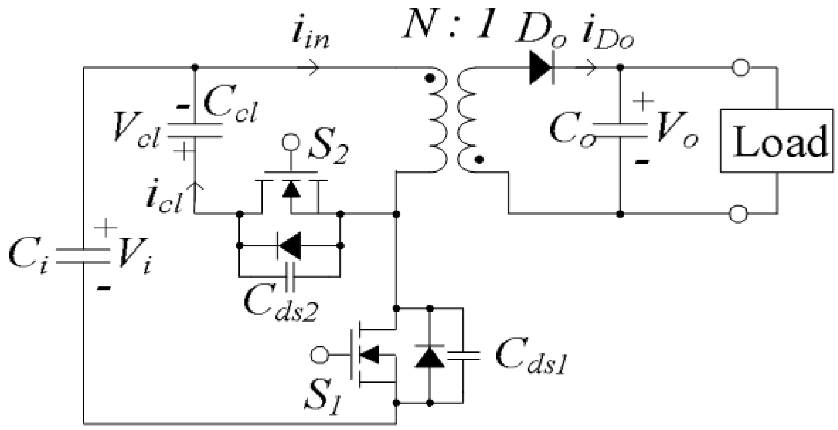

Figure 2.10: Basic Circuit of the Active-Clamped Flyback Converter. (Source: Kim et al., 2006)

2.8 Actuators of Snake Robot

To mimic the locomotion of a biological snake, there should be a mechanism involved. One possible mechanism would be the DC servo motor. The choice of motor and drives as well as mechanical transducer is a very important step in servo system design. Otherwise, non-optimal selection leads to poor system performance and increased installation and maintenance costs. (Ohm, 2006)

The first step in selecting a proper system would be to conduct the load analysis. Servo motor should have just enough speed, peak torque, and root mean square (rms) torque capabilities, to meet the load requirement as well as the cost objective. Equally important is selecting the type and size of the drive and power supply to meet the system requirements. (Ohm, 2006)

When selecting a drive, it should be able to supply enough current and voltage to the motor to meet both peak and rms torque requirements. When selecting a servo drive, its interface must be checked. Some examples of interface are analogue velocity command, and pulse type such as A-B pulse format and pulse & direction format. Some drives will feature position control function integrated into the amplifier. Consideration for type and resolution of the feedback device, input/output (I/O) and other features must be made. (Ohm, 2006)

The power supply in a servo system fundamentally delivers DC power to a servo amplifier. The power output rating of a power supply must exceed or equal to the combined average power of all servo drives operating simultaneously. The average power of an individual servo drive is based on the power calculation of rms torque and speed. (Ohm, 2006)

2.9 Summary of the Literature Review

A short summary of the literature review can be tabulated as below:

Table 2.2: A summary of the reviews

Author	Title	Year	Interest	Remarks
Y. M. Lai	Power Electronics Handbook (Chapter 20)	2001	Switching regulator.	The advantages of switching regulators for multiple loads.
			Different topologies of switching regulator.	The reasoning behind different topologies and their applications.
Joseph L. Jones, Anita M. Flynn, Bruce A. Seiger	Mobile Robots: Inspiration to Implementation (2nd edition)	1999	Linear regulator.	The disadvantages of linear regulators in power distribution and power losses.
Quevedo, Goodwin	Control of EMI from Switched-Mode Power Supplies via Multi-Step Optimization	2004	The disadvantages of SMPS and existence of EMI in the circuit.	EMI problem in the SMPS will reduce the performance of the dc-dc converter. Possible solutions are listed.
Fang Lin Luo, Hong Ye, and Muhammad H. Rashid	Power Electronics Handbook (Chapter 17)	2001	Switching regulators in the form of dc-to-dc converter.	Types of dc-dc converter.
			The inheritance problem, the parasitic element effects on dc-dc converters.	The power losses and performance drop due to the fast switching of the dc-dc converter.

Toshimichi Saito, Shin'taro Tasaki, and Hiroyuki Torikai	Winner Takes All (WTA)-Based Interleaved Buck Converter for Low Voltage and High Current Applications	2005	Interleaved buck converter	The circuit layout of multi-phase buck converter
Dariusz Czarkowski	Power Electronics Handbook (Chapter 13)	2001	Types of Buck Converter	Different types of buck converter; Buck converter and synchronous buck converter
Shulin Liu, Jian Liu	Design of Intrinsically Safe Buck DC/DC Converters	2005	Expressions and calculations of buck converters to determine the operating range	Calculations of buck converters, particularly operating range of the converter and value of inductor required
O. García, P. Zumel, A. de Castro, and J.A. Cobos	High Current DC-DC Converter with SMT Components	2006	Interleaved synchronous buck converter	Multi-phase synchronous buck converter using surface mounted technology
Keeney, McWhorter	A Highly Efficient Inductorless Voltage Regulator	1969	An improvement to the flyback converter.	Reduce power losses at no-load condition where the motor starts to operate and when the power flow only to the motor but not the load.

Jong Hyun Kim, Myung Hyo Ryu, Byung Duk Min, Eui Ho Sang	A Method to Reduce Power Consumption of Active-Clamped Flyback Converter at No-Load Condition	2006	Selection of servo motors and drives based on mechanical and power parameters.	Step-by-step and calculation for the load to select proper servo motors and for power to select suitable drives.
Dal Y. Ohm	Selection of Servo Motors and Drives	2006	The servo motor load response	Understanding the power requirement of servo motors
Grigore V.	Topological Issues in Single-Phase Power Factor Correction	2001	Understanding the operating region of buck converter and its improvements using ZVS-QS	Buck converter, ZVS-QS Buck converter

CHAPTER 3

METHODOLOGY

3.1 Project Overview

The snake-like robot will be separated into three different parts of tasks, namely the mechanical part, the electronics and electrical part, and the programming part. Thus, a team is formed of three person with each person takes a part.

This report takes the tasks of electronics and electrical part (highlighted box in Figure 3.1). The electronics part mainly deals with the electronics components and circuits construction that will be used in the robot, and the electrical wiring of the electronics circuits. Critical electronics components that must be included in the robot are the voltage switching regulator, MOSFET gate driver circuit, and voltage feedback circuit. As for the electrical part, the critical consideration is for the wiring of the circuits, motors and sensors on the robot.

Below are the flow graph of the tasks and the project overview of the snake-like robot design project:

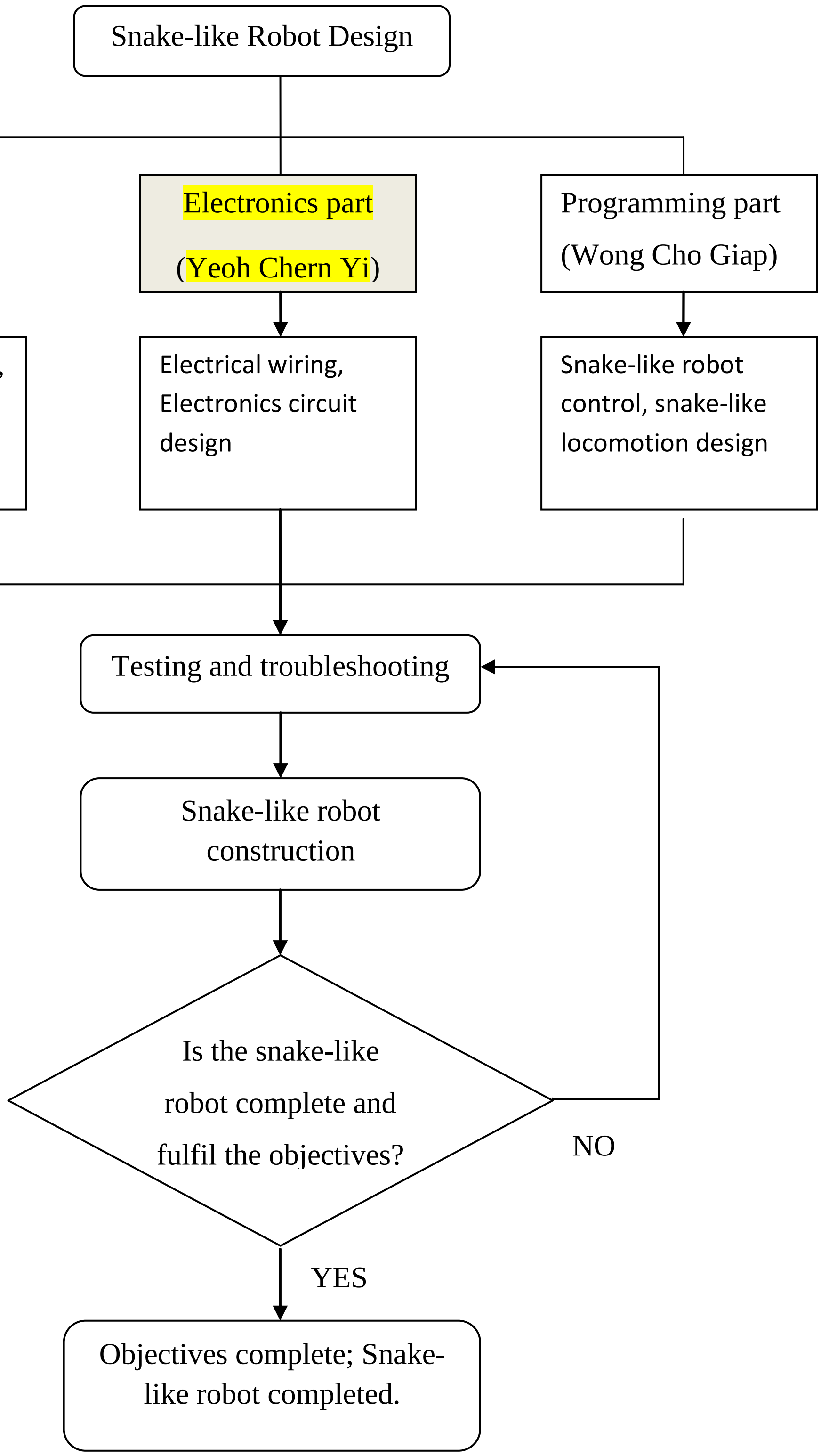

Figure 3.1: The Flow Graph for the Snake-Like Robot Design Project.

3.2 Identify the Potential Circuit for Power Management

In mobile robot, managing the power supply is an important task. It would determine the operating time of the mobile robot when not connected to any main sources. One consideration of the feasibility of a mobile robot is also regarding how long the robot can survive in the outside environment with no contact.

Thus, it is much important to ensure that the power supply onboard of the robot is managed efficiently to minimize power losses and to maintain optimum performances of the robot. One such solution for power management is to use switching voltage regulator

The suitable switching voltage regulator to be used would be the dc-dc converter, mainly because the mobile robot would be running on dc power source such as battery. For the consideration of the converter choices, some points must be emphasized so that a good power management for the mobile robot can be built. The important points to be included are:

- The converter must be able to supply adequate voltage and current to maintain the operations of motors on the robot.
- A steady output voltage must be achieved. Switching converters use fast-switching components to turn on and turn off the circuits in order to minimize the power losses at the load. This will create a ripple effect on the output voltage, thus, a steady state is hard to be reached.

For this project, the interest will be on the buck regulator as it is low-cost and the circuit is simple to be built and used.

3.3 Calculations

To measure the performance of the circuits, some calculations will be done to verify the performance stated of the circuits.

One method to judge the performance of a circuit is to perform theory calculations. By starting from theory calculations, time and effort can be saved when a prototype of the circuit is built to test in real world. Theory calculations involve identifying the input and output power, the suitable components to use in the circuit to provide optimum performance, and the suitable operating region of the circuit to provide the necessary results.

Few conditions will be set as the desired output results. Given the input supply will be from LiPo (lithium polymer) battery (refer Appendix C) with the rating of maximum voltage of 12.6 V and to be used down to 10 V. The switching frequency will be set to be used from 30 kHz to 70 kHz. The desired output voltage will be 6.7 V to satisfy the voltage requirement of the motors at the output. As for the output, maximum ratings will be taken to ensure that the circuit is capable to operate until the highest possible load on the output. The summary of the operating specification is listed as below:

Table 3.1: Summary of Operating Specification for the Converter Circuit.

Specification	Value	Unit
Input Voltage (LiPo battery 11.1 V 2200 mAh)	Min : 10 Max: 12.6	Voltage (V)
Output Voltage	6.7	Voltage (V)
Maximum Output Current	4	Ampere (A)
MOSFET Switching Frequency	Min: 30 Max: 70	Kilo Hertz (kHz)

The output load will be the servo motor planned to be used for the robot's mechanical actuations. The servo motor has the specification stated as below:

Table 3.2: Summary of Estimated Specification for the Output Load.

Specification	Value	Unit
Model	C55R	Cytron
Voltage (maximum)	7	V
Torque (maximum)	0.01325	N-m
No-load current	100	mA
Stall current	1	A
No load speed	6.16	rad/sec

3.3.1 Planning of the Converter Circuit

To start planning for the circuit, either P- or N-channel MOSFET should be used. After some consideration, Negative-channel MOSFET (N-MOSFET) is preferred due to its advantages of being easier to control than Positive-channel MOSFET when the input supply voltage is not high. The MOSFET driver for N-MOSFET is also simpler to be built. A buck converter is first planned by using IRF540N and the MOSFET driver would be built using pulse-generating circuit.

As for the load, it is planned that the converter will handle a maximum load of four dc servo motors connecting in parallel at a single time. With each of the motor has rated stall current of 1 A, the maximum rating of the current load will be 4 A. Any load operating under the maximum rating specified is considered safe and acceptable.

3.3.2 Calculations of Buck Converter

Suitable components have to be identified first so that to give first insight of what and how the components would behave when they are put into a circuit. The components that would be mentioned are MOSFET, required converter operation and passive components (capacitors and inductors), power loss and efficiency associated to the converter, converter duty cycle, MOSFET gate driver, and feedback signal to the gate driver.

3.3.2.1 Operating Mode of Converter

To ensure that the circuit does not enter current limit at maximum load there must be a value of current in the output inductor. This is determined by the boundary between Continuous Conduction Mode (CCM) and Discontinuous Conduction Mode (DCM) is calculated through the given equation,

$$L = \frac{(V_{in_{max}} - V_{out})}{V_{in_{max}}} \times \frac{V_{out}}{V_{in_{max}}} \times \frac{1}{f_{min}} \times \frac{1}{LIR \times I_{out_{max}}} \tag{3.1}$$

Where LIR is the inductor-current ratio, $\frac{\Delta I}{I_{out}}$

ΔI is the output ripple current

$I_{out_{max}}$ is the maximum output current

$V_{in_{max}}$ is the maximum supply voltage

V_{out} is the output voltage

f is the switching frequency

(Schelle D. et. al, 2006)

Peak current through the inductor determines the inductor's required saturation-current rating. Saturating the inductor core decreases the converter efficiency, while increasing the temperatures of the inductor, the MOSFET and the diode. The peak inductor current is obtained through the equation,

$$I_{peak} = I_{\ out_{max}} + \frac{\Delta I}{2} \tag{3.2}$$

A good practice for choosing the ripple current is to be not greater than 30% of the output current. It provides a balance between efficiency and load transient response. Increasing the LIR quickens the load-transient response and vice versa.

(Schelle D. et. al, 2006)

Assume a LIR of 0.3, which gives output ripple current, ΔI, of 1.2 A. Using the set of operating conditions for the converter, from the Equation 3.1, the minimum required inductance value, L, is approximately 7 µH. From the Equation 3.2, the peak current, I_{peak}, is calculated to be 4.6 A. It is presumable to account for circuit tolerances and differences between the actual and calculated values, and thus, it is acceptable to increase the calculated rating by 20%. Therefore, the maximum rating of I_{peak} is 5.52 A.

3.3.2.2 Output capacitor

The output capacitor filters the inductor ripple current and is required to minimize the overshoot and ripple present at the output voltage of a buck converter. Large overshoots and large voltage ripple is caused by low output capacitance. Another problem caused by insufficient output capacitance is high equivalent-series resistance (ESR) in the output capacitor. The capacitor must be large enough to prevent overshoot of voltage due to the stored inductor energy. The output capacitance is obtained through the equation,

$$C_o = \frac{L(I_{peak})^2}{(V_{shoot}+V_{out})^2-{V_{out}}^2} \tag{3.3}$$

where V_{shoot} is the output voltage overshoot

V_{out} is the output voltage

(Schelle D. et. al, 2006)

The total output voltage ripple is obtained through the equation,

$$\Delta V = \frac{1}{2C_o} \times \frac{V_{in_{max}}-V_{out}}{L} \times (\frac{V_o}{V_{in_{max}}} \times \frac{1}{f})^2 + (\Delta I \times ESR_{C_o}) \tag{3.4}$$

A general recommendation is to keep the output voltage ripple to be less than 2% of the output voltage. To solve for the ESR, the equation is given by,

$$ESR_{C_o} = \frac{1}{\Delta I} \times \left(\Delta V - \frac{1}{2C_o} \times \frac{V_{in_{max}}-V_{out}}{L}(\frac{V_{out}}{V_{in_{max}}} \times \frac{1}{f_{min}})^2\right) \tag{3.5}$$

(Schelle D. et. al, 2006)

To choose an output capacitor, the maximum output voltage overshoot must be set. Thus, assume the maximum output voltage overshoot, V_{shoot}, to be 10 mV, the output capacitance, C_o, is calculated to be 1590.55 µF by using Equation 3.3. Considering fault tolerance of 20%, the minimum output capacitor is 1908.66 µF. The closest available value for the minimum output capacitor is 2200 µF. As to calculate the ESR value of the output capacitor, assume the output voltage ripple, ΔV, to be 0.134V, the calculated ESR_{C_o} will be 61.51 mΩ, using Equation 3.5. Therefore, it is recommended to find a capacitor that has lower ESR value than 61.51 mΩ. One method to achieve equivalent or lower than calculated ESR value is to connect multiple low-ESR capacitors in parallel.

The Equivalent Series Resistance (ESR) of capacitor varies from different manufacturers and they are unique to each other and do not available in the datasheet. Thus, capacitors are measured to obtain its ESR values using inductance, capacitance and resistance (LCR) meter. The table below listed the average ESR values for each of the capacitance value used:

Table 3.3: Summary of ESR Value for Capacitors

Capacitor		ESR value (average)
Polyester	103K	66.5 Ω
Ceramic	102K	14.50 kΩ
	103K	50 Ω
	104K	58 Ω
Electrolytic	1 μF	9 Ω
	22 μF	2.07
	47 μF	0.6 Ω
	220 μF	0.45
	330 μF	0.04
	1000 μF	0.032
	2200 μF	0.035 Ω

It is in the opinion that the output capacitor is connected in parallel with a combination of ceramic, polyester, and electrolytic capacitors. Electrolytic capacitors have higher storage capacity value than the other two but it does little in filtering ripples of current and voltage at high frequency. Therefore, smaller values of capacitors are used to filter out the ripples at higher frequency due to their higher discharge rate than electrolytic capacitor. Thus, a combination of 2200 μF electrolytic capacitor, with 0.1 μF and 0.001 μF ceramic capacitors, and 0.01 μF polyester capacitor serves as the decoupling capacitors, will be used.

By referring to their ESR values for each type of capacitor respectively, the total value of ESR of the output capacitor will be the summation of the resistance value in parallel configuration. Thus, the ESR_{C_o} will be approximately 34.96 mΩ. The value is within the calculated value for output capacitor ESR.

3.3.2.3 Input Capacitor

Input capacitor, C_{in}, must be calculated and used such that it can handle the amount of ripple current given. The input capacitor value is obtained through the equation,

$$I_{in-rms} = I_{out_{max}} \frac{\sqrt{V_{out}(V_{in}-V_{out})}}{V_{in}}, \text{ where } I_{in-rms} \text{ is the ripple current.} \qquad (3.6)$$

(Schelle D. et. al, 2006)

From the calculation of the above Equation 3.6, the ripple current rating, I_{in-rms}, is approximated to be 2 A. Assuming fault tolerance of 20%, the minimum ripple current rating 2.4 A. Ripple current rating of the capacitor should be greater than half of the output current.

For best performance, low-ESR capacitors should be placed in parallel with higher capacitance capacitors to provide best input filtering for the converter. It is recommended that 10 µF to 22 µF per ampere of output current is set for capacitance value for the input capacitor. A thought of design for the input capacitor is to connect electrolytic capacitor, ceramic capacitor, and polyester capacitor in parallel to achieve high storage capacity, good filtering, and low-ESR value. Considering the input ripple current is high, a combination of two 2200 µF electrolytic capacitor, 0.1 µF and 0.001 µF ceramic capacitor, and 0.01 µF polyester capacitor will be used.

Based on the Table 3.3 for the capacitor ESR values, the total combination of the input capacitors gives an approximate total ESR value of 17.5 mΩ. The total input capacitance is 4400 μF with a total of 0.111 μF as the input decoupling capacitor.

3.3.2.4 Diode

For the diode selection, power dissipation is the limiting factor. The average power dissipation by diode is calculated through the equation,

$$P_{diode} = (1 - \frac{V_{out}}{V_{in_{max}}}) \times I_{out_{max}} \times V_D \tag{3.7}$$

where V_D is the voltage drop of the diode (0.7V for silicon diode and 0.3 for Schottky diode)

For a reliable operation over the input voltage range, the reverse-repetitive maximum voltage must be greater than the input voltage ($V_{RRM} \geq V_{in_{max}}$). The diode must also have forward-current specification that is greater than the maximum output current ($I_{Fav} \geq I_{out_{max}}$).

(Schelle D. et. al, 2006)

Assuming if silicon diode is used, as such, the calculated power dissipation by diode using Equation 3.7 is 1.31 W. Considering a fault tolerance of 20%, the power loss at the diode is 1.573 W.

3.3.2.5 MOSFET

To select a suitable MOSFET, the maximum junction temperature, T_{Jmax}, and maximum ambient temperature, T_{Amax}, of the MOSFET must be known. T_{Jmax} must not exceed 115 ^oC to 120 ^oC and T_{Amax} should not exceed 60 ^oC. The temperature rise of the MOSFET is the difference between T_{Jmax} and T_{Amax}, given by the equation,

$$T_{Jrise} = T_{Jmax} - T_{Amax} \tag{3.8}$$

Thus, the maximum rise of MOSFET temperature is set to 55 ^oC.

(Schelle D. et. al, 2006)

The maximum power dissipated in the MOSFET can be obtained from the allowable maximum rise in MOSFET temperature. The equation is given as,

$$P_{D_{TOT}} = \frac{T_{Jrise}}{\Theta_{JA}} \tag{3.9}$$

where Θ_{JA} is junction-to-ambient thermal resistance.

(Schelle D. et. al, 2006)

A best estimation for Θ_{JA} is 62 $^oC/W$. By using this value, the maximum power dissipation of the MOSFET, $P_{D_{TOT}}$, in Equation 3.9, is calculated to be 0.89 W. Power dissipation in the MOSFET is caused by the on-resistance and switching losses. On-resistance loss is calculated by the equation,

$$P_{D_{RDS}} = \frac{V_{out}}{V_{in_{min}}} \times I_{out_{max}}{}^2 \times R_{DS(on)HOT} \tag{3.10}$$

where $R_{DS(on)HOT}$ is the hot on-resistance

$R_{DS(on)25°C}$ is the on-resistance at 25 ^oC.

(Schelle D. et. al, 2006)

The value of temperature at junction of particular on-resistance, T_{Jhot}, may be estimated. A recommendation is to have temperature coefficient of 0.5%/^{o}C as to provide a good indicator for maximum on-resistance at any given temperature. Thus, the hot on-resistance is obtained through the equation,

$$R_{DS(on)HOT} = [1 + 0.005(T_{Jhot} - 25°C)]R_{DS(on)25°C} \quad (3.11)$$

(Schelle D. et. al, 2006)

Assuming the on-resistance loss is approximately 60% of the total MOSFET losses, the maximum allowable on-resistance at 25 ^{o}C is obtained through the equation,

$$R_{DS(on)25°C} = \frac{V_{in_{min}}}{V_{out}} \times \frac{1}{{I_{out_{max}}}^2 \times [1 + 0.005(T_{Jhot} - 25°C)]} P_{D_{TOT}} \times 60\% \quad (3.12)$$

(Schelle D. et. al, 2006)

Assuming the MOSFET is to be operated until 110 ^{o}C, by using the set values given, the maximum allowable $R_{DS(on)25°C}$ is 34.84 mΩ (from Equation 3.12) and the $R_{DS(on)HOT}$ is 49.65 mΩ (from Equation 3.11). Hence, going with Equation 3.10, the on-resistance loss, $P_{D_{RDS}}$ is calculated to be 0.532 W.

To calculate the switching losses, the equation is given by,

$$P_{Dsw} = \frac{C_{RSS} \times {V_{in_{max}}}^2 \times f \times I_{out_{max}}}{I_{Gate}} \quad (3.13)$$

where C_{RSS} is the reverse-transfer capacitance of the MOSFET.

I_{Gate} is the peak gate-drive source/sink current at the gate

f is the mean value of MOSFET switching frequency, $f = \frac{f_{max} + f_{min}}{2}$

(Schelle D. et. al, 2006)

The reverse-transfer capacitance is obtained through the MOSFET datasheet. Choosing an available MOSFET datasheet for IRF540N [24], the information for the C_{RSS} given by the datasheet is 120 pF. Assuming the required gate current to be 1 A, the calculated switching losses, P_{Dsw}, with Equation 3.13, is 3.81 mW.

By recalculating and summing the on-resistance losses and switching losses, the net dissipated power is

$$P_{Dsw} + P_{D_{RDS}}. \tag{3.14}$$

With all the values obtained, the net dissipated power is calculated to be 0.536 W.

3.3.2.6 Buck Converter Efficiency and Power Loss

Minimizing the power loss of the converter could extend the battery life and reduce heat dissipation. The total power loss throughout the converter is listed as below:

Table 3.4: List of Power Loss Associated to the Converter.

Type of power losses	Estimation or Calculation
Input capacitor ESR loss	$P_{C_{in_{rms}}} = {I_{in-rms}}^2 \times ESR_{C_{in}}$
Inductor (dc resistance) DCR loss	$P_{DCR_{rms}} = (I_{out} + \Delta I \times \sqrt{2})^2 \times DCR_L$
Output capacitor ESR loss	$P_{C_{o_{rms}}} = (\Delta I \times \sqrt{3})^2 \times ESR_{C_o}$
PCB copper loss	Assuming a net copper loss of 0.75 W

The efficiency of the converter can therefore be summed and accounted for the power losses in the converter. The equation is given by,

$$\eta = \frac{V_{out} \times I_{out}}{((V_{out} \times I_{out}) + P_{C_{in_{rms}}} + P_{DCR_{rms}} + P_{C_{o_{rms}}} + P_{Dsw} + P_{D_{RDS}} + P_{diode} + 0.75)} \quad (3.15)$$

(Schelle D. et. al, 2006)

Arranging the estimation values from the calculation, the table below listed the values required to build the prototype circuit:

Table 3.5: Resistance Value for the Capacitor and Inductor in the Circuit.

Types of resistance	Value
Input capacitor ESR, $ESR_{C_{in}}$	17.5 mΩ
Output capacitor ESR, ESR_{C_o}	34.9 mΩ
Inductor DCR, DCR_L (measured)	0.004 Ω

Thus, the power loss for each of the component in the circuit is listed as below:

Table 3.6: Power Loss in Components in the Circuit.

Type of power losses	Estimation or Calculation
Input capacitor ESR loss	$P_{C_{in_{rms}}} = 2.4^2 \times 17.5 \times 10^{-3} = 0.1008\, W$
Inductor (dc resistance) DCR loss	$P_{DCR_{rms}} = (4 + 1.2 \times \sqrt{2})^2 \times 0.004 = 0.1298\, W$
Output capacitor ESR loss	$P_{C_{o_{rms}}} = (1.2 \times \sqrt{3})^2 \times 34.9 \times 10^{-3} = 0.1508\, W$
Net dissipated power in MOSFET	$P_{Dsw} + P_{D_{RDS}} = 0.536\, W$
Dissipated power by diode	$P_{diode} = 1.57\, W$
PCB copper loss (estimated)	0.75 W

Hence, from the Equation 3.16 and the values obtained from Table 3.5, the calculated efficiency is 0.89 or 89%.

3.3.2.7 Summary of Calculations

The summary of the calculation results (refer Appendix H) on the circuit's component selection requirements are listed in the table below:

Table 3.7: Summary of Calculation and Measured Results.

	Parameter	Value
Input	Input Ripple Current, I_{in-rms}	2.4 A
Inductor	Inductance, L	7 µH
	Inductor DCR, DCR_L	0.004 Ω
	Inductor Peak Current, I_{peak}	5.52 A
Output	Voltage overshoot, V_{shoot}	10 mV
	Output Voltage Ripple, ΔV	0.134 V
	Output Current Ripple, ΔI	1.2 A
Capacitor	Input Capacitor, C_{in} (2×2200 µF, 0.1 µF, 0.01 µF, 0.001µF)	4400.111 µF
	Total Input capacitor ESR, $ESR_{C_{in}}$	17.5 mΩ
	Output Capacitor, C_o (2200 µF, 0.1 µF, 0.01 µF, 0.001 µF)	2200.111 µF
	Total Output Capacitor ESR, ESR_{C_o}	34.96 mΩ
Diode	Silicon diode voltage drop, V_D	0.7 V
MOSFET	On-Resistance at 25 °C, $R_{DS(on)25°C}$	34.96 mΩ
	Hot On-Resistance, $R_{DS(on)HOT}$	49.81 mΩ
	Reverse-Transfer Capacitance, C_{RSS}	120 pF

3.3.2.8 Duty Cycle of Buck Converter

The duty cycle of the converter determines how long the MOSFET is kept on, allowing more current to flow from input to the output. Duty cycle of the MOSFET conduction could be obtained through the given equation,

$$D = \frac{V_{out}}{V_{in_{min}}} \tag{3.16}$$

Assuming the minimum required duty cycle is determined by the output voltage, 6.7 V, and the minimum average input supply voltage, 10 V, thus, the minimum duty cycle can be set to approximate of 0.67 or 67%.

3.3.2.9 MOSFET Gate Signal

The operation of turning MOSFET on or off is controlled by a pulse width modulation (PWM) signal at the MOSFET gate. Therefore, to drive the MOSFET on/off, a PWM signal must be fed through a driver to the MOSFET gate. For the MOSFET to turn on and off properly, it requires certain amount of current to charge and discharge the MOSFET since MOSFET gate is capacitive.

To provide a PWM signal, timer NE 555 is used. The timer is capable to provide required frequency signal for the converter.

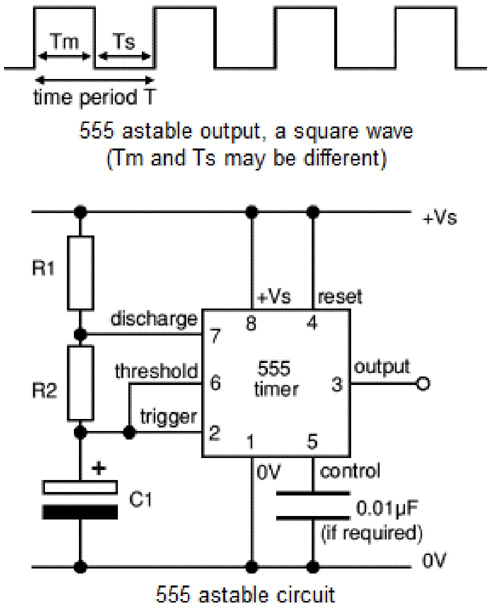

Figure 3.2: Basic Connection Diagram for Timer 555. (Source: Hewes J., 2010)

The mark time, T_m, is the time interval of output high. The space time, T_s, is the time interval of output low. By adjusting the resistor R1 and R2, the duty cycle of the output can be controlled. A general equation to select the resistor R2 is through the equation,

$$R_2 = \frac{0.7}{f \times C1} \tag{3.17}$$

where *f* is the switching frequency

C1 is the value of the capacitor C1

The selection value of R1 and R2 must be in the range of 1 kΩ to 1 MΩ. If the duty cycle is to be 50%, R1 is determined by $R1 = \frac{R2}{10}$.

If the set maximum switching frequency is 70 kHz, from Equation 3.17, then the value of R2 would be 10 kΩ.

The minimum required duty cycle is 71%. Thus, to determine the duty cycle of the switching frequency, if the duty cycle is above 50%, the equation is given by,

$$Duty\ Cycle, D = \frac{T_m}{T_m + T_s} = \frac{R1 + R2}{R1 + 2R2} \tag{3.18}$$

$$T_m = 0.7 \times (R1 + R2) \times C1$$
$$T_s = 0.7 \times R2 \times C1$$

Thus, using Equation 3.18, the calculated value of R1 is 5 kΩ.

3.3.2.10 MOSFET Gate Signal Amplifier

The specified timer NE 555 could sink or source up to only 200 mA. This is not enough to charge or discharge the gate of a high-side MOSFET as the higher load at the source terminal of the MOSFET (load), the higher current is needed at the MOSFET gate. Therefore, the current source must be obtained externally, outside the timer. To switch-on the MOSFET, the required voltage at the gate referenced to the source (voltage gate-to-source, V_{gs}) must be above 4V. To switch-on the MOSFET, the required V_{gs} must be below 2V. The 4V and 2V is the threshold voltage gate-to-source ($V_{gs(th)}$) for the MOSFET to switch-on and switch-off respectively. Therefore, a higher-than-input-supply voltage is required at the MOSFET gate.

One method is to amplify the voltage and current using transistor amplifier. Transistor is a current driven device and could be used to amplify current or voltage. One configuration is to use two transistors, PNP and NPN, to form a Class B amplifier or known as push-pull amplifier.

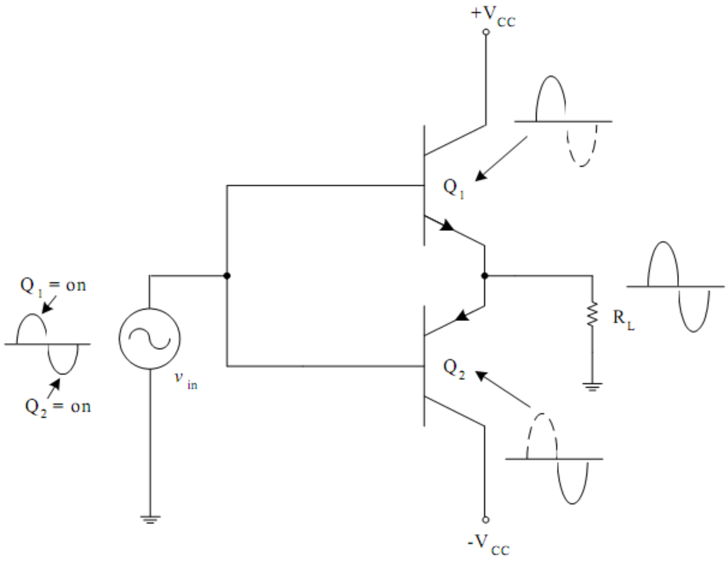

Figure 3.3: Push-Pull Amplifier. (Source: Lecture 9: Power Amplifier – Class B, 2011)

The amplifier depends on each of the transistor to conduct on alternating half-cycles of the input. The idea of using push-pull amplifier comes from a buck converter design (Figure 3.4) which utilizes the same concept to provide gate signal to the MOSFET.

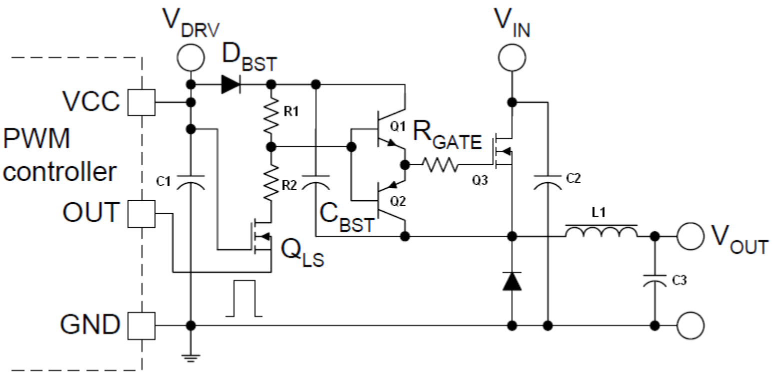

Figure 3.4: Push-Pull Amplifier as MOSFET Gate Driver. (Source: technogamma, personal communication, March 11, 2008)

Thereby, a push-pull amplifier (Figure 3.5) is constructed for the similar purpose of amplifying the gate signal. During the signal input high, Q1 is biased above cut-off and conduction results through the transistor R_L. The result will be an output on the signal input high. During the signal output low, Q1 returned to the cut-off state and Q2 is biased above cut-off. At this time, the result will be an output on the signal input low.

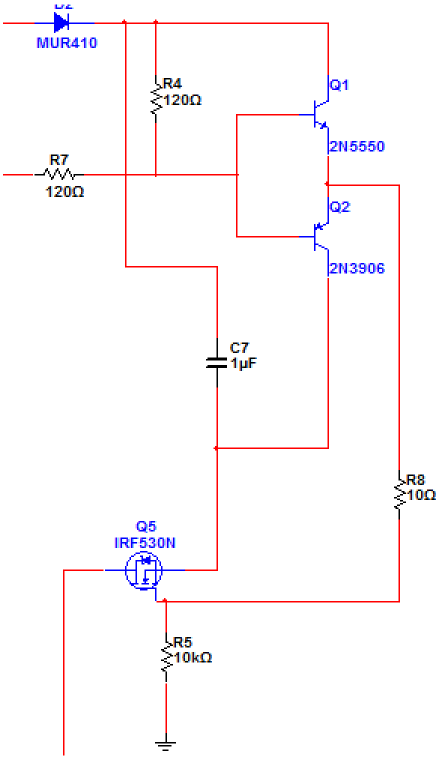

Figure 3.5: Constructed Push-Pull Amplifier.

Similarly, the same amplifier is used to draw enough current to the MOSFET gate. The resistor R4 is used to deliver base current to Q1. Capacitor C7 is the boost capacitor tied to the source of the MOSFET so that it could provide more current to the Q1 collector. The collector of the Q2 is connected to the source terminal of the MOSFET such that the gate signal (output signal from the amplifier) is referenced to the MOSFET source. This is because the turn on and off of the MOSFET depends on the gate-to-source voltage.

3.3.2.11 Voltage Feedback to the Converter

To control the voltage of the output, there must a feedback signal from the output to the input so as to increase or decrease the input supply. In this case of converter, the rate of the MOSFET gate switching on and off must change accordingly to the output. If the output voltage is increasing above the limit, the MOSFET gate must turn off longer than it turns on and vice versa for when the output voltage is decreasing below the limit.

The control of the switching of the MOSFET gate is done by timer 555 inputting a PWM signal. On-board the timer 555, there is a CONTROL pin (pin 5) which is used to adjust the frequency of the PWM signal up to a certain extend. The function of the pin is to the threshold and trigger pin. When using the CONTROL pin, the timer 555 will be under voltage-controlled mode. At default the voltage at the CONTROL pin is 2/3 of the IC input supply, V_{cc}. If there is an external voltage applied to the pin, the control voltage can be varied. If control voltage is increased, the capacitor takes a longer time to charge and discharge. Hence, the frequency decreases and duty cycle increases.

An idea to create a feedback voltage to the CONTROL pin is shown in Figure 3.6 below:

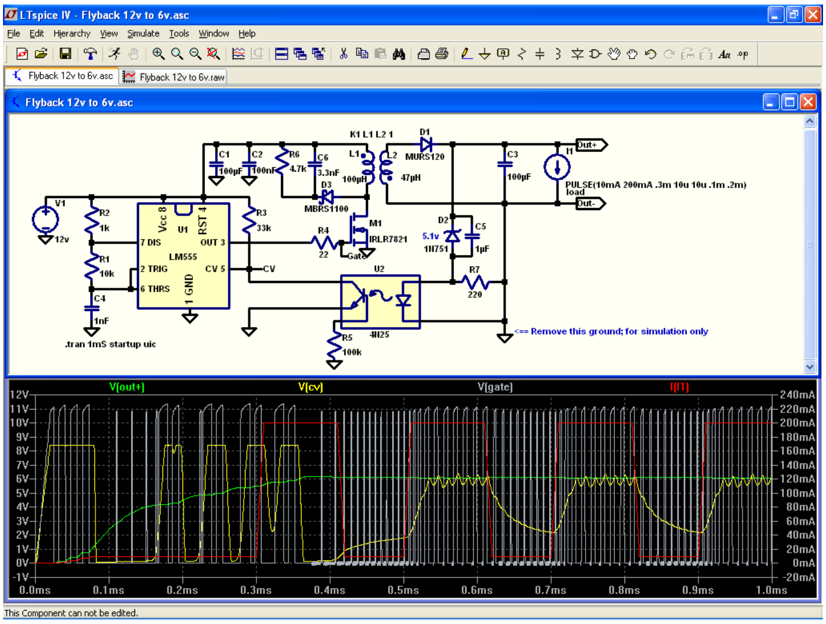

Figure 3.6: Optocoupler as Voltage Feedback. (Source: SgtWookie, personal communication, December 10, 2010)

To create a feedback voltage to the CONTROL pin, an optocoupler is used. The output voltage terminal is connected to the LED pin (pin 1) through a zener diode and capacitor in parallel. The emitter pin is connected to the ground with the collector pin connected to the timer 555 CONTROL pin. At the CONTROL pin, there is an external voltage source connected and a capacitor connected between the THRESHOLD pin (pin 6) and CONTROL pin. When the output voltage is above the zener voltage, the diode is reverse-biased. A small amount of current will flow through the diode and giving a signal at the base of the optocoupler. Once there is a signal at the base pin, current will flow from the collector to the ground at the emitter, thereby, reducing the voltage at the CONTROL pin and reduces duty cycle. When the output voltage is below the zener voltage, the diode is forward-biased and the optocoupler does not conduct, thereby, voltage at the CONTROL pin will increase and duty cycle increases. The wiring of the circuit is shown in Figure 3.7.

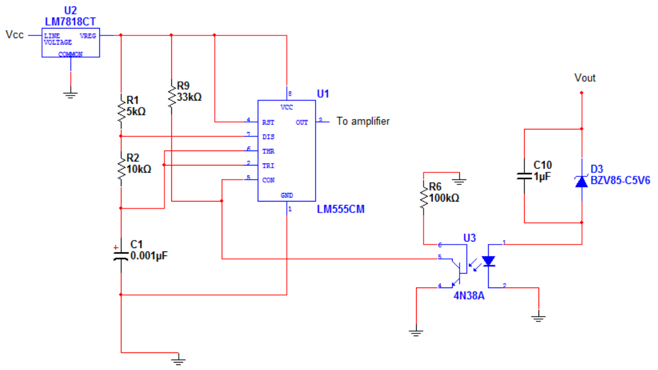

Figure 3.7: An Example of the Optocoupler Connected to the Timer 555 CONTROL Pin.

3.4 Circuit Construction and Simulation

Based on the both calculated and given specification values, a circuit is constructed (Figure 3.8). The circuit will be simulated and later constructed as a prototype for testing.

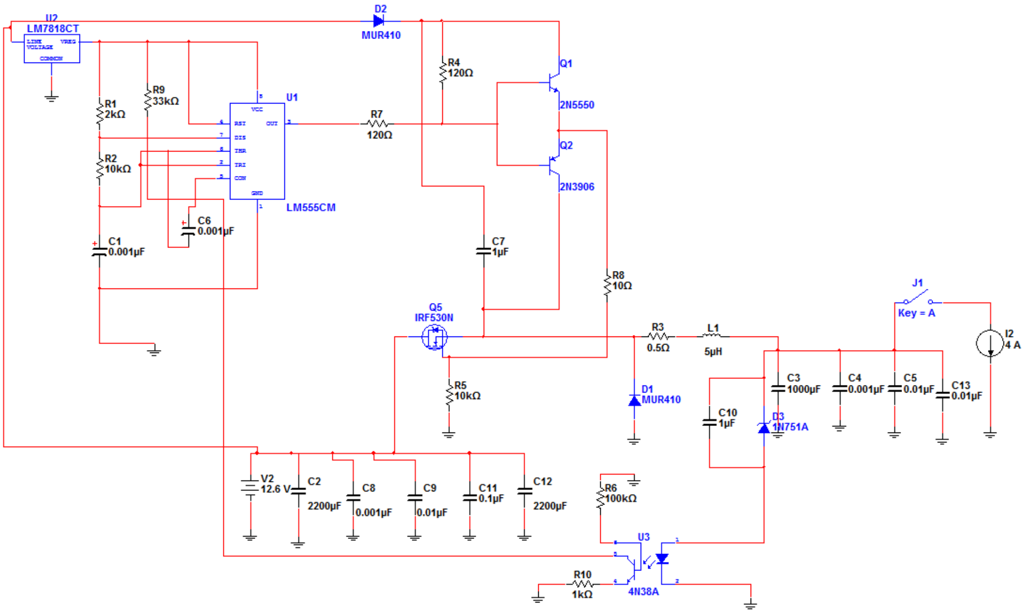

Figure 3.8: Constructed Buck Converter Circuit.

The circuit consist of a buck converter which is driven using PWM signal from the timer 555. A push-pull amplifier is included to amplify the voltage and current through the MOSFET gate. As for the feedback for the circuit, an optocoupler is used to adjust the frequency of the PWM signal so that the MOSFET could switch on and off at closest approximate interval to provide the desired output voltage.

For the simulation, the circuit will be tested on its transient load, transient input, startup and steady state to obtain information on its operating characteristics in different conditions. (Refer Appendix F for test figures)

3.4.1 Transient Load Simulation on the Buck Converter

Transient load test measures the circuit's conditions when it is applied with a fluctuating current at the load. The current will oscillate from 4 A to 0.4 A at a given period cycle. The input voltage is set to its mean value of 11.3 V. This test is to observe the circuit's response to a variation of current at the output given a fixed input supply. The load transient specification is given as below:

Signal Type	Pulse
I1: Initial Current	4 A
I2: Peak Current	0.4 A
T_d: Initial Delay Time	100 µs
T_r: Rise Time	50 µs

T_f: Fall Time	50 µs
Pw: Pulse Width	500 µs

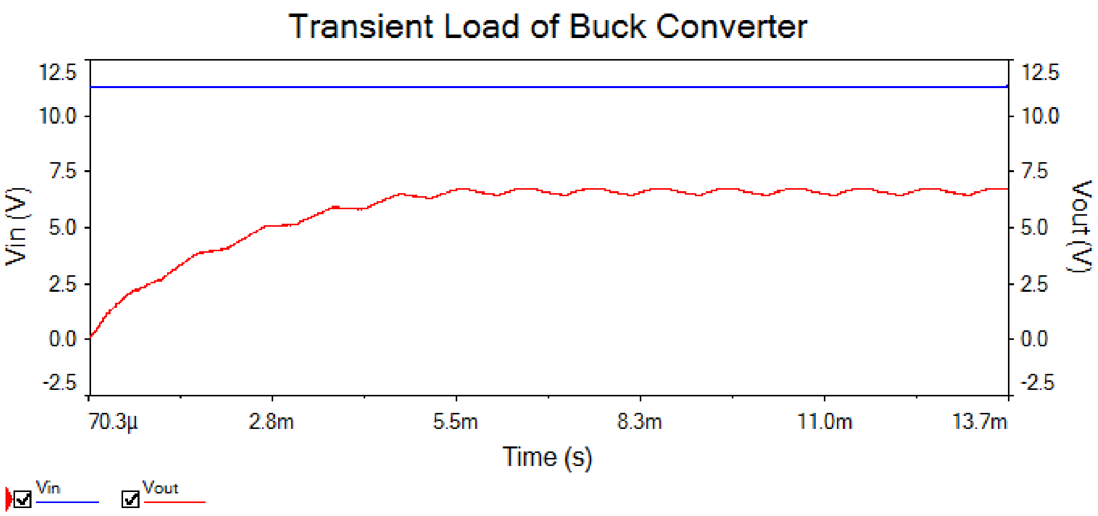

Figure 3.9: Voltage Responses of V_{in} and V_{out} for Transient Load.

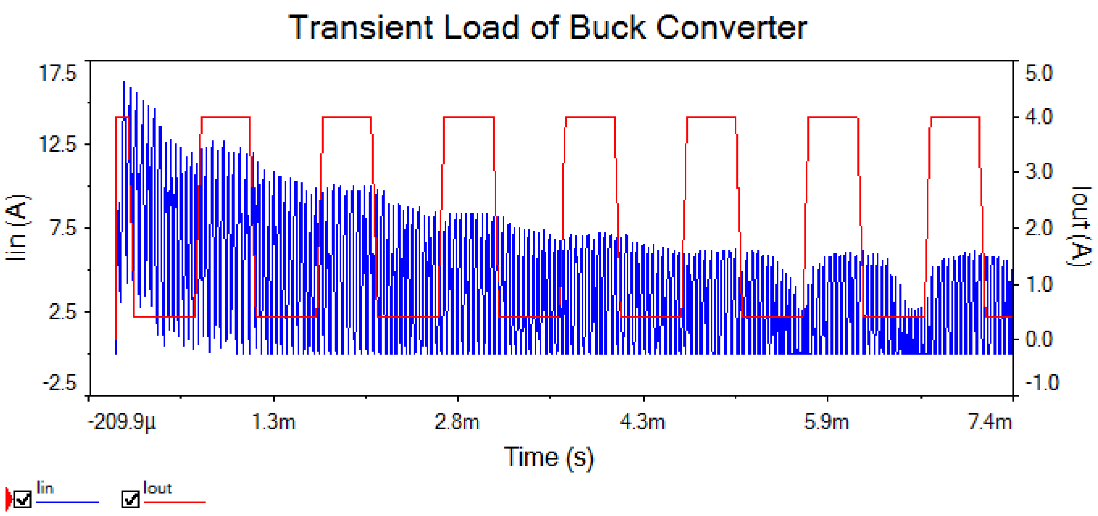

Figure 3.10: Current Responses of I_{in} and I_{out} for Transient Load.

At the output voltage (Figure 3.9), the voltage oscillates between approximate ranges of 6.3 V and 6.7 V with a voltage ripple of 0.4 V. The output current waveform (Figure 3.10) decreases and increases according to the waveform of its output voltage. As the output voltage increases, the output current also increases the peak current to allow more power to dissipate at the load. The input current could be observed with the same pattern except for certain time delay. At initial period, the input current could reach up to 15 A. At steady interval, the input current oscillates between approximate ranges of 6 A and 0A.

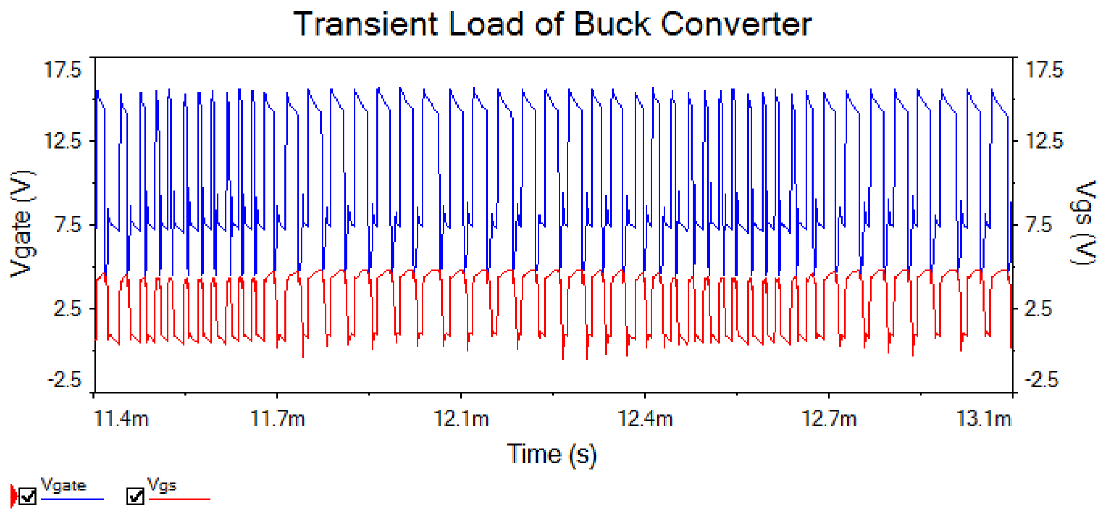

Figure 3.11: Signal MOSFET Gate Responses of V_{gate} and V_{gs} for Transient Load.

At the MOSFET gate (Figure 3.11), the gate voltage oscillates between approximate ranges of 16V and 4.8V. As for the gate-to-source voltage (V_{gs}), the waveform oscillates between approximate ranges of 5V and 1.2V when the output voltage is below 6V. As the output voltage is above 6V, the switching frequency increases thereby reducing the switch-on time of the MOSFET and also the amplitude of V_{gs}. At both time intervals, the waveform oscillates between approximate ranges of 4V and 1.2V. At both situations, the MOSFET is able to switch-on and switch-off properly.

3.4.2 Transient Input Simulation on the Buck Converter

Transient input test measures the circuit's conditions when it is applied with a fluctuating voltage at the input when driving a load at maximum output current of 4 A. The current will oscillate from 10 V to 12.6 V at a given period cycle. The maximum load current is set to 4 A. The input transient specification is given as below:

Signal Type	Pulse
V1: Initial Voltage	10 V
V2: Peak Voltage	12.6 V
T_d: Initial Delay Time	100 µs
T_r: Rise Time	50 µs
T_f: Fall Time	50 µs
Pw: Pulse Width	500 µs

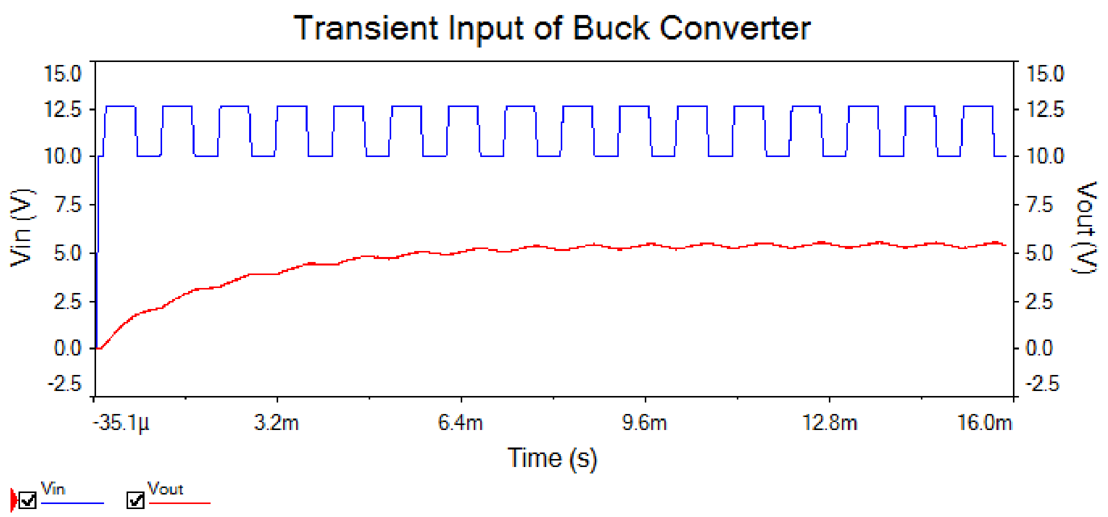

Figure 3.12: Voltage Responses of V_{in} and V_{out} for Transient Input.

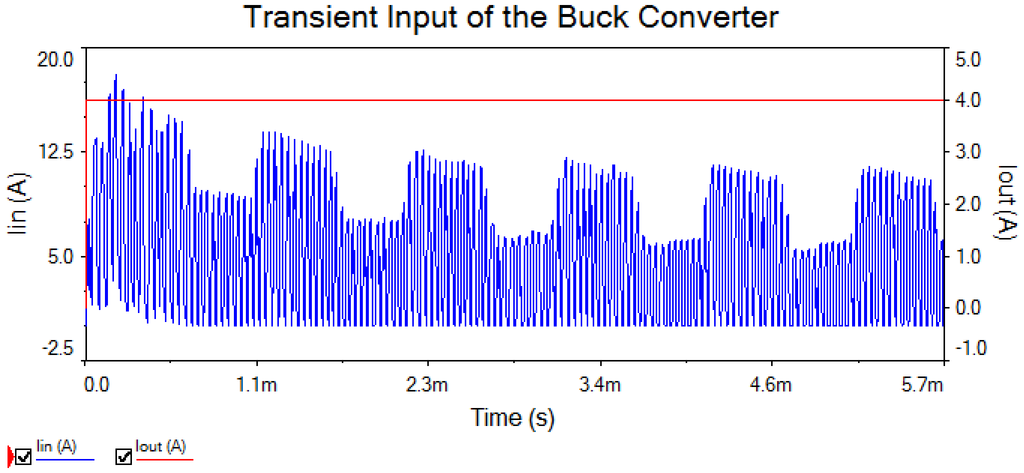

Figure 3.13: Current Responses of I_{in} and I_{out} for Transient Input.

At the input voltage (Figure 3.12), the voltage forms a trapezoidal waveform that oscillates between approximate ranges of 10 V and 12.6 V. As the input voltage increases to peak voltage, the input current increases to allow more power to dissipate at the load. At the output voltage, the voltage oscillates between approximate ranges of 5.2 V and 5.4 V with a voltage ripple of 0.2 V.

Observing Figure 3.13, at initial period, the input current could reach up to 15 A. After reaching steady condition, the input current forms a trapezoidal waveform that oscillates between approximate ranges of 12 A and 0 A. The input current could be observed with the same pattern as the input voltage except for certain time delay.

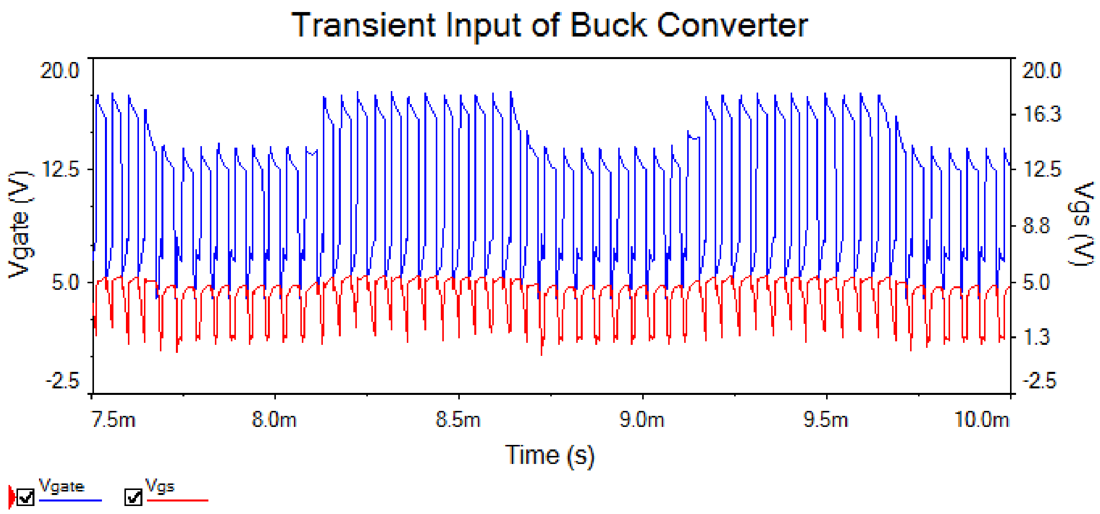

Figure 3.14: Signal MOSFET Gate Responses of V_{gate} and V_{gs} for Transient Input.

At the MOSFET gate (Figure 3.14), the gate voltage oscillates between approximate ranges of 14 V and 4.8 V when the input voltage is at low 10 V. The gate-to-source voltage oscillates between approximate ranges of 5 V and 1V. When the input voltage is at peak 12.6 V, the gate oscillates between approximate ranges of 16 V and 4 V. As for the gate-to-source voltage, the waveform oscillates between approximate ranges of 5.5 V and 1.2 V. The decrease in the amplitude of the gate voltage is due to a minimum input voltage of 10V. However, at both situations, the MOSFET is able to switch-on and switch-off properly.

3.4.3 Startup Simulation on the Buck Converter

Startup test is to test the condition of the circuit during the startup stage. The startup measures the input voltage from 0 V up to its mean input voltage of 11.3 V. The load will be represented by a resistive load of 1.675 Ω. The test is mainly to observe the condition of the circuit during its startup with a load in demand of maximum current. The startup input source is set with the condition:

V1: Initial Voltage	0 V
V2: Peak Voltage	11.3 V
T_d: Initial Time Delay	50 µs
T_r: Rise Time	50 µs

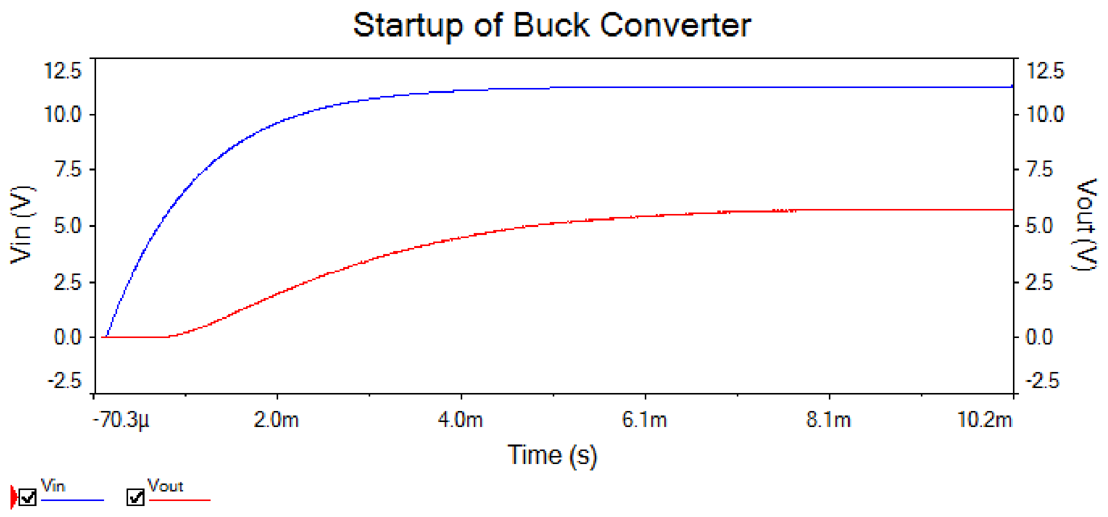

Figure 3.15: Voltage Responses of V_{in} and V_{out} for Startup Stage.

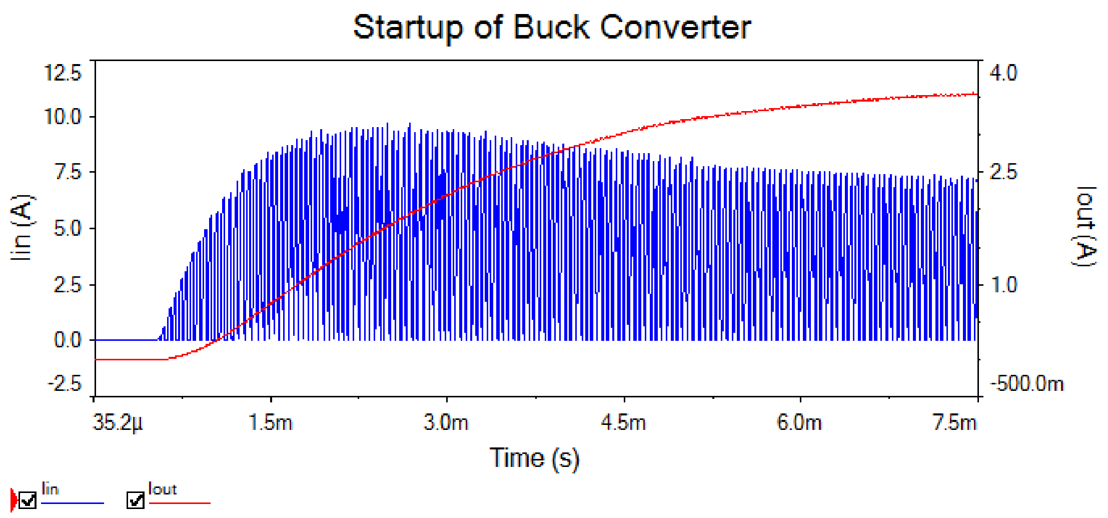

Figure 3.16: Current Responses of I_{in} and I_{out} for Startup Stage.

At the input voltage (Figure 3.15), the voltage slowly rises from 0 V to 11.3 V. During the startup initial period, the input current waveform (Figure 3.16) rises up to 10 A before falling to a steady oscillating waveform between approximate ranges of 0A and 7.5A. The buck converter operates on discontinuous input current and also due to inductor charging, thus, having a high current overshoot during the startup stage.

The output voltage rises slower than the input voltage due to circuit requires charging up before the voltage will reach the load. The output voltage has ripple voltage less than 40 mV. The output current has ripple current less than 20 mA. The output current has the same waveform pattern as the output voltage. It is observed that the output does not reach its maximum values of 6.7 V and 4 A. The maximum output voltage recorded is 5.7 V and the maximum output current recorded is 3.6 A.

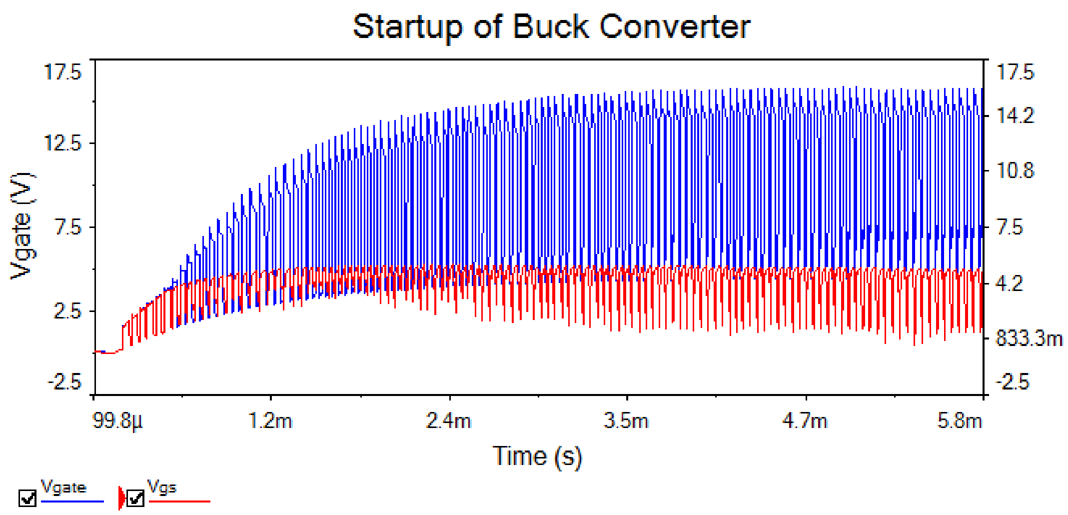

Figure 3.17: Signal MOSFET Gate Responses of V_{gate} and V_{gs} for Startup Stage.

At the MOSFET gate, the amplitude gate voltage increases as the input voltage increases. At steady condition where the input voltage nearly reaches 11.3V, the gate voltage oscillates between approximate ranges of 16V and 4.8V. As for the gate-to-source voltage, the waveform oscillates between approximate ranges of 5.2 V and 0.8 V. The MOSFET is able to switch-on and switch-off properly.

3.4.4 Steady State Simulation on the Buck Converter

Steady state test is to test the circuit operating with the mean of input supply of 11.3 V and the maximum load current of 4 A under a steady state condition.

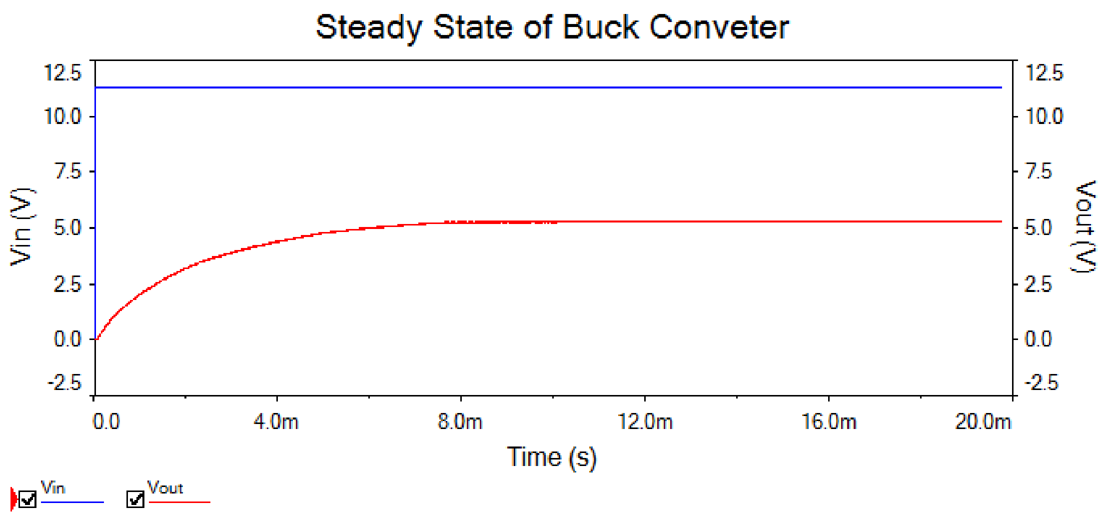

Figure 3.18: Voltage responses of V_{in} and V_{out} for Steady State.

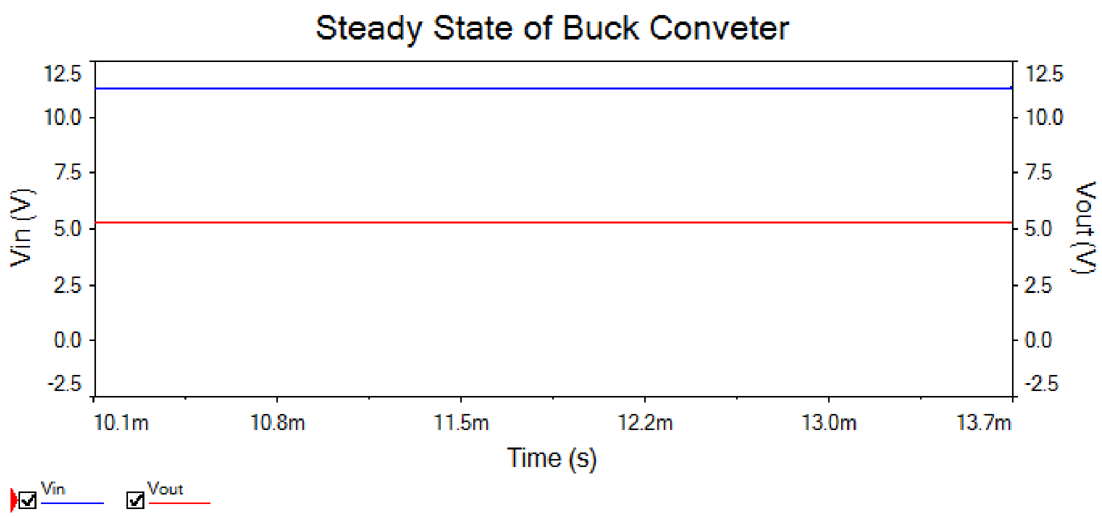

Figure 3.19: Voltage Responses of V_{in} and V_{out} for Steady State (Zoomed In).

From Figure 3.19, the circuit reaches a steady state after 10 ms. The output voltage can be seen with an average ripple voltage of 0.04V at a mean output voltage value of 5.22 V but does not have any voltage overshoot.

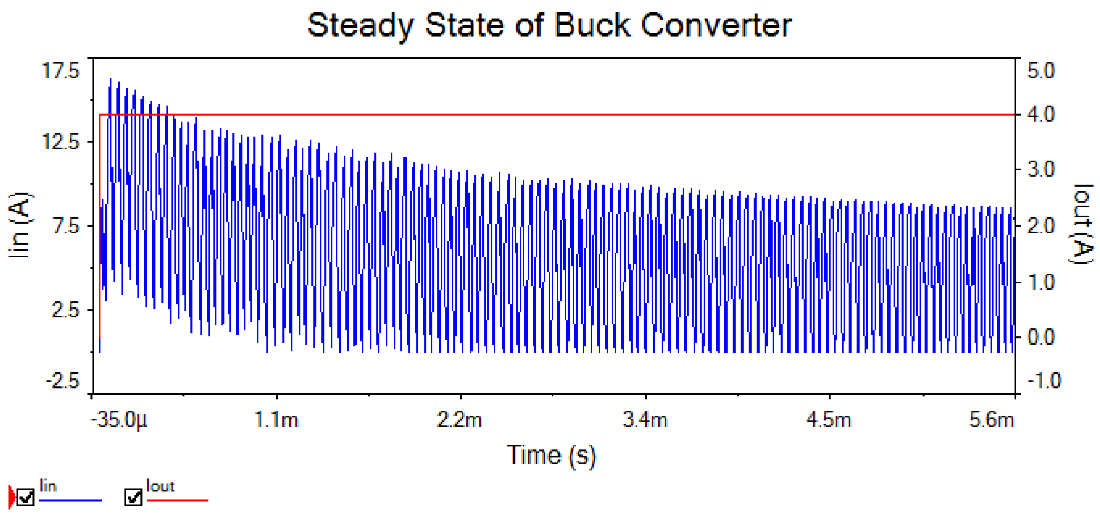

Figure 3.20: Current Responses of I_{in} and I_{out} for Startup Stage.

Observing the Figure 3.20, at the start of the simulation, it is pointed before that the input current will have a high overshoot of current up to 13 A when the load demands a maximum current before the circuit is charged up. However, at steady state, the input current will oscillate between an approximate ranges of 0 A and of 10 A.

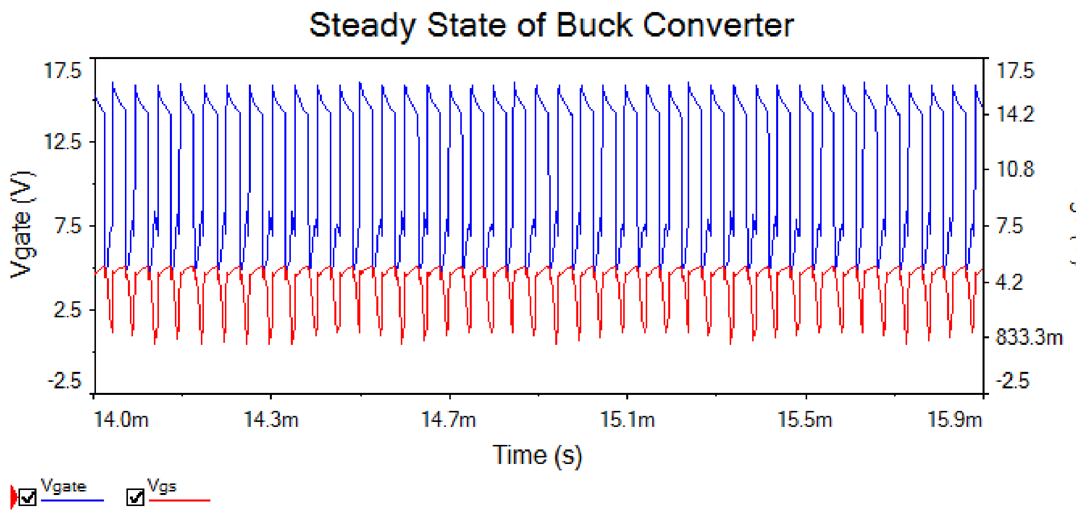

Figure 3.21: Signal MOSFET Gate Responses of V_{gate} and V_{gs} for Steady State (Zoomed In).

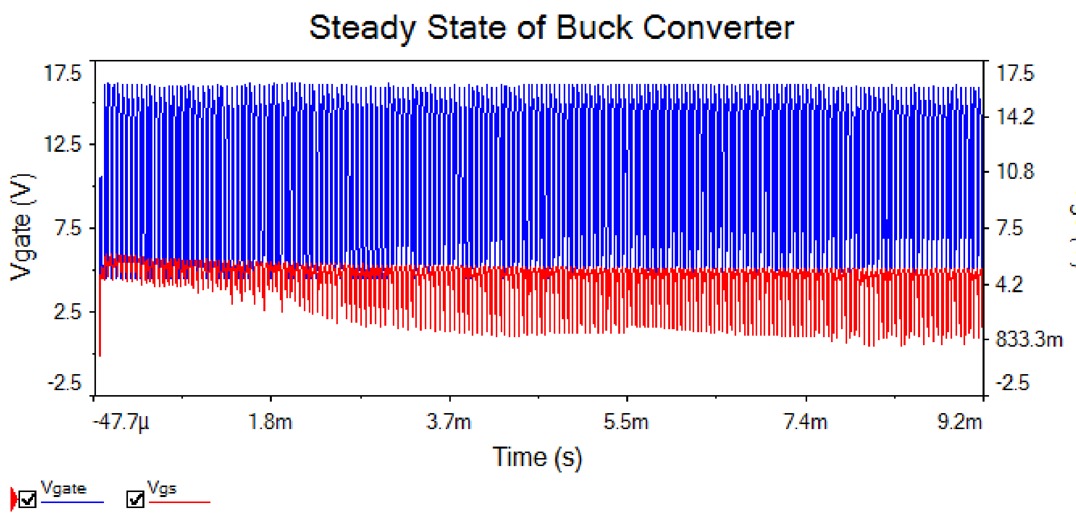

Figure 3.22: Signal MOSFET Gate Responses of V_{gate} and V_{gs} for Steady State.

At the MOSFET gate (Figure 3.21), the amplitude gate voltage is constant as the input voltage is constant as well. At steady condition the gate voltage oscillates between approximate ranges of 16 V and 4.8 V. As for the gate-to-source voltage, the waveform oscillates between approximate ranges of 5 V and 1.2 V. Since the output voltage does not reach the maximum value of 6V, there is no change to the switching frequency. The MOSFET is able to switch-on and switch-off properly.

3.5 Buck Converter in a Single Chip

There are many readily available buck converters in the market. Some chip designs are complex and comes with many functions and safety operation functions such as current limiting, thermal shutdown protection, and overvoltage protection. Other chip designs feature simple circuitry without extra features as compared to those complex chip designs. However, both types of chip designs require external basic components to complete a regulator circuit.

An example of non-synchronous, integrated-switch buck regulator is the LM2678T-ADJ by National Semiconductor. It features adjustable output voltage and an embedded feedback circuitry inside the chip. The switching frequency is fixed at 260 kHz by its internal oscillator. The use of the manufacturer's online circuit designer software called WEBENCH Power Designer will generate a model circuit based on the operating requirements and using the chip.

Using the operating requirements of the project, a model circuit (Figure 3.23) was generated. The simulation and operating values were automatically generated as well.

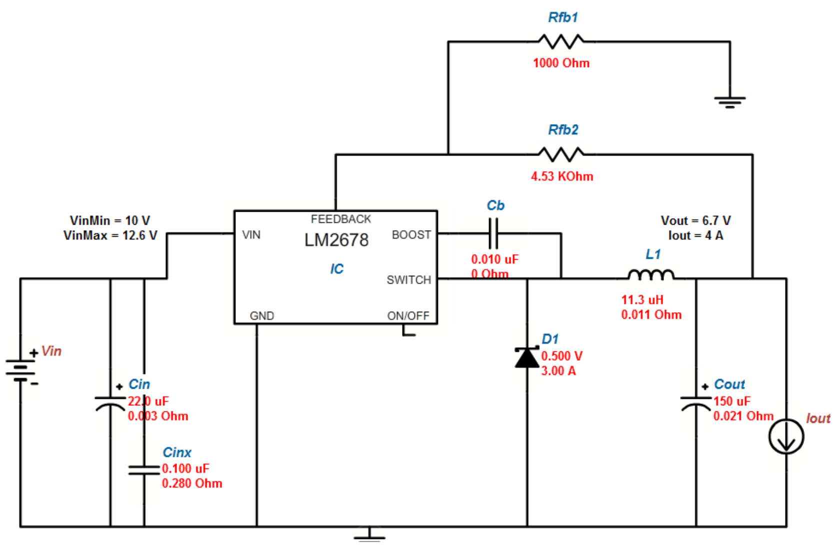

Figure 3.23: The Model Circuit for LM2678.

The simulation can be set to monitor the current and voltage at different points and components on different set of tests. The tests include transient input, transient load, steady state, and startup. (Refer Appendix G)

3.5.1 Simulation of Transient Input for LM2678

Transient input test involves the circuit operating with an input source fluctuating between its initial input voltage and peak output voltage at a given delay time. The load at this test is set to be fixed at maximum value. The transient input source is set with the condition:

R: Source Resistance	10 mΩ
Signal Type	Pulse
V1: Initial Voltage	10 V
V2: Peak Voltage	12.6 V
T_d: Initial Delay Time	100 µs
T_r: Rise Time	50 µs
T_f: Fall Time	50 µs
Pw: Pulse Width	500 µs

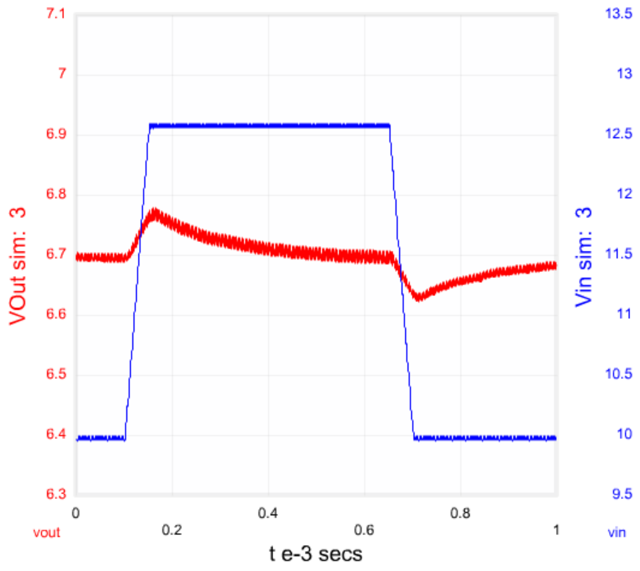

Figure 3.24: The Simulation Chart of V_{in} and V_{out} at Transient Input.

From the waveform simulated (Figure 3.24), the load voltage can be seen to rise and fall with the same rise and fall time of the input voltage. It is observed that the mean load voltage is an approximate value of 6.73 V. When the input voltage does not change, the load voltage will increase or decrease to this mean value.

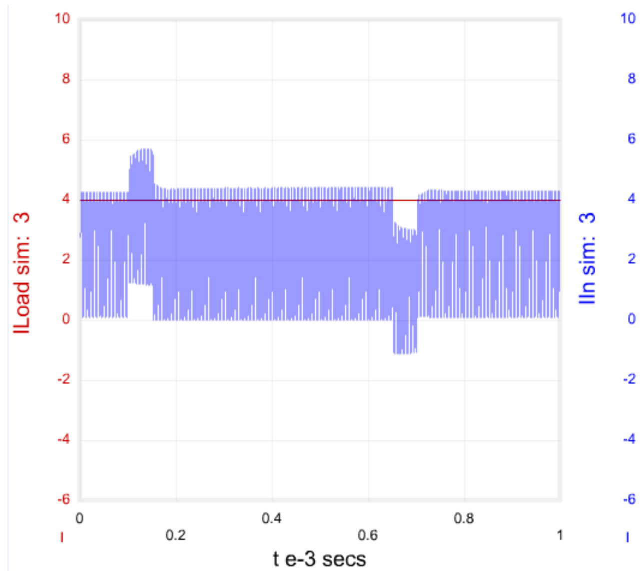

Figure 3.25: The Simulation Chart of I_{load} and I_{in} at Transient Input.

From the waveform simulated (Figure 3.25), the load current can be seen to have a maximum current value of 4 A. The input current is seen to be oscillating between 0 A and 4 A. However, during its rise time, the input current will have an approximate overshoot surge of 5.8 A and a low of 1 A. At its fall time, the opposite is observed where the input current will have an approximate fall of -1.8 A and an approximate high of 2.8 A. A negative value means there is a back-emf current to the input.

3.5.2 Simulation of Transient Load for LM2678

Transient load test involves the circuit operating with a fixed mean input supply and the load current is pulsing between a minimum value and maximum value within a time period. The transient input source is set with the condition:

Signal Type	Pulse
I1: Initial Current	4 A
I2: Peak Current	0.4 A
T_d: Initial Delay Time	100 µs
T_r: Rise Time	50 µs
T_f: Fall Time	50 µs
Pw: Pulse Width	500 µs

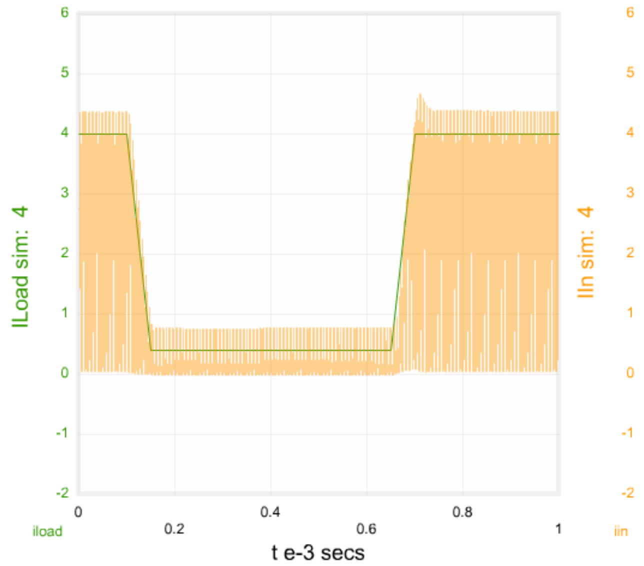

Figure 3.26: The Simulation Chart of I_{load} and I_{in} at Transient Load.

From the waveform simulated (Figure 3.26), the input current can be seen to rise and fall with the same rise and fall time of the input voltage. However, when the load current is at its low of 0.4 A, the input current is seen to have oscillating between an approximate value of 0.5 A and 0 A with a ripple current of approximately 0.5 A. At the fall time, the input current is seen to be falling accordingly from an approximate high of 3.8 A to 0.5 A. At the end of the rise time of the load current, the input current has an approximate peak of 4.6 A before reaching a steady state at an approximate value of 3.8A with a ripple current of approximately 0.5 A.

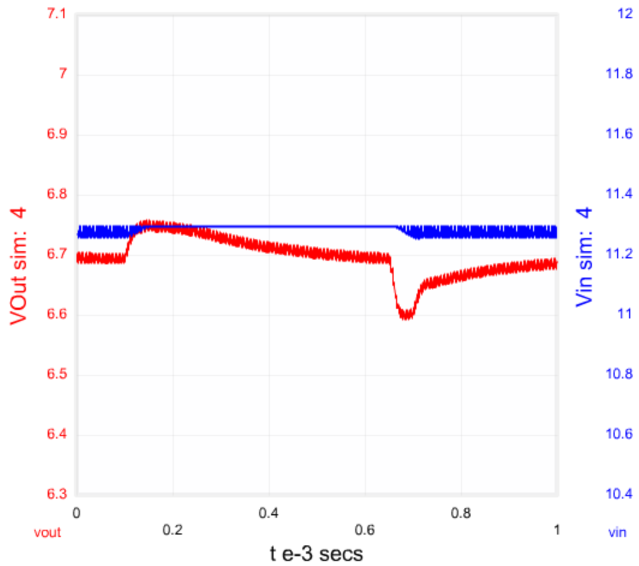

Figure 3.27: The Simulation Chart of V_{in} and V_{out} of the Circuit at Transient Load.

From the waveform simulated (Figure 3.27), the load voltage is seen to be oscillating with the same rise and fall time, with an approximate peak of 6.75 V and an approximate low of 6.6 V. The load voltage will settle at an approximate mean value 6.73 V. The input current is seen to have a steady voltage value of 11.3 V except that when the load current is high the input voltage falls slightly below 11.3 V.

3.5.3 Simulation of Steady State for LM2678

Steady state test is to test the circuit operating with the mean of input supply and the maximum load current. The steady state input source is set with the condition:

R: Source Resistance	10 mΩ
V: Input Voltage	11.3 V

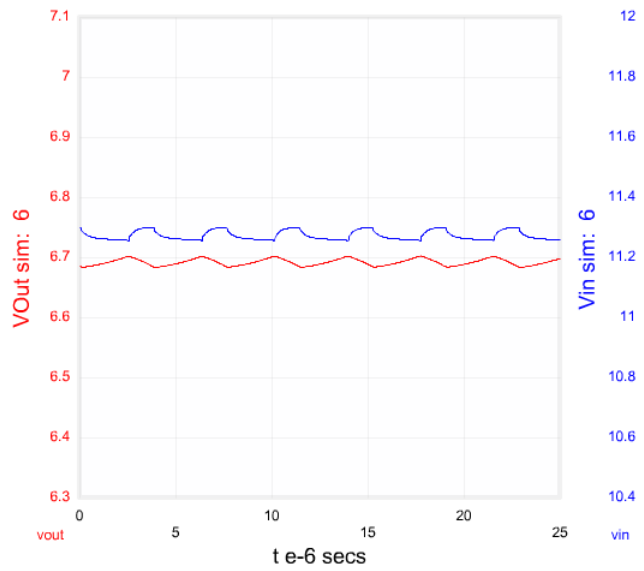

Figure 3.28: The simulation chart of V_{out} and V_{in} at Steady State.

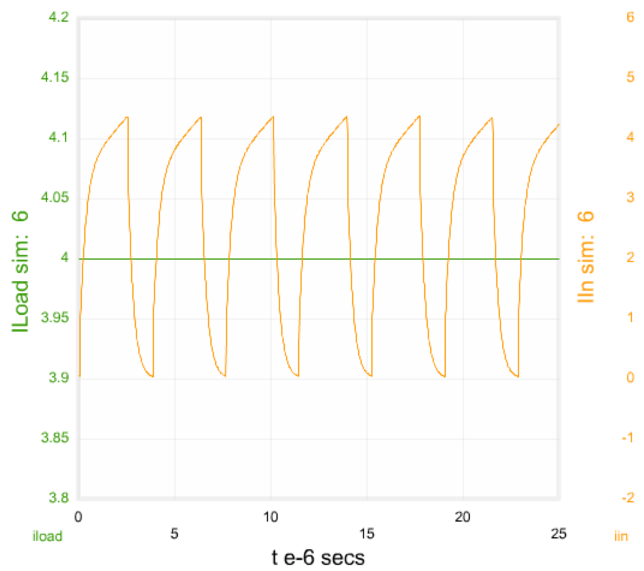

Figure 3.29: The simulation chart of I_{in} and I_{out} at Steady State.

Observing both Figure 3.28 and Figure 3.29, at the input side, the voltage waveform and current waveform have the opposite peaks and lows. When the input voltage is high, the input current is low and vice versa. The input voltage has a peak of 11.3 V and an approximate low of 11.28 V whereas the input current has a high of 4 A and a low of 0 A. This means that the input current is discontinuous.

As for the output load side, the load current has a fixed current value of 4 A. The load voltage forms a saw-tooth waveform with an approximate peak of 6.7 V when the input current is high. The load voltage has an approximate low of 6.68 V when the input current is low at 0 A.

3.5.4 Simulation of Startup for LM2678

Startup test is to test the condition of the circuit during the startup stage. The startup measures the input voltage from zero voltage up to its mean input voltage. The load will be represented by a resistive load of 1.675 Ω with a current load of 4 A. The startup input source is set with the condition:

R: Source Resistance	10 mΩ
V1: Initial Voltage	0 V
V2: Peak Voltage	11.3 V
T_d: Initial Time Delay	50 µs
T_r: Rise Time	50 µs

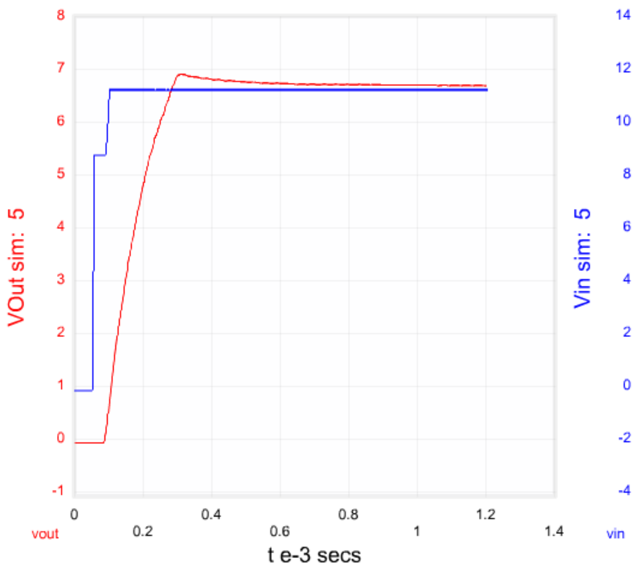

Figure 3.30: The simulation chart of V_{in} and V_{out} of the circuit at Startup.

The input voltage waveform (Figure 3.30) is seen to rise from 0 V to 11.3 V with a step of 50 μs. The output load voltage is seen to rise from 0 V when the input voltage is approximately 4.5 V. The load voltage is seen to overshoot to an approximate value of 6.9 V before reaching a steady state of 6.7 V.

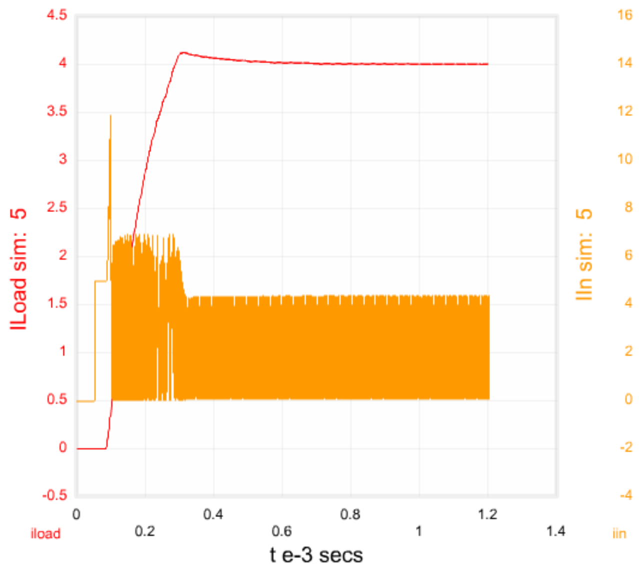

Figure 3.31: The simulation chart of I_{load} and I_{in} at Startup.

From the Figure 3.31, the load current waveform has a similar shape as its load voltage waveform. As for the input current waveform, the input current has an overshoot up to 12 A when the input voltage reaches a peak of 11.3 V. When the load current increases from 0 A, the input current is approximately 5 A. Before the load current reaches its steady state of 4 A, the input current oscillates between an approximate value of 7 A and 0 A. Once the load current reaches its steady state, the input current is seen to oscillate between 4 A and 0 A. A ripple current of approximately 1.2 A is seen at the steady state.

3.6 Wiring of Components

The various electronic components, motors, and input supplies will need to be connected together in order to complete the whole circuits. Therefore, printed circuit board (PCB) will be used as a platform for all of these connections. Instead of using plenty of jumper cables, the wire is ‘printed’ on the board forming pathways connecting the components together. The components in this project consist of analogue and digital components. Integrated circuits (ICs), sensors, passive elements such as resistors, capacitors, inductors, and diodes fall in the category of digital components. Servo motors and DC geared motors fall in the category of analogue components.

A good design of PCB is to separate analogue and digital signal planes. Since analogue signal is sensitive to noises and digital signal, albeit robust to noise, may carry noise in their signal, the two different signals are not a good mix together. However, their ground planes can be combined since both of the signals will return to the same common ground which is the negative terminal of the input supply.

The components must be placed as close as possible to the ground so that the signals have the shortest travel path back to the common ground. It is advisable to create thick pathways if it is intended to carry high current through it to the components. Thicker pathways will enable more current to flow through and reduce heat buildups.

For the motor loads, it is good to include a freewheeling diode connected in parallel to reduce the back-emf sources from the motors, due to their inductance characteristics, when the input supply is cutoff. For the input and output, decoupling capacitors are recommended to protect the components from initial current surges and incoming signal noises.

A sample of the self-built layout for the PCB is shown in Figure 3.32 below.

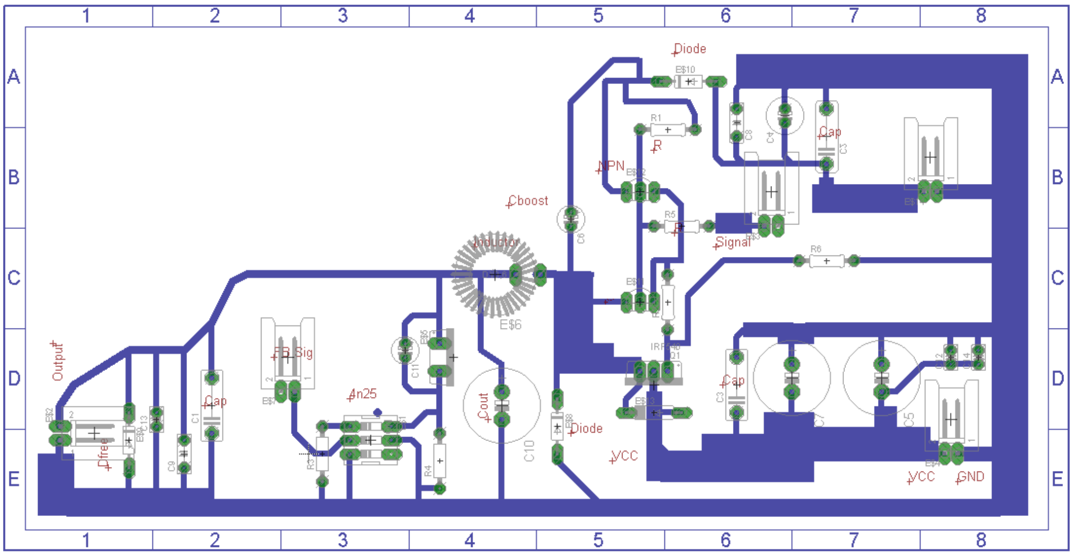

Figure 3.32: A Layout of PCB for a Part of Constructed Buck Converter. (Refer Appendix E)

CHAPTER 4

RESULTS AND DISCUSSION

4.1 Results Overview

A test circuit is constructed to assess the performance of the converter. A few tests were carried out to observe the validity of the results shown in the simulation. The test would include the measuring the output voltage and input current for a variety of resistive loads. Another circuit comprises LM2678T-ADJ will be made as a comparison for the constructed buck converter.

Comparisons between the simulation results between the constructed buck converter and LM2678T-ADJ will be discussed. The difference between the simulation results and experimental results will be discussed as well.

4.2 Circuit Construction

The proposed buck converter design was constructed on breadboard for testing and experiment (Figure 4.1). The recommended circuit design using manufacturer's software circuit design for LM2678T-ADJ was also constructed on separate breadboard for similar purposes.

The tests included for the experiment were listed as below:

1. Measure output current and voltage of no-load.
2. Monitoring output voltage at different value of resistive load.
3. Monitoring output current for selected resistive load.

Due to restriction of space on the breadboard, the circuit has to be cramped in little spaces available and a lot of jumper cables would be used to connect to components at different pin terminals. As such, there would be compromise in the experimental results with little power losses due to the jumper cables. One solution would be using decoupling capacitors to balance out the effect of inductance carried by the jumper cables. The remaining wire inductance, if available, was assumed to be negligible as the inductance value of the inductor of the converter was large compared to the wire inductance. Therefore, the purpose of the converter was to supply enough power to the output load. The switching frequency of the converter was limited from 30 kHz to 70 kHz. The range of this switching frequency could be considered low as compared to other buck converters available in the market, where their switching frequencies varies from a minimum of 200 kHz up to the range of megahertz, MHz.

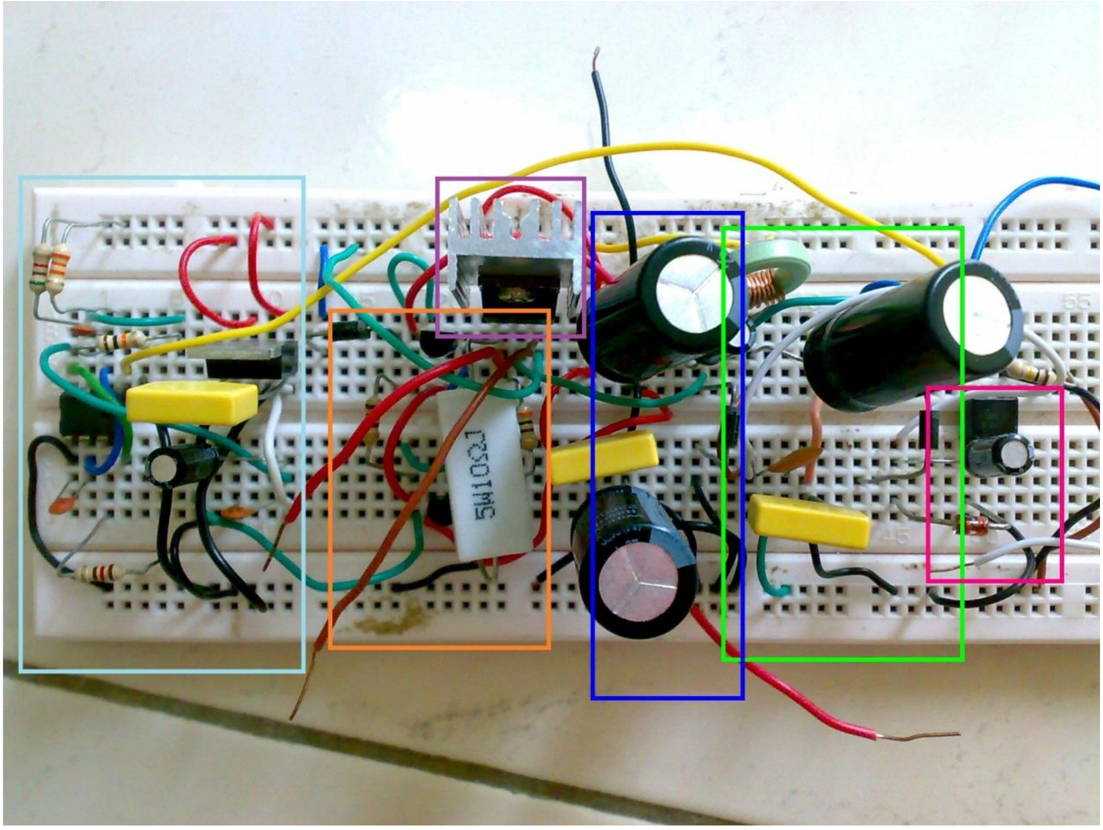

Legend

- Timer 555
- Push-Pull Amplifier
- MOSFET IRF540N
- Topology of Buck Converter
- Optocoupler
- Input Capacitor

Figure 4.1: The Constructed Buck Converter on Breadboard.

The bill of material for the constructed buck converter was listed as below. The list of components will be separated into categories of DC-DC converter circuit, pulse-width-modulation (PWM) signal, signal amplifier, and feedback voltage.

Table 4.1: Bill of Material for DC-DC Converter Circuit.

Component	Quantity	Value / Description
MOSFET	1	IRF540N
Input Capacitor	2	2200 µF
	1	0.1 µF
	1	0.01 µF
	1	0.001 µF
Inductor	1	7 µH
Fast Recovery Diode	3	UF 4007
Output Capacitor	1	2200 µF
	1	0.1 µF
	1	0.01 µF
	1	0.001 µF

Table 4.2: Bill of Material for PWM Signal.

Component	Quantity	Value / Description
Timer	1	NE 555
Resistors	1	5 kΩ
	1	10 kΩ
	1	33 k Ω
Capacitor	2	0.001 µF
Voltage Regulator 12 V	1	LM7812

Table 4.3: Bill of Material for Signal Amplifier.

Component	Quantity	Value / Description
PNP Transistor	1	2N3906
NPN Transistor	1	2N5550
Capacitor	1	1 μF
Resistors	1	10 Ω
	2	120 Ω
	1	10 kΩ
Fast Recovery Diode	3	UF 4007

Table 4.4: Bill of Material for Feedback Voltage.

Component	Quantity	Value / Description
Optocoupler	1	4N25
Capacitor	1	1 μF
Resistors	1	100 kΩ
Zener Diode	1	1N4734 (5.6 V)

On the LM2678T-ADJ circuit, additional decoupling capacitors were added on the input and output of the circuit. The decoupling capacitors function to reduce noise at the input and act as temporary current storage between the delay time for the output capacitor to discharge and recharge. The LM2678T-ADJ circuit requires only basic components such as an inductor, capacitors, and resistors. The bill of material for LM2678T-ADJ circuit was listed as below

Table 4.5: Bill of Material for LM2678T-ADJ Circuit.

Component	Quantity	Value / Description
DC-DC Converter	1	LM2678T-ADJ
Resistors	1	3 kΩ
	1	1.5 kΩ
	1	1 kΩ

Capacitor	1	0.01µF
	2	0.1 µF
	1	1 µF
	1	22 µF
	1	220 µF
Inductor	1	12 µH
Fast Recovery Diode	1	UF 4007

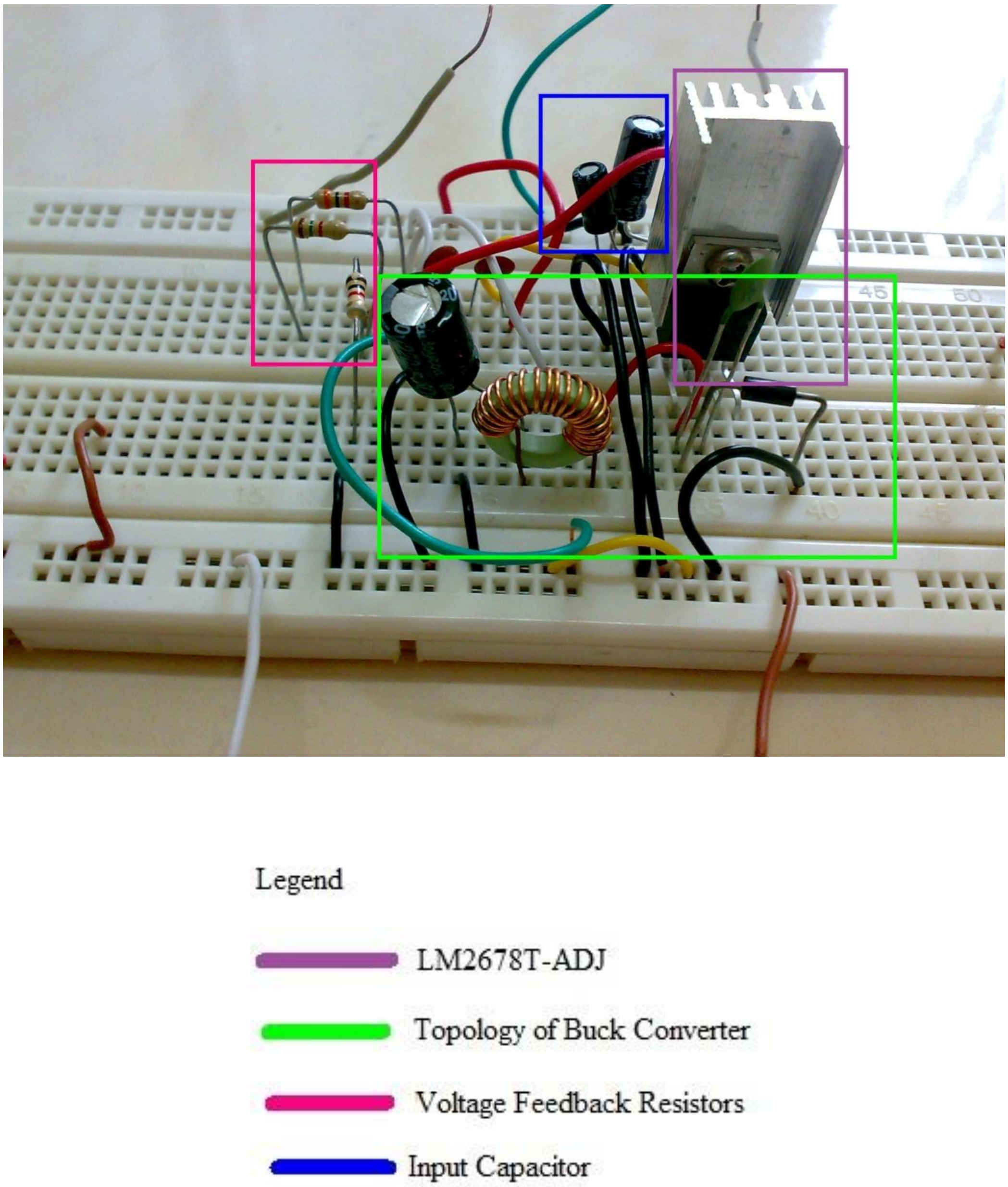

Figure 4.2: The Constructed Circuit of LM2678T-ADJ.

4.3 Experimental Results

The circuits constructed were tested inside a lab using available power source such as power supply unit. The power supply unit was set to 12 V as the preferred input voltage for experiment.

One of the test in experiment was to measure the input current and voltage at no-load. Based on the simulation results, both constructed buck converter and LM2678T-ADJ required a minimum value of current in the circuits due to the charging of the inductor. The results were taken using multimeter and were listed as below:

Table 4.6: Experimental Results for No-Load.

Constructed Buck Converter		LM2678T-ADJ	
Output Voltage (V_{rms}) (V)	Output Current (I_{rms}) (mA)	Output Voltage (V_{rms}) (V)	Output Current (I_{rms}) (mA)
6.7	0.7	6.73	0.536

The tested resistive loads had resistance value of 3.3 Ω, 5.1 Ω, 33 Ω, 51 Ω with a rated power of 5 W. The output voltage was measured using multimeter. Hence, the readings were referred to its root-mean-squared voltage (V_{rms}), where the voltage effectively reached the load. The results for the experiment were listed in the table below:

Table 4.7: Experimental Results for Resistive Load.

Resistance (Ω)	Constructed Buck Converter	LM2678T-ADJ
	Output Voltage (V_{rms})	Output Voltage (V_{rms})
3.3	5.64	-
5.1	5.64	-
33	5.51	6.72
51	5.47	6.76

The output voltage results were also captured on oscilloscope since the actual readings of the output voltage could be fluctuating from its peak voltage. The oscilloscope results for the constructed buck converter were shown as below:

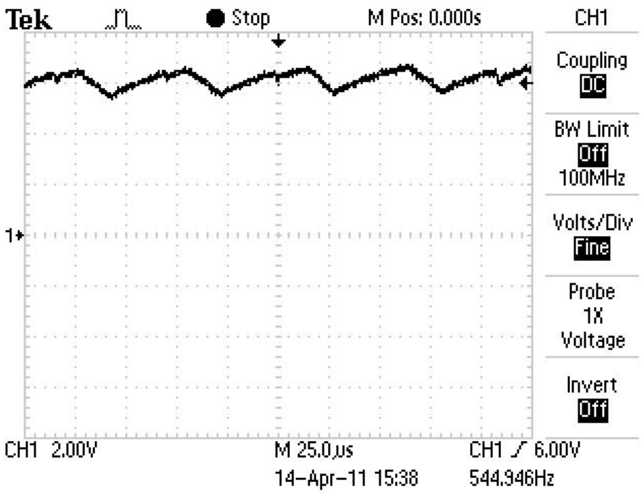

Figure 4.3: The Waveform of Output Voltage for 3.3 Ω

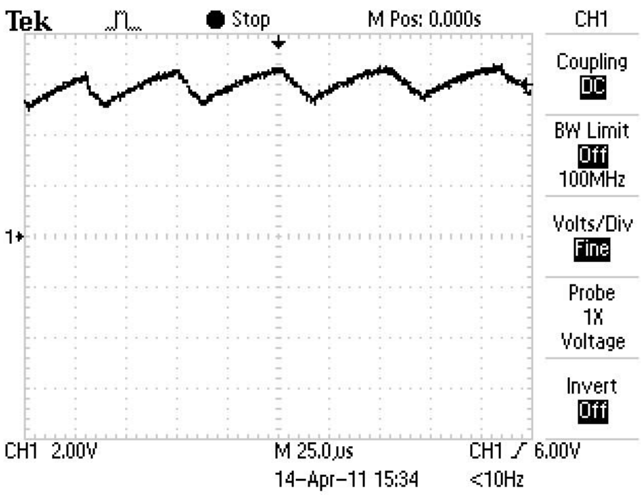

Figure 4.4: The Waveform of Output Voltage for 5.1 Ω

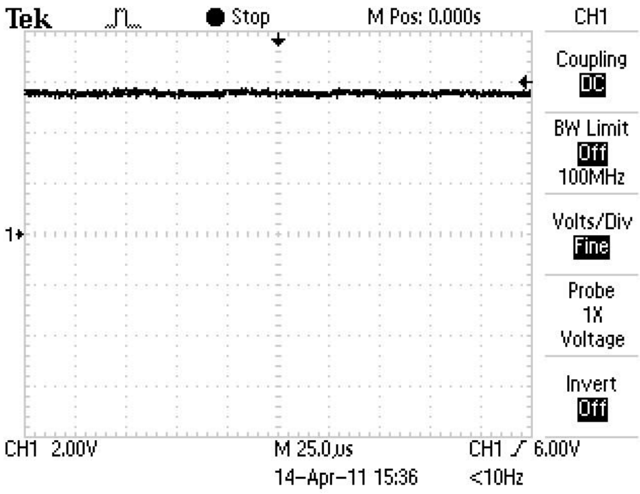

Figure 4.5: The Waveform of Output Voltage for 33 Ω

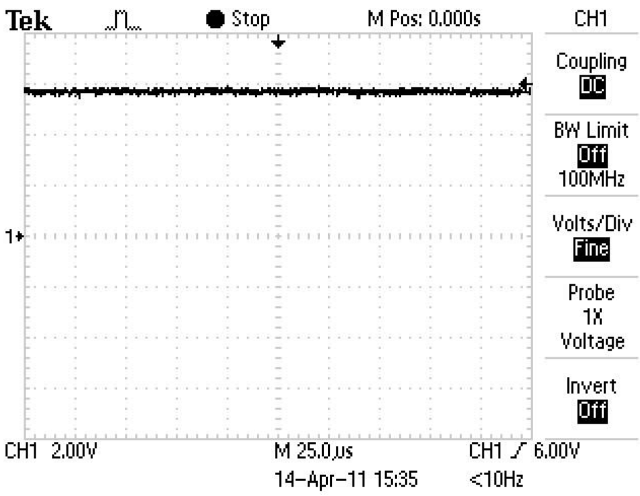

Figure 4.6: The Waveform of Output Voltage for 51 Ω

By using another 5 W 22 Ω resistor to be placed in parallel with all the experimental resistance values, the resistive load obtained was 1.682 Ω which is close to the required resistive load of 1.675 Ω to obtain an output of 6.7 V 4 A. The oscilloscope result was shown as below:

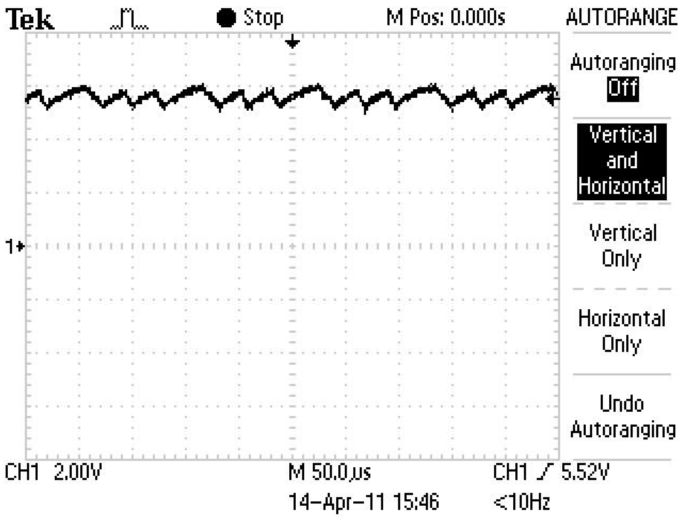

Figure 4.7: The Waveform of Output Voltage for 1.682 Ω

The oscilloscope results for the LM2678T-ADJ were shown as below:

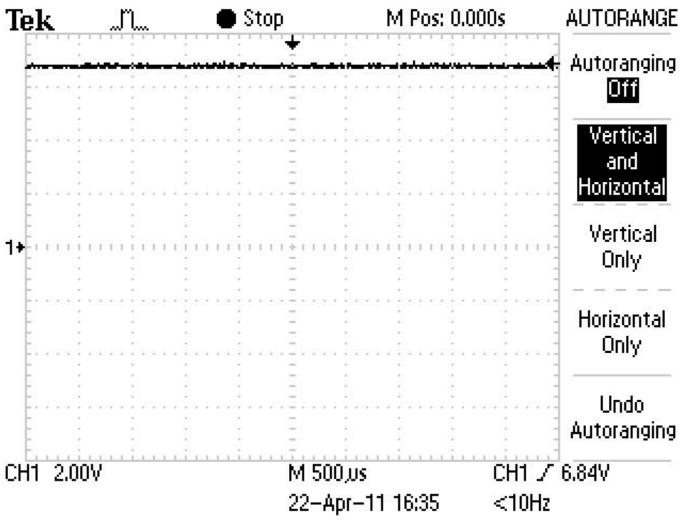

Figure 4.8: The Waveform of Output Voltage for 33 Ω (LM2678)

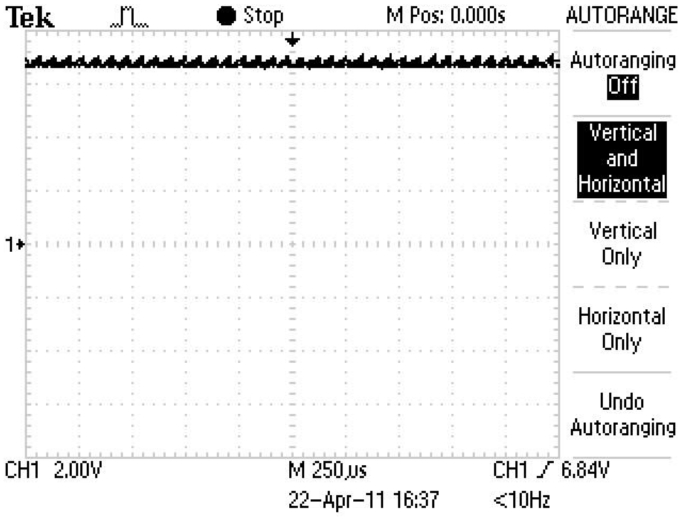

Figure 4.9: The Waveform of Output Voltage for 51 Ω (LM2678)

It was also in interest to know the output current waveform so as to identify the general characteristics of the buck converters. Thus, for the constructed buck converter, the output current for 3.3 Ω and 1.682 Ω were measured with oscilloscope.

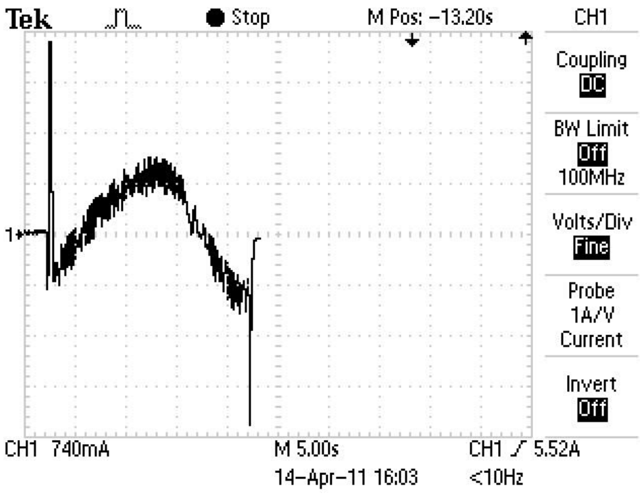

Figure 4.10: The Waveform of Output Current for 3.3 Ω

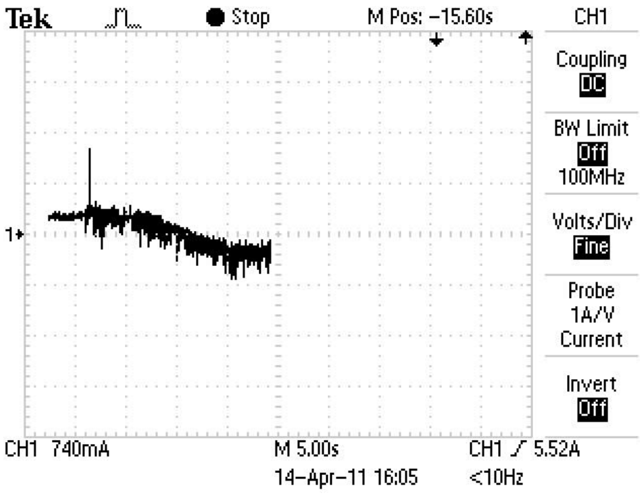

Figure 4.11: The Waveform of Output Current for 1.682 Ω

As for LM2678T-ADJ, the output current waveform for 1.682 Ω was measured with oscilloscope. However, in this case, a sealed-lead acid (SLA) battery with rating of 12V 7 Ah was used due to insufficiency of bench-top power supply unit to start the circuit.

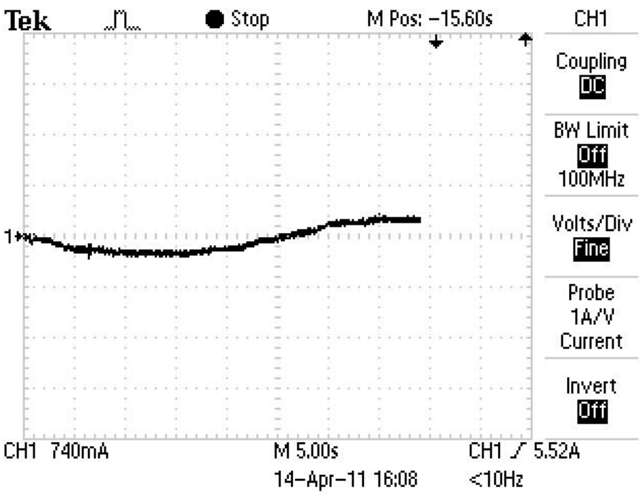

Figure 4.12: The Waveform of Output Current for 1.682 Ω (LM2678)

The gate voltage and gate-to-source voltage of the IRF540N MOSFET for the constructed buck converter were measured with oscilloscope to determine the turn-on and –off cycles of the MOSFET.

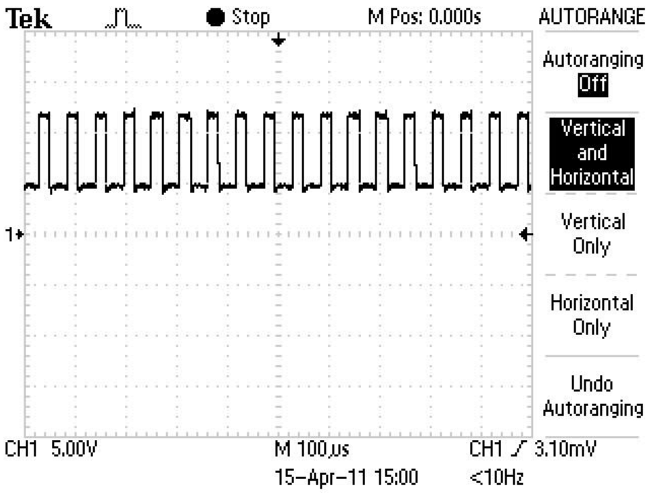

Figure 4.13: The Waveform of Gate Voltage for IRF540N MOSFET

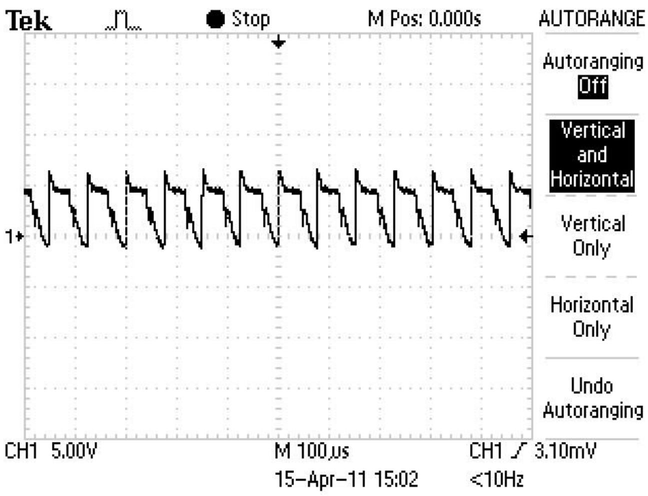

Figure 4.14: The Waveform of Gate-to-Source Voltage for IRF540N MOSFET

4.4 Discussion

There were anomalies in the readings of input current for the constructed buck converter when simulations were done. The input current was an unacceptable value of twice higher than the recorded input current for LM2678T-ADJ. Further considerations were taken and therefore, a practical experiment was carried out to identify the characteristics of the constructed buck converter and LM2678T-ADJ.

4.4.1 Discussions on the simulations

From the simulation results for constructed buck converter and LM2678T-ADJ obtained, there is one point of concern; the value of input current. For the constructed buck converter circuit simulations, the input current is twice the value of current obtained from the simulations of LM2678T-ADJ. Upon pin-pointing, as seen in Figure 4.15, the current from the input supply to output load, much of the input current is detected flowing into the output capacitor. The possible reason could be the output capacitor in the simulation is continuously charging.

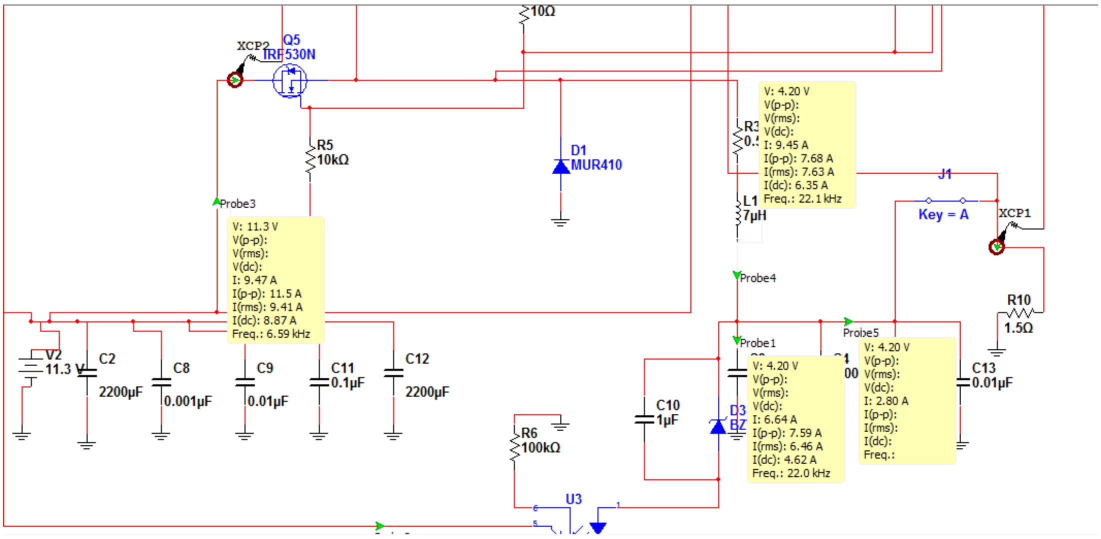

Figure 4.15: Simulation Result Showing the Current Flow from Input to Output.

Despite having recorded unusual high current for the constructed buck converter in the simulations, the simulated waveforms of voltage and current for input and output have the same waveform patterns when compared with simulated waveforms obtained for LM2678T-ADJ.

It is noted that in both circuits, the input current is discontinuous where the input supply momentarily 0 A. This is one characteristic of the buck converter which it is operating with discontinuous input current.

It is observed that the constructed buck converter rarely have voltage overshoots and the ripple voltage of the output voltage is within estimated range. For LM2678T-ADJ, there would be minor voltage overshoots at the output when the input voltage is increasing or decreasing.

In both of the circuits, they are observed with noticeable current overshoots during the startup of the circuits where the inductor initially draws higher current than expected ratings. Ripple currents at the output current are observed for both of the circuits but are within the estimated range.

For the constructed buck converter, it is observed that the current is always lagging behind voltage. This condition suggests that the circuit is slightly inductive. As for LM2678T-ADJ, its simulations suggest the voltage and the current is in phase.

4.4.2 Discussions on the Experimental Results

With no-load, the constructed buck converter would draw a minimum current of 0.7 mA, whereas the LM2678T-ADJ would draw a minimum current of 0.536 mA. Therefore, it is unsafe to use the circuit with no load as the current will be dissipated inside the circuit, causing the circuit to overheat and fail. As a precaution the MOSFET in the constructed buck converter and LM2678T-ADJ (buck converter chip) must be attached with heat-sink.

When measuring the output voltage for given resistive loads, the constructed buck converter gave readings ranging from 5.47 V to 5.64 V, as compared to input voltage of 6.7 V. This is because of freewheeling diode and zener diode in the circuit with each has an average voltage drop of 0.7 V. Accounting for those voltage drops at both diodes would roughly reach the measured output voltage.

Observing the waveforms for the output current for both of the circuits (figure 4.10 to Figure 4.12), the waveforms showed the output currents of both circuits drop below 0 A. These are due to the reason of light-load conditions at the output. As the loads require less current than expected, the output loads flows the current back to the inductor, resulting the output currents to drop below 0 A.

Observing the output current waveform of Figure 4.10 of the constructed buck converter, there are noticeable current overshoots at the output load during the initial startups of the circuit. The current overshoots could be a few times higher than normal value for the output current. This current overshoot is due to output current phase lags output voltage phase, building more current at the output.

However, by observing the output current waveform for LM2678T-ADJ, the output current starts by dropping below 0 A to a maximum low of – 150 mA before increasing to a maximum of 150 mA. There is no current overshoot observed in the waveform. For a comparison, a similar pattern could be observed in Figure 4.11 for the constructed buck converter but it exhibits more ripple currents and a current overshoot at initial time.

The reason for the constructed buck converter to have more ripple currents and current overshoot is due to ripple voltages of the output voltage, as seen in Figure 4.3 to Figure 4.7. At lower resistive load, the output voltage exhibits more ripple voltages. As the resistive load value increases, the output voltage can be seen to have with little or no voltage ripples, as seen in Figure 4.5 and Figure 4.6.

For LM2678T-ADJ, the output voltages waveforms shown in Figure 4.8 and are observed with little ripple voltages whereas the voltage ripples are more visible in Figure 4.9. As compared to output voltage waveforms of the constructed buck converter of similar resistive load values (Figure 4.5 and Figure 4.6), there is no ripple voltages visible to naked eyes. The reason that more ripples are observable for higher resistance value (in Figure 4.9) is due to lower current dissipated at the 5 W 51 Ω resistor, causing current buildup in the inductor.

The difficulty for the MOSFET gate to turn-on and –off depends on its gate-to-source voltage. The MOSFET gate must have higher high voltage than the voltage source and have lower low voltage than the voltage source. The voltage source refers to the output voltage of 6.7 V. The MOSFET gate turns on at 4 V and turns off at 2 V. Therefore, the gate voltage must have at least 12 V at its high and at least 4 V at its low. Therefore, by using the push-pull amplifier, the required gate signal could be obtained as shown in Figure 4.13. The gate-to-source voltage waveform is shown in Figure 4.14, where it has a high of approximately 4 V and a low of approximately -1 V. When the voltage waveform goes high, there is a voltage overshoot of approximately 1 V.

CHAPTER 5

CONCLUSION

5.1 Conclusion

In the constructed buck converter, the main importance is the driving of the MOSFET. The switching –on and –off of the MOSFET depends on the gate-to-source voltage threshold. For the MOSFET used in the circuit to turn on, the required gate-to-source voltage is 4 V and above. As for it to turn off, the gate-to-source voltage is 2 V and below. Between the drain terminal and the source terminal of the MOSFET, there is an internal resistance. The internal resistance, R_{ds}, specifies how much power dissipation on the MOSFET and the value of resistance seen by the MOSFET between the input supply and the output load. In the datasheet, the listed low R_{ds} refers to when the gate-to-source voltage is of 10 V. At this point of voltage, the MOSFET is fully turn-on, allowing nearly all the input power to flow to the load with little or no resistance by the MOSFET which can be negligible. As the input supply source is limited and the circuit construction is kept to simplest as possible using off-the-shelf electronic components, the gate-source voltage can only be kept operated between 5.5 V and 1.2 V, which fulfilled the condition for the MOSFET to turn-on and turn-off.

Despite obtaining different results for constructed buck converter when compared to LM2678T-ADJ for both simulation and experimental, constructed buck converter showed similar characteristics as with LM2678T-ADJ. Thus, it can be assumed that the constructed buck converter fulfills its function as a step-down voltage converter which is also a step-up current converter. It is concluded that buck converter is suitable for low-voltage high-current applications. Thus, one objective of this project, which is to implement a suitable dc-dc converter for low-voltage high-current applications, is achieved.

Comparing to linear regulator, the power loss of the regulator comes from the voltage drop at the regulator, the difference between the input voltage and output voltage, before the regulated voltage reaches the output load. Thus, if the output load is rated at lower voltage, more voltage drop would occur at the regulator. The voltage drop would then be dissipated as heat, times the amount of current from the input supply. The input current and the output current in linear regulator are equal. Thus, the higher input voltage and the lower output voltage, the heat dissipated would be higher and leads to lower efficiency of the regulator. Therefore, it is concluded that switching regulator is much more efficient compared to linear regulator in low-voltage high-current applications. Another objective of this project, which is to achieve high efficiency for low-voltage high-current applications, is achieved.

CHAPTER 6

RECOMMENDATIONS AND FUTURE IMPROVEMENTS

6.1 Recommendations and Future Improvements

The constructed buck converter has plenty of rooms for improvements. Some of recommendations that could be featured are listed as below:

1. Current limiting circuit for the input and output.
2. Implement soft-switching function so that the input current will be continuous in buck converter using ZVS technique.
3. Modification of the buck converter into buck-boost converter for better circuit efficiency.
4. Increase the ability of buck converter through multi-phase and also synchronous.

The constructed buck converter mentioned in this project has only implemented with fuse as an input current limiter. Though the fuse could function well in terms of disconnecting the input supply from the circuit when the input current is higher than the limit set for circuit, the blow up time for the fuse varies depending on how high the current exceeds the rating of the fuse. Thus, a better solution would be to implement a current limiting circuit in the constructed buck converter so that the circuit could protect itself from excessive current. Furthermore, it would be inconvenient to change fuse everytime when it is blown up.

The soft-switching technique enables a buck converter to operate with a continuous input current. This would make the buck converter to be a fourth-order converter that belongs to the fourth-generation dc-dc converter. Soft-switching could reduce the input and output ripple currents, switching losses and also the EMI of the circuit.

Buck-boost converter is a bridge between buck converter and boost converter. It offers higher efficiency compare to either single buck converter or boost converter could offer. However, the output of the buck-boost converter is an inverting output. Therefore, for general use of non-inverting output, the buck-boost converter has to be modified where two buck-boost converters is arranged in cascading order (refer Appendix A).

Buck converter can be designed to be as multi-phase (or interleaved) where buck converters are connected in parallel to increase its current handling and performance. Synchronous buck converter is spotted with two MOSFETs; one MOSFET at high-side and one MOSFET at low-side. The low-side MOSFET is used to reduce conduction losses on the buck converter. These two improvements could increase the efficiency of the buck converter and could handle higher current rating compared to a single acting buck converter.

REFERENCE

Lai, Y. M. (2001). Power Supplies. In Muhd. H. Rashid (Ed.), Power Electronics Handbook (pp. 487 – 494). Canada: Academic Press.

Luo, F. L., Ye, H., & Rashid, Muhd. H. (2001). DC/DC Conversion Technique and Nine Series Luo-Converters. In Muhd. H. Rashid (Ed.), Power Electronics Handbook (pp. 335 – 402). Canada: Academic Press.

Czarkowski D. (2001). DC-DC Converters. In Muhd. H. Rashid (Ed.), Power Electronics Handbook (pp. 335 – 402). Canada: Academic Press.

Grigore V. (2001). Topological Issues in Single-Phase Power Factor Correction. Institute of Intelligent Power Electronics Publications, 6, 36-65.

Saito T., Tasaki S., & Torikai H. (2003). WTA-Based Interleaved Buck Converters for Low-Voltage High-Current Applications. Industrial Electronics Society, 1, 652-655. doi: 10.1109/IECON.2003.1280058

García O., Zumel P., de Castro A., & Cobos J. A. (2006). Automotive DC-DC bidirectional converter made with many interleaved buck stages. Power Electronics, IEEE Transactions, 3, 578-586, doi: 10.1109/TPEL.2006.872379

Jones, J.L., Flynn, A. M., & Seiger, B. A. (1999). Mobile Robots: Inspiration to Implementation (2nd ed.). USA: A K Peters, Ltd.

Quevedo, D. E., & Goodwin, G. C. (Eds.). (2004). Proceedings from American Control Conference 2004: Control of EMI from Switched-Mode Power Supplies via Multi-Step Optimization. Boston, Massachusetts: IEEE.

Keeney, C. G., & McWhorther, M. (1969). A Highly Efficient Inductorless Voltage Regulator. Journal of IEEE Solid-State Circuits Society, 4(4), 192-195.

Kim, J. H., Ryu, M. H., Min, B. D., & Sang E. H. (Eds.). (2006). Proceedings from IECON 2006: A Method to Reduce Power Consumption of Active-Clamped Flyback Converter at No-Load Condition. Paris: IEEE.

Drivetech, Inc. (2006). Selection of Servo Motors and Drives. Virginia: Ohm D. Y.

Anscombe, R., Bryant, A., Buckingham, R., Ferguson, G., Graham, A., Lichon, M., Parry, N., Brandrick, P., Redman, M., Summers, M., & Green, B. (2006). Snake-arm robots: a new approach to aircraft assembly. United Kingdom: SAE International.

Anscombe, R., Bryant, A., Buckingham, R., Ferguson, G., Graham, A., Lichon, M., & Parry, N. (2006). Snake-arm Robots Conduct Nuclear Maintenance. Finland: IYNC.

Dowling, K. (1997). Limbless Locomotion: Learning to Crawl with a Snake Robot. Pittsburgh: Carnegie Mellow University.

Science Daily. (2006, Dec. 25). Snake-Like Robot And Steady-Hand System Could Assist Surgeons. Science Daily. Retrieved from http://www.sciencedaily.com/

Gibson, T. (2010, Jul. 23). Army technology expands snake-robotics. www.army.mil. Retrieved from http://www.army.mil/-news/

Thomas, K. K. (2008, Nov. 2). Robotics in Biomemics-Snake Robot. Available from http://www.newtechpapers.com/ECpapers/Snake%20Robots.doc

Dragland, Â. (2005/2006). Snake robot to the rescue. Retrieved from http://www.ntnu.no/gemini/2006-01e/snakerobot.htm

technogamma. (2008, March 11). MOSFET High Voltage driver (High Side) problem [Msg 1]. Message posted to http://forum.allaboutcircuits.com/showthread.php?t=15675&highlight=high+side+mosfet+gate+driver

SgtWookie. (2010, December 10). Floating Power Supply? [Msg 23]. Message posted to http://forum.allaboutcircuits.com/showthread.php?p=285808

Schelle D., & Castorena J. (2006). Buck-Converter Design Demystified. Retrieved from http://powerelectronics.com/mag/606PET25.pdf

Hewes J. (2010). 555 and 556 Timer Circuits. Retrieved from http://www.kpsec.freeuk.com/555timer.htm

Lecture 9 Power amplifier- Class B. [PDF Document]. Retrieved from http://www.ee.cityu.edu.hk/~hkng/doc07_08/L09%20Power%20Amplifier%20(Class%20B%20and%20C).pdf

International Rectifier. IRF540N Datasheet (2001) [PDF Document] Retrieved from http://www.irf.com/product-info/datasheets/data/irf540n.pdf

APPENDICES

APPENDIX A: Journal of Non-Inverting Buck-Boost Converter

A High Efficiency, Non-Inverting, Buck-Boost DC-DC Converter

Mark Gaboriault
Allegro MicroSystems
115 Northeast Cutoff
Worcester, MA 01606 USA
mgaboriault@allegromicro.com

Andrew Notman
Allegro MicroSystems
Stuart House, Eskmills Park
Musselburgh, East Lothian
EH21 7PB Scotland

***Abstract*— Portable electronics applications often require a system voltage that is within the range of fully-charged to semi-discharged batteries, for example 3.3V output from a 2.8V to 4.2V Lithium-Ion battery input.**

The optimal solution to this requirement is a high-efficiency, non-inverting buck-boost, DC-DC converter, providing a programmable constant output voltage, typically from single cell Li-ion, multi-cell NiMH, or Alkaline power sources. This solution uses a control scheme which provides automatic and smooth transition through boost, buck-boost and buck modes.

Keywords - Buck, Boost, Converter, Regulator, Cuk, SEPIC

I. INTRODUCTION

A common power management problem, especially for battery powered portable electronics applications, is the need to provide a regulated output voltage from a battery voltage which, when charged or discharged, can be greater than, less than, or equal to the desired output voltage.

There are several existing solutions to this problem, each with significant drawbacks. However, Allegro MicroSystems has developed a solution (patent pending) for a buck-boost converter IC which maximizes efficiency, minimizes ripple noise on input and output, and minimizes external component requirements and associated cost.

II. EXISTING SOLUTIONS

There are several solutions being utilized today, including: cascaded boost & buck converter; classic 4-switch buck-boost converter; cascaded boost converter & linear regulator; SEPIC converter; and Cuk converter.

The proposed solution has advantages over all of these alternatives. Most notably are improved efficiency and the simplification of external components required for control loop(s) and/or compensation. A more detailed discussion of the cascaded boost & buck converter and classic 4-switch buck-boost converter follows.

A. Drawbacks of Cascaded Boost & Buck Converter

A schematic of this solution is shown in Fig. 1.

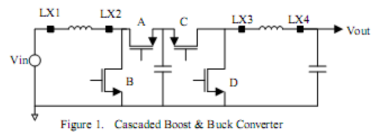

Figure 1. Cascaded Boost & Buck Converter

Because this topology incorporates two DC-DC converters butted together, there is twice the losses associated with just a single converter and it therefore invariably provides poor efficiency.

There is also a high number of external components required - inductors and decoupling capacitors, as well as the compensation networks required for each of the two controllers. These components use up valuable circuit board area and add to the cost associated with this function.

At power up there is also a tendency for a large instantaneous current demand from the input supply, since the first stage is normally a boost converter and has to charge its output capacitor. Each of the supplies must also be sequenced properly to ensure proper operation at start-up.

B. Drawbacks of Classic 4-Switch Buck-Boost Converter

A schematic of this solution is shown in Fig. 2.

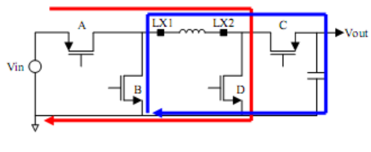

Figure 2. Classic 4-Switch Buck-Boost Converter

0-7803-8269-2/04/$17.00 (C) 2004 IEEE

This converter is based on an H-Bridge topology where each of the input and output pairs of transistors are activated as diagonal pairs in every cycle. The first path (A-D pair) enables charging of the inductor, while the second path (B-C pair) shows the inductor charging the capacitor.

Notice that in any cycle, each of the four switches turn on and off precisely once every cycle. In either a Buck or a Boost converter, only two switches turn on and off per cycle. Therefore the switching losses of the Classic 4-Switch converter may be double those of a Buck or Boost converter.

The output to input voltage ratio is given by: D/(1-D) where D is the duty cycle. When the input voltage equals the output voltage, D is 0.5, or 50%. The inductor current (neglecting ripple current) is given by Iload/(1-D), in this case 2*Iload.

Because the inductor current is twice the load current, the resistive losses are *four* times that of a Buck or low duty cycle Boost converter.

The physical size of the inductor must also be larger to accommodate this extra current without saturating. Furthermore, as the output capacitor must carry the full output current during the PWM on-time (D), and the charge current during the PWM off-time, the output capacitor must have low equivalent series resistance (ESR).

III. Ideal Solution

To mitigate disadvantages as described in Section II, it is ideal to have a four-switch DC-DC converter that changes mode of operation depending on the input and output voltages.

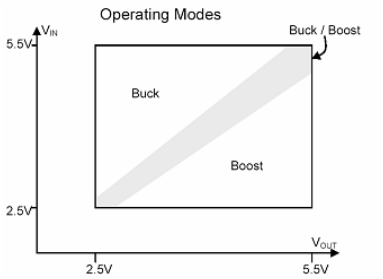

Figure 3. A8440 Operating Modes

The controller changes modes to make the H-bridge look like a Buck converter for Vin>>Vout and a Boost converter for Vin<<Vout. The solution introduces a Buck-Boost Mode for Vin~Vout, where the direct connection of input to output via the inductor is maximized. The direct connection ensures a more continuous DC current, as opposed to the high peak current experienced in a classic Four-switch Buck-Boost. It also minimizes stress on both input and output capacitors and reduces ripple voltage.

Fig. 3 illustrates the three modes of operation. The input and output voltages correspond to the 2.5V to 5.5V rating of the A8440 buck-boost converter IC.

A. Design

The Buck and Boost transfer functions are combined into a single differential modulation scheme, and controlled from one source - labeled "VCONT". The Buck-Boost region is designated as a combination of Buck and Boost regions of control. By using Time-Division-Multiplexing of fixed high duty cycle Buck and low duty cycle Boost pulses, an overall Buck-Boost transfer function is achieved.

The mix of Buck and Boost pulses required to achieve the regulated output voltage is controlled by a Delta-Sigma function that monitors one of the outputs from the error-amplifier.

The Buck-Boost region only allows a limit of 1:7 and 7:1 Buck to Boost pulse ratios. Outside these limits the conventional Boost or Buck mode control takes over.

(Please note: Allegro patents pending regarding this control scheme)

B. Features and Functions

The A8440 buck-boost converter IC incorporates the following features and functions:

- Enable / Soft start
- UVLO – undervoltage lockout
- Thermal protection circuit
- Up to 2MHz clock generation and external synch
- Two modes of operation:
  - PWM (full power) and PFM/Hysteretic mode (low power, e.g. 50mA or less)
- Overcurrent Limits:
  - 2A in PWM mode
    (600mA operation in hysteretic mode)
  - -0.4A reverse current limit

C. Control Law

Fig. 4 illustrates the control law of the DC-DC converter without an output load. The curve will scale as the load changes. The value of "VCONT" (when compared to reference voltages "VBUL" and "VBOL") determines which mode is selected.

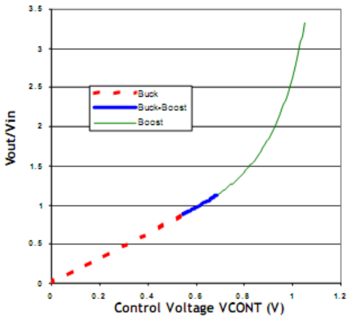

Figure 4. Buck-Boost Control Function

The Buck region is a perfectly linear function of the control voltage, the Buck-Boost region has a slight curvature, and the Boost region is very non-linear as one would expect from a function like 1/(1-D).

Any discontinuities built in due to the piecewise linear nature of the control law are eliminated by the high loop gain of the system.

In practice, the control regions actually overlap so all Vout/Vin ratios can be achieved. This, taken together with the very small amount of hysteresis in the slow mode-comparators at the cross-over points, ensures that a single mode is selected.

D. Differential Modulation

The control voltage VCONT is the output of the error amplifier which controls the duty cycle. VCONT & VCONTB are differential error amplifier signals with a common-mode voltage of VCM = VTOP/2, where VTOP is a bandgap reference voltage.

The mode of operation is controlled by comparing VCONT with both VBUL (the control voltage limit for Buck mode) and VBOL (the control voltage limit for Boost mode).

The switching waveforms are generated from the outputs of two fast comparators that compare the ramp waveform with VCONT and VCONTB. The following sections describe the differential modulation scheme which selects one of the three operating modes.

1) Buck Mode Operation (Fig. 5): VCONT is below both VBUL and VBOL, so the slow comparators monitoring VCONT select *Buck* mode.

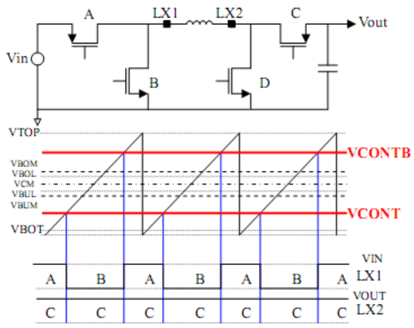

Figure 5. Differential Modulation - Buck Mode

As VCONT rises, VCONTB falls and the A-C region decreases while the A-D region increases. *Only the C-D switch pair changes state during the cycle.*

2) Boost Mode Operation (Fig. 6): VCONT is above both VBUL and VBOL, so the system selects *Boost* mode.

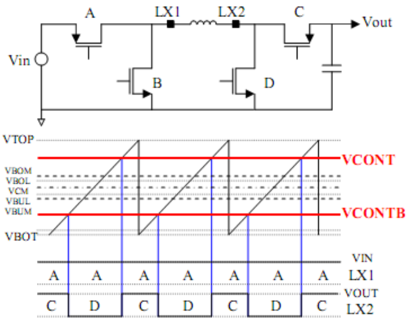

Figure 6. Differential Modulation - Boost Mode

As VCONT rises, VCONTB falls and the A-C region decreases while the A-D region increases. *Only the C-D switch pair changes state during the cycle.*

3) Buck-Boost Mode Operation (Fig. 7): VCONT is between VBUL and VBOL, so the system selects *Buck-Boost* mode. The example in Fig. 7 is for Vout just below Vin, such that there are more Buck pulses (AC-BC) than Boost pulses (AD-AC).

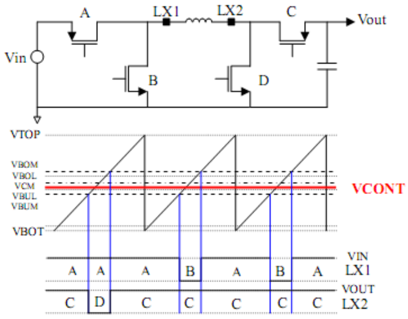

Figure 7. Differential Modulation - Buck-Boost Mode

The Delta-Sigma circuit is active, and gives a data stream with respect to the VCONT level. The Delta-Sigma gives a data stream that is a given mixture of ones and zeroes:

- '1' = 15% duty cycle - Boost pulse
- '0' = 85% duty cycle - Buck pulse

When VCONT is equal to VBOL, the resultant output is 11111110111111101…or when VCONT is equal to VBUL, the result is 000000010000001…In the case of Fig. 7, this result is 001001001001…

F. Performance

1) Inductor Current in Buck-Boost Mode: Fig. 8 shows an example of the ripple current for the extreme case of seven Buck pulses followed by one Boost pulse. "Real-world" data is shown for a system operating at 1MHz with a 10uH inductor and regulating the output to 3.3V.

Overall ripple current is no greater than that of a Buck converter operating at 5.5V input and regulating to 2.5V output (though at a much lower frequency).

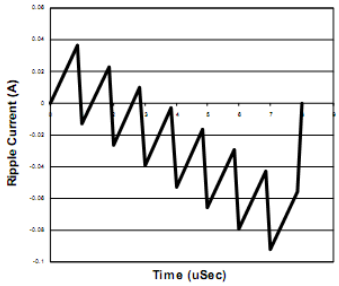

Figure 8. Buck-Boost Mode Ripple Current

2) Measured Efficiency: Fig. 9 shows actual data taken at Vout = 3.3V@100mA, 1MHz switching frequency.

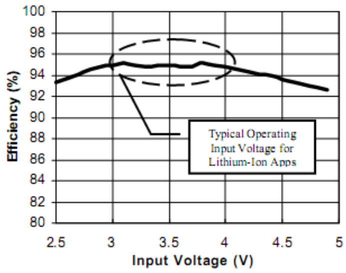

Figure 9. Measured Efficiency at 100mA load, 1MHz

Note that an efficiency of 95% efficiency in the Buck-Boost region is achieved. There is a slight dip due to the Delta-Sigma function circuitry as Vout nears Vin in buck-boost mode. However, this dip is far less significant than that which would appear for a *four*-switch buck-boost converter.

IV. Conclusion

Allegro's A8440 Buck-Boost DC-DC converter IC provides a regulated output voltage from an input voltage above, below, or equal to the input voltage - thus solving a problem encountered often in designing power supplies for portable electronics.

The design incorporates two n-channel and two p-channel power switches and employs synchronous rectification to maximize efficiency with minimum external components.

This solution is optimal because only two switches are in operation during any clock cycle. In the buck-boost region the output capacitor is less stressed, as the time the converter connects the input to the output via the inductor is maximized.

Therefore the key advantages of this solution are:

1) *Improved Efficiency* - No need to run at double load current, synchronous rectification utilized, and only two switches needed in any given clock period.

2) *Reduced Output Noise* – Minimizes the time when the output capacitor supplies the load.

3) *Minimal External Components* - Thus minimizing costs.

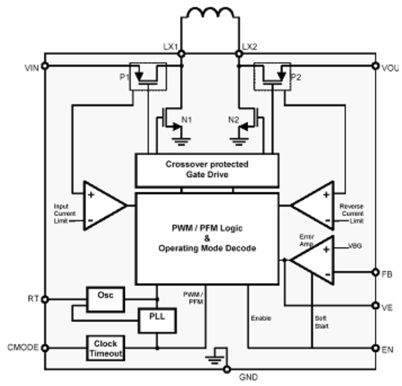

Figure 10. A8440 Buck-Boost IC Block Diagram

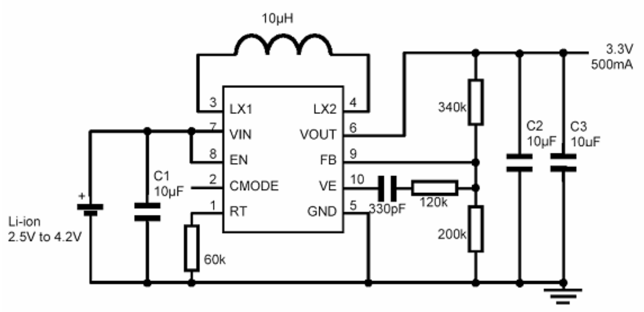

Figure 11. Typical Application Using A8440 Buck-Boost Converter IC

APPENDIX B: LM2678S/T-ADJ Design Documentation

National Semiconductor

WEBENCH® Design Report

Design : 1195735/11 LM2678S-ADJ
Design 11 - LM2678S-ADJ
WEBENCH® Design : LM2678_ADJ_Buck_None

VinMin = 10.0V
VinMax = 12.6V
Vout = 6.7V
Iout = 4.0A

Device = LM2678S-ADJ
Topology = Buck
Creation date = 4/14/11 8:57:50 AM
Total BOM Cost = $5.36
Total Pd = 2.86 W
Footprint = 633.0 mm2
BOM Count = 9

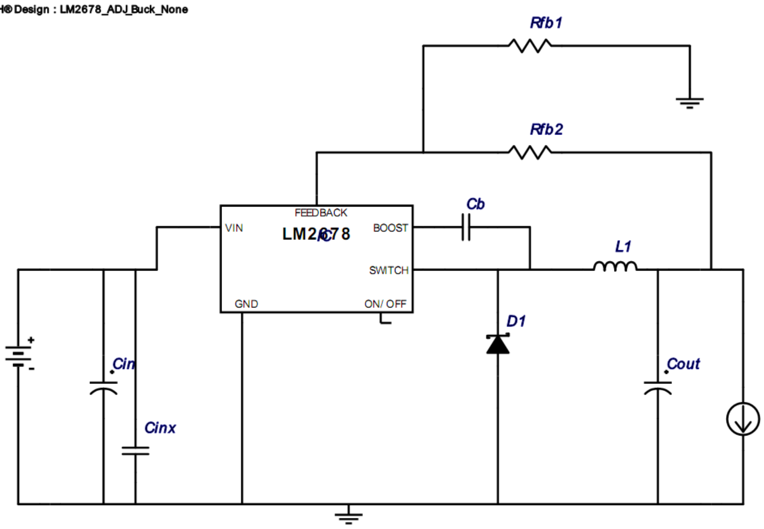

Electrical BOM

#	Name	Manufacturer	Part Number	Qty	Price	Properties	Footprint
1.	Cb	Yageo America	CC0805KRX7R9BB103 Series= X7R	1	$0.01	Cap= 10.0 nF ESR= 0.0 Ohm VDC= 50.0 V IRMS= 0.0 A	0805 13mm2
2.	Cin	TDK	C4532X7R1E226M Series= X7R	1	$0.45	Cap= 22.0 µF ESR= 3.0 mOhm VDC= 25.0 V IRMS= 2.5 A	1812 39mm2
3.	Cinx	AVX	08053C104KAT2A Series= X7R	1	$0.01	Cap= 100.0 nF ESR= 280.0 mOhm VDC= 25.0 V IRMS= 0.0 A	0805 13mm2
4.	Cout	Nippon Chemi-Con	APXE100ARA151MF80G Series= PXE	1	$0.57	Cap= 150.0 µF ESR= 21.0 mOhm VDC= 10.0 V IRMS= 2.88 A	CAPSMT_62_F80 74mm2
5.	D1	Diodes Inc.	B340A-13-F	1	$0.13	VF@Io= 500.0 mV VRRM= 40.0 V	SMA 37mm2
6.	IC	National Semiconductor	LM2678S-ADJ	1	$3.25	Switcher	TS7B 199mm2

#	Name	Manufacturer	Part Number	Qty	Price	Properties	Footprint
7.	L1	Coilcraft	MLC1565-113MLB	1	$0.92	L= 11.3 µH DCR= 10.6 mOhm	 MLC1565 243mm2
8.	Rfb1	Vishay-Dale	CRCW04021K00FKED Series= CRCW..e3	1	$0.01	Res= 1,000 Ohm Power= 63.0 mW Tolerance= 1.0%	0402 8mm2
9.	Rfb2	Vishay-Dale	CRCW04024K53FKED Series= CRCW..e3	1	$0.01	Res= 4.53 kOhm Power= 63.0 mW Tolerance= 1.0%	0402 8mm2

Op Vals

#	Name	Value	Category	Description
1.	Cin IRMS	1.592 A	Current	Input capacitor RMS ripple current
2.	Cout IRMS	332.671 mA	Current	Output capacitor RMS ripple current
3.	IC Ipk	4.576 A	Current	Peak switch current in IC
4.	Iin Avg	2.354 A	Current	Average input current
5.	L Ipp	1.152 A	Current	Peak-to-peak inductor ripple current
6.	M Irms	3.03 A	Current	Q Iavg
7.	BOM Count	9.0	General	Total Design BOM count
8.	FootPrint	633.0 mm2	General	Total Foot Print Area of BOM components
9.	Frequency	260.0 kHz	General	Switching frequency
10.	IC Tolerance	24.0 mV	General	IC Feedback Tolerance
11.	M Vds Act	553.374 mV	General	
12.	Mode	CCM	General	Conduction Mode
13.	Pout	26.8 W	General	Total output power
14.	Total BOM	$5.36	General	Total BOM Cost
15.	D1 Tj	115.228 degC	Op_Point	D1 junction temperature
16.	Cross Freq	35.126 kHz	Op_point	Bode plot crossover frequency
17.	Duty Cycle	57.386 %	Op_point	Duty cycle
18.	Efficiency	90.346 %	Op_point	Steady state efficiency
19.	IC Tj	77.189 degC	Op_point	IC junction temperature
20.	ICThetaJA	26.0 degC/W	Op_point	IC junction-to-ambient thermal resistance
21.	IOUT_OP	4.0 A	Op_point	Iout operating point
22.	Phase Marg	59.526 deg	Op_point	Bode Plot Phase Margin
23.	VIN_OP	12.6 V	Op_point	Vin operating point
24.	Vout p-p	24.481 mV	Op_point	Peak-to-peak output ripple voltage
25.	Cin Pd	7.606 mW	Power	Input capacitor power dissipation
26.	Cout Pd	2.324 mW	Power	Output capacitor power dissipation
27.	Diode Pd	852.281 mW	Power	Diode power dissipation
28.	IC Pd	1.815 W	Power	IC power dissipation
29.	L Pd	186.56 mW	Power	Inductor power dissipation
30.	Total Pd	2.864 W	Power	Total Power Dissipation
31.	Vout OP	6.7 V	Unknown	Vin operating point

Design Inputs

#	Name	Value	Description
1.	ErrorFeature	I	Error feature
2.	Iout	4.0 A	Maximum Output Current
3.	Iout1	4.0 Amps	Output Current #1
4.	SoftStart	0.0 ms	Soft Start Time (ms)
5.	SyncFeature	I	External Sync feature
6.	VinMax	12.6 V	Maximum input voltage
7.	VinMin	10.0 V	Minimum input voltage
8.	Vout	6.7 V	Output Voltage
9.	Vout1	6.7 Volt	Output Voltage #1
10.	base_pn	LM2678	National Based Product Number
11.	customfreq	Y	Use Customer Frequency
12.	onOff	I	On/Off feature
13.	optfactor	3.0	Optimization factor to tune up the design
14.	pricefactor	0.0	Price factor to tune up the design cost
15.	ta	30.0 degC	Ambient temperature

Design Assist

1. **LM2678** Product Folder : http://www.national.com/pf/LM/LM2678.html : contains the data sheet and other resources.

National's WEBENCH simulation tools attempt to recreate the performance of a substantially equivalent physical implementation of the design. Simulations are created using National's published specifications as well as the published specifications of other device manufacturers. While National does update this information periodically, this information may not be current at the time the simulation is built. National does not warrant the accuracy or completeness of the specifications or any information contained therein. National does not warrant that any designs or recommended parts will meet the specifications you entered, will be suitable for your application or fit for any particular purpose, or will operate as shown in the simulation in a physical implementation. National does not warrant that the designs are production worthy.

You should completely validate and test your design implementation to confirm the system functionality for your application prior to production.

Use of National's WEBENCH simulation tools is subject to National's Site Terms and Conditions of Use. Prototype boards based on WEBENCH created designs are provided provided AS IS without warranty of any kind for evaluation and testing purposes and are subject to the terms of the Evaluation License Agreement.

APPENDIX C: Pictures of Components

Picture of component: Input supply LiPo battery 11.1 V 2200 mAh.

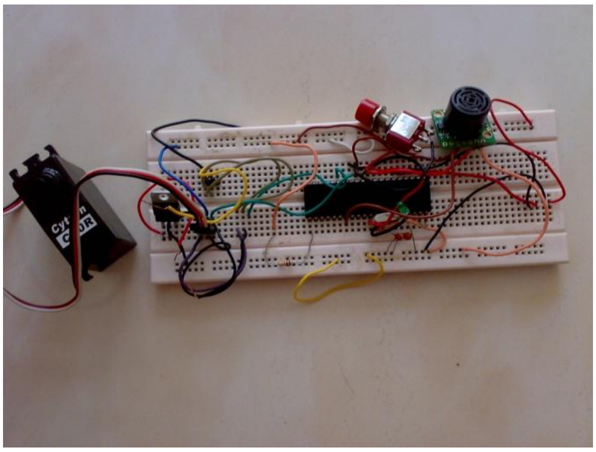

Picture of components on breadboard: microcontroller, ultrasonic sensor, and servo motor.

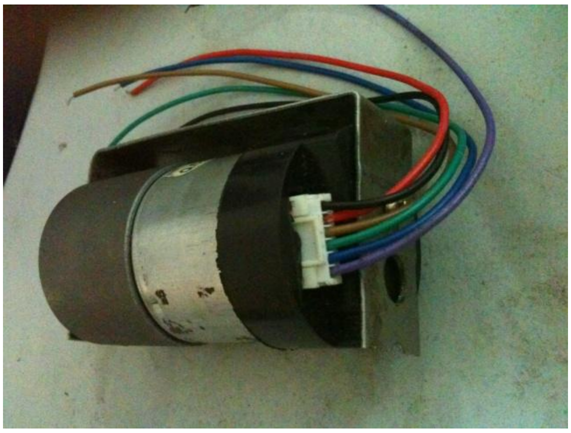

Picture of component: DC Geared motor.

APPENDIX D: Construction of Snake Robot

Picture of servo motors: connection to the robot as actuators for its joints.

Picture of servo motors: connection to the robot as actuators for a single joint. (Side view)

Picture of snake robot: Complete construction.

APPENDIX E: Layout of the PCBs for the circuits

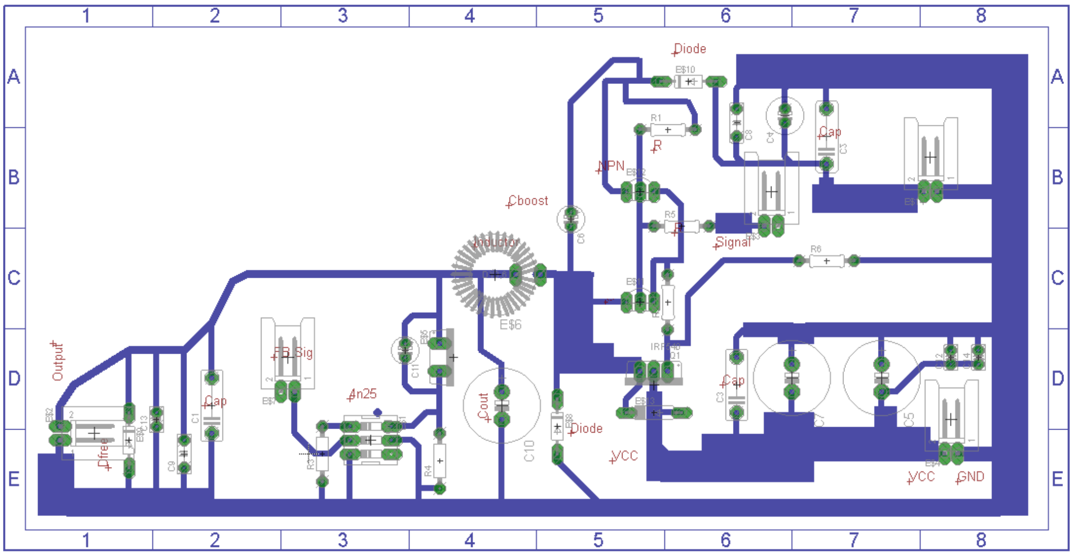

Picture of PCB: DC-DC converter, feedback voltage, and MOSFET gate amplifier parts of constructed buck converter

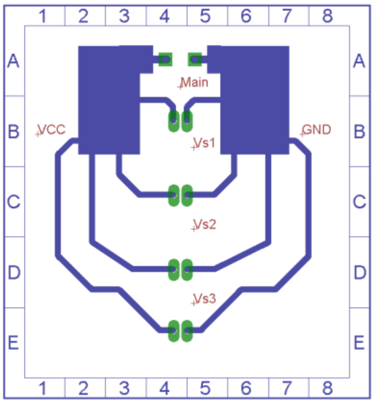

Picture of PCB: Battery point connecting the input supply to various circuits

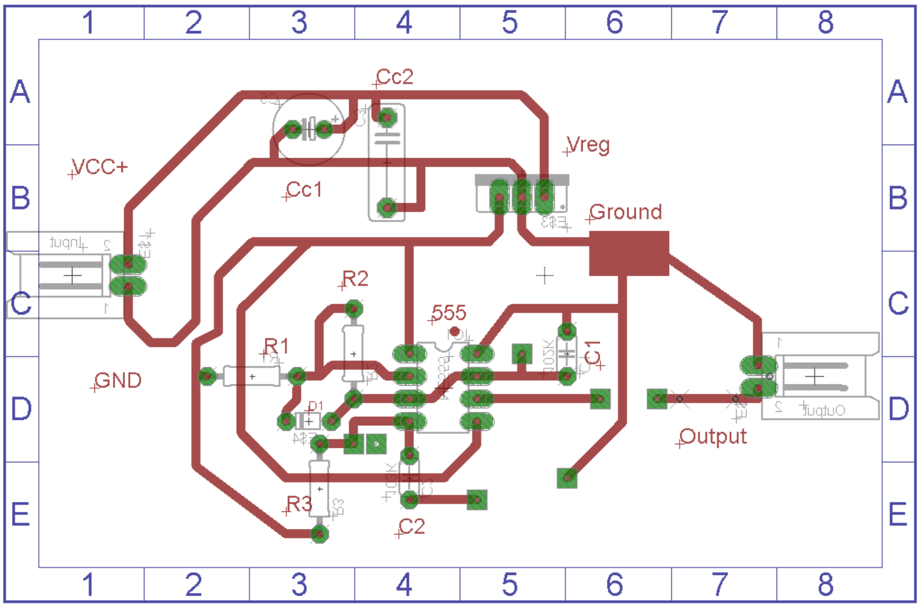

Picture of PCB: Timer 555 part of constructed buck converter

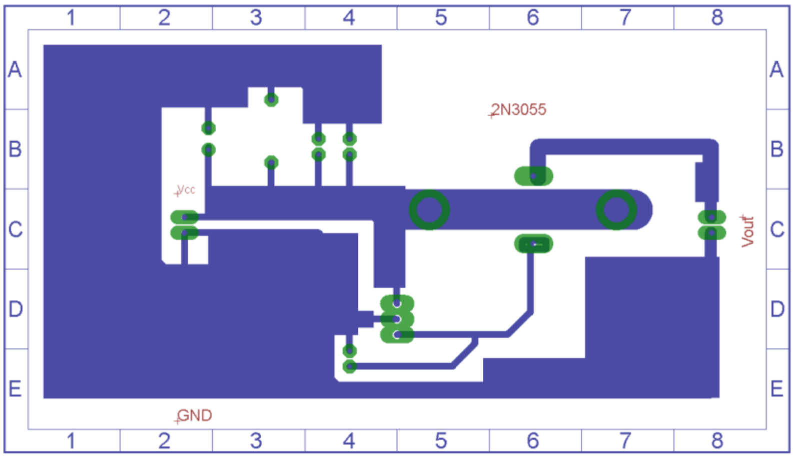

Picture of PCB: Linear Regulator

APPENDIX F: Tests for Constructed Buck Converter

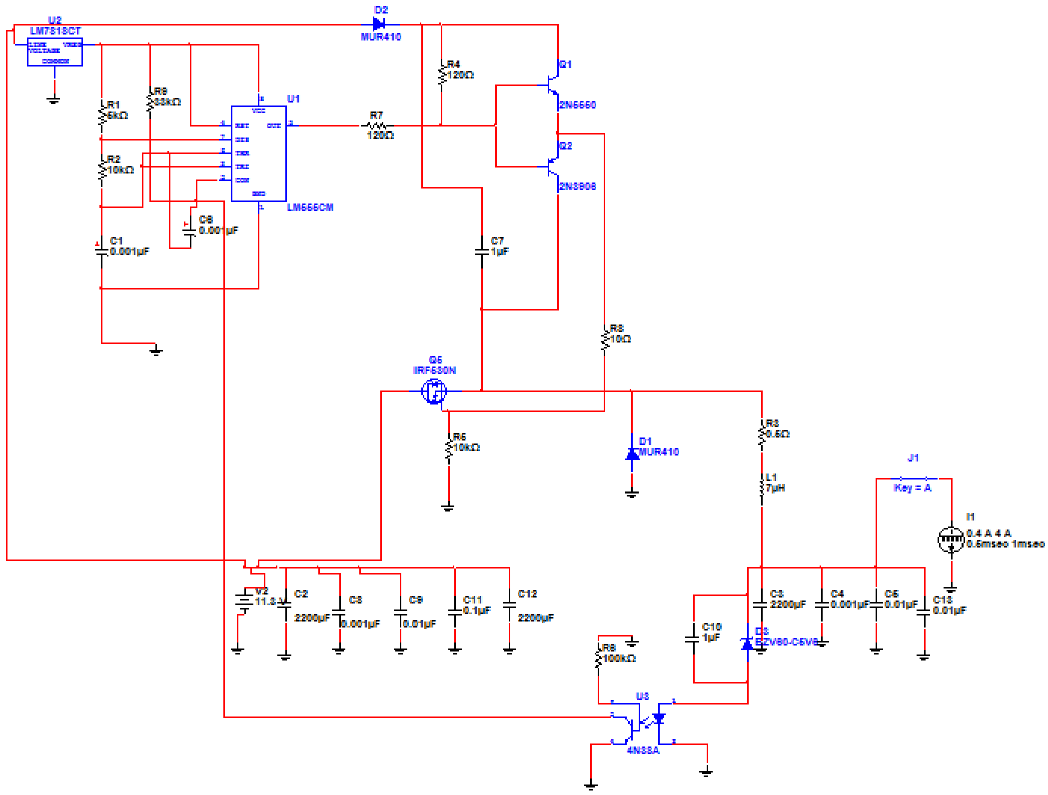

Figure i: Transient Load Test for Constructed Buck Converter

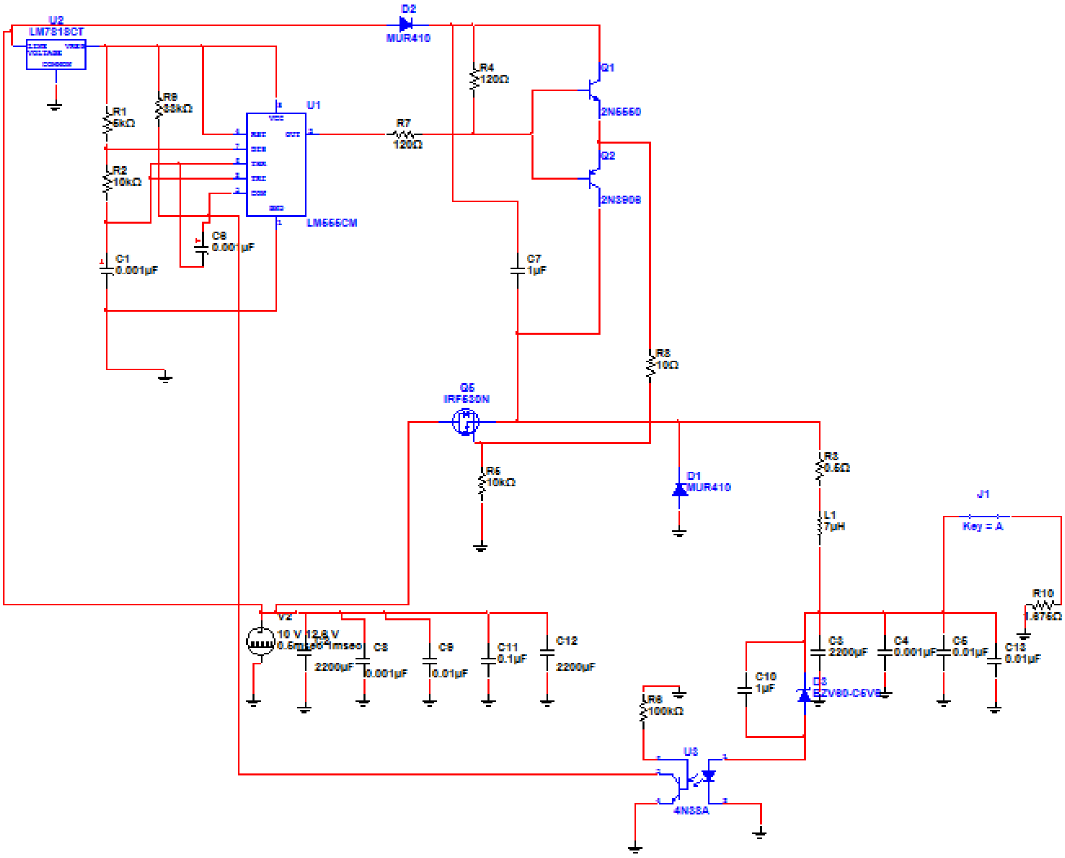

Figure ii: Transient Input Test for Constructed Buck Converter

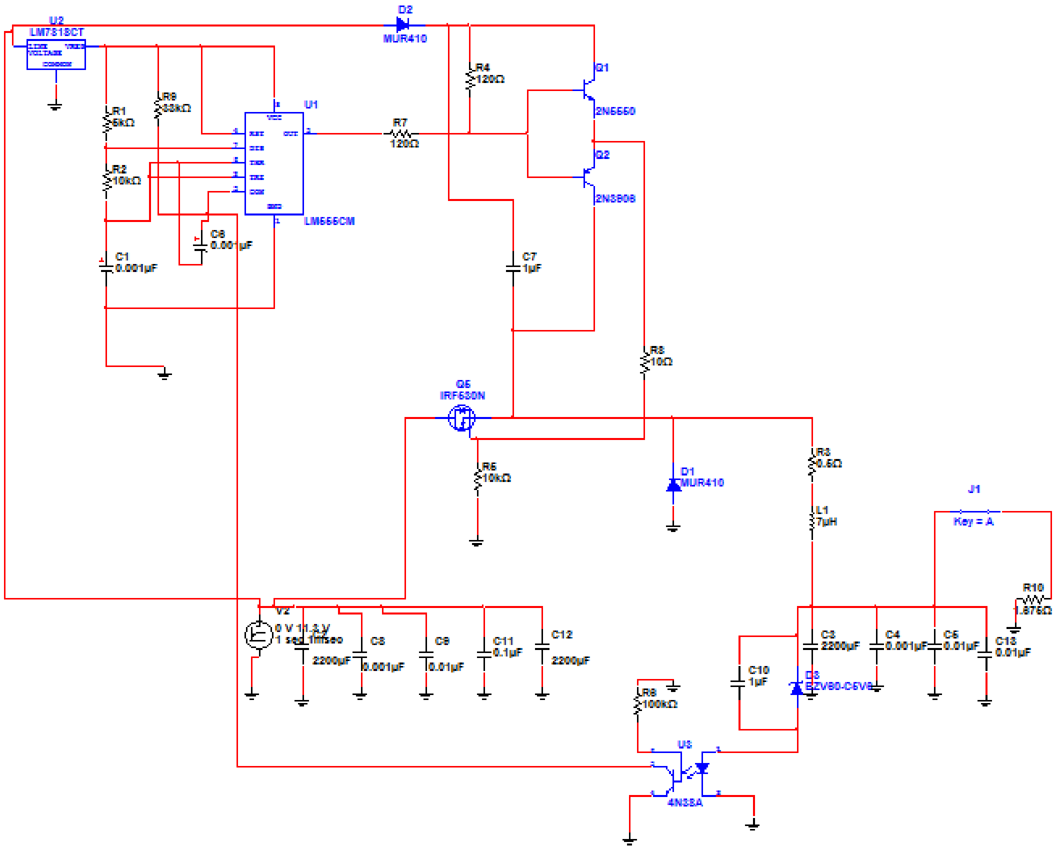

Figure iii: Startup Test for Constructed Buck Converter

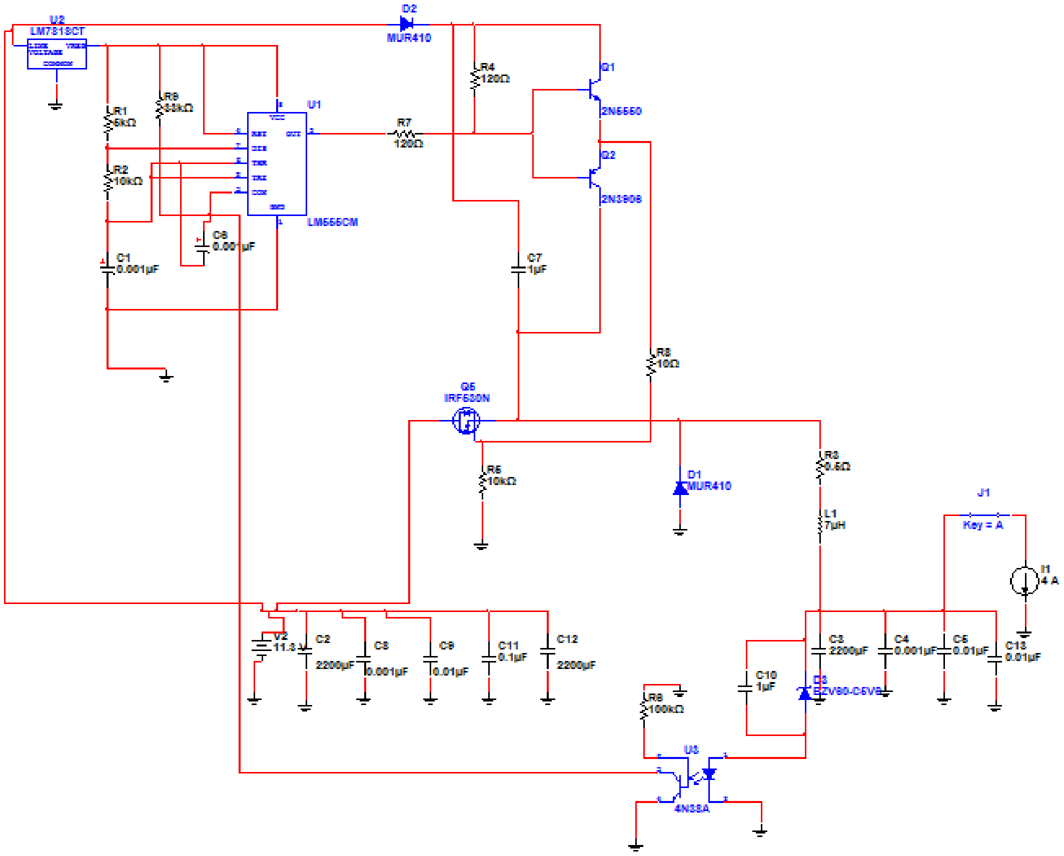

Figure iv: Steady State Test for Constructed Buck Converter

APPENDIX G: Tests for LM2678T-ADJ

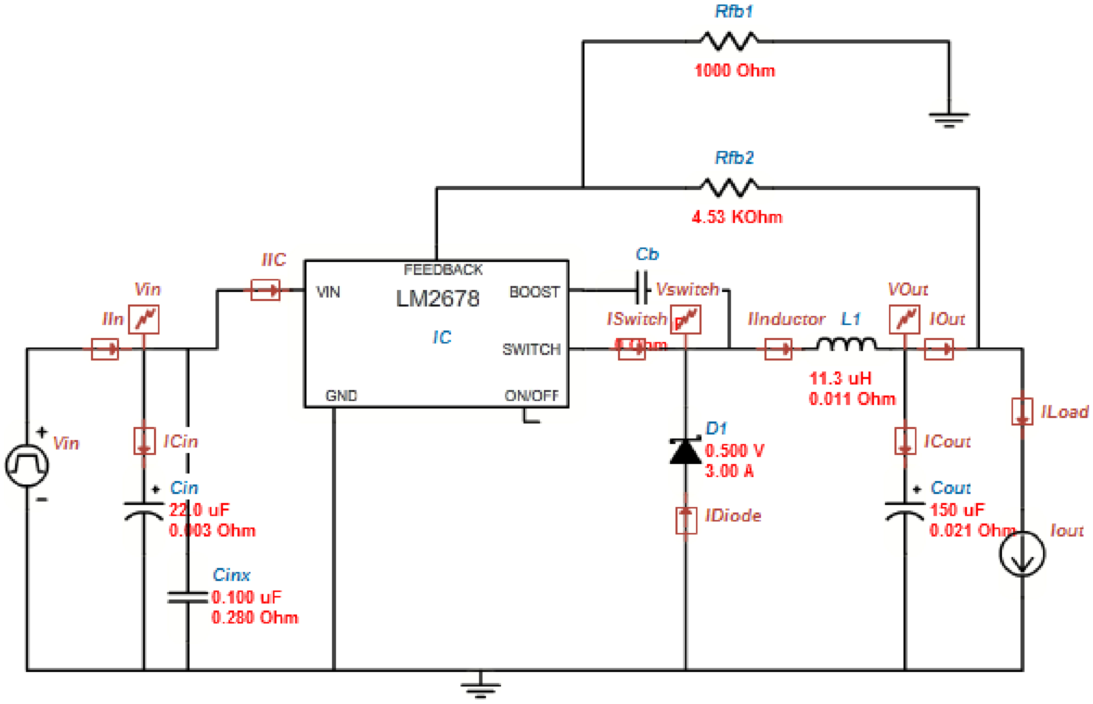

Figure v: Transient Input Test for LM2678T-ADJ

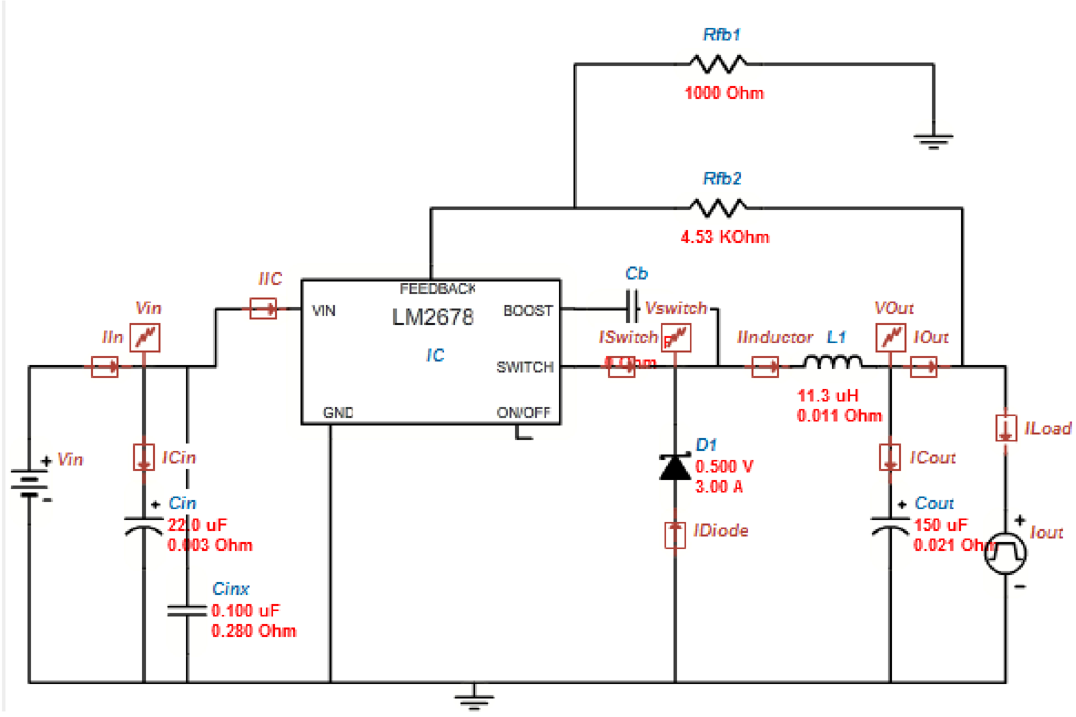

Figure vi: Transient Load Test for LM2678T-ADJ

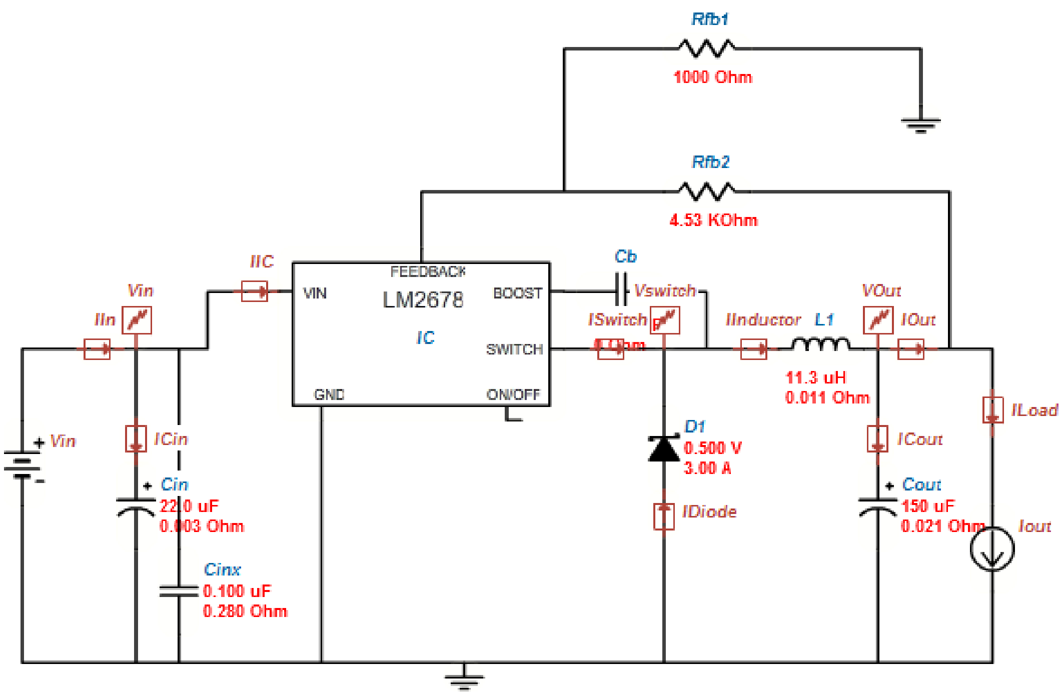

Figure viii: Steady State Test for LM2678T-ADJ

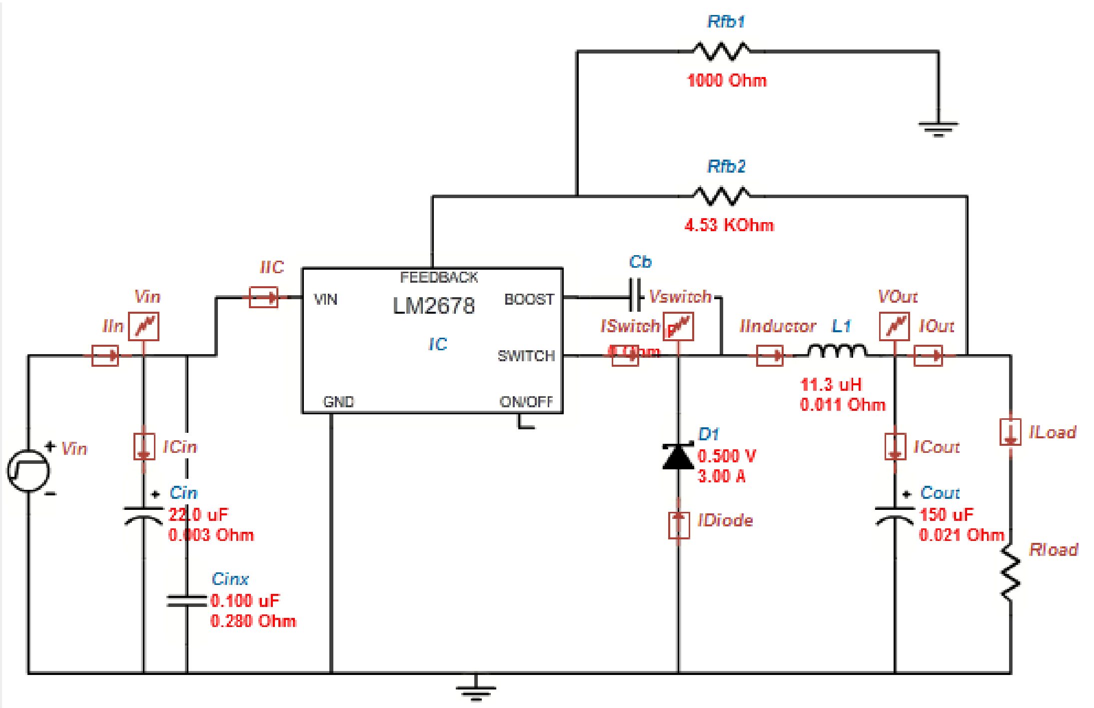

Figure vii: Startup Test for LM2678T-ADJ

Appendix H: Calculations for the Buck Converter

```
Vin_max = 12.6;
Vout = 6.7;
fmin = 30 × 10^3;
fmax = 70 × 10^3;
Vin_min = 10;
Iout_max = 4;
```

The Output Inductor Value (Eq 3.1)

$L_{\text{ripple}} = 0.3;$

$$L = \frac{\left(V_{in_{max}} - V_{out}\right)}{V_{in_{max}}} \times \frac{V_{out}}{V_{in_{max}}} \times \frac{1}{f_{min}} \times \frac{1}{L_{\text{ripple}} \times I_{out_{max}}}$$

6.91645×10^{-6}

∴ Assume L to be 7 μH.

The Peak Current Through Inductor (Eq 3.2)

$\triangle I = L_{\text{ripple}} \times I_{out_{max}}$

$$I_{(\text{peak})_{\text{cal}}} = I_{out_{max}} + \frac{\triangle I}{2}$$

$I_{peak} = I_{(\text{peak})_{\text{cal}}} \times 1.2$

1.2

4.6

5.52

∴ The peak current is 5.52 A after tolerance of 20%.

The Output Capacitor Value (Eq 3.3)

$V_{shoot} = 10 \times 10^{-3}; \ L = 7 \times 10^{-6};$

$$C_{o\text{cal}} = \frac{L\left(I_{peak}^{2}\right)}{(V_{shoot} + V_{out})^{2} - V_{out}^{2}}$$

$C_o = 1.2 \times C_{o\text{cal}}$

0.00159055

0.00190866

∴ Assume a common available capacitor value of $\boldsymbol{C_o}$ = 2200 μF.

Calculated required ESR for the Output Capacitor (Eq 3.5)

$\triangle V = 0.02 \times V_{out}; C_o = 2200 \times 10^{-6};$

$$ESR_{C_o} = \frac{1}{\triangle I} \times \left(\triangle V - \frac{1}{2\,C_o} \times \frac{V_{in_{max}} - V_{out}}{L} \left(\frac{V_{out}}{V_{in_{max}}} \times \frac{1}{f_{min}} \right)^2 \right)$$

0.0615149

∴ The maximum value of ESR output capacitor cannot exceed 61.51 mΩ.

ESR value of Output Capacitor to be used in the project circuit

$$ESR_{C_o} = \left(\frac{1}{0.035} + \frac{1}{58} + \frac{1}{14.5 \times 10^3} + \frac{1}{66.5} \right)^{-1}$$

0.0349604

∴ The ESR value of output capacitor , 34.96 mΩ, is less than calculated maximum vaule of ESR output capacitor.

Input Ripple Current (Eq 3.6)

$$I_{in-rms\,\mathrm{cal}} = I_{out_{max}} \frac{\sqrt{V_{out}\left(V_{in_{max}} - V_{out}\right)}}{V_{in_{max}}}$$

$I_{in-rms} = 1.2 \times I_{in-rms\,\mathrm{cal}}$

1.99596

2.39516

∴ The input ripple current is estimated to be 2.4 A after tolerance of 20%.

ESR of Input Capacitor to be used in the project circuit

$$ESR_{C_{in}} = \left(\frac{1}{0.035} + \frac{1}{0.035} + \frac{1}{58} + \frac{1}{14.5 \times 10^3} + \frac{1}{66.5} \right)^{-1}$$

0.0174901

∴ The ESR value of the input capacitor is 17.5 mΩ.

Average Power Dissipation on the Diode (Eq 3.7)

$V_D = 0.7;$

$$P_{diode\,\mathrm{cal}} = \left(1 - \frac{V_{out}}{V_{in_{max}}} \right) \times I_{out_{max}} \times V_D$$

$P_{diode} = P_{diode\,\mathrm{cal}} \times 1.2$

1.31111

1.57333

∴ The estimated power diode loss is 1.573 W.

Maximum Power Dissipation on MOSFET (Eq 3.9)

$$T_{J\,rise} = 55;\ \Theta_{J\,A} = 62;\ P_{D_{TOT}} = \frac{T_{J\,rise}}{\Theta_{J\,A}}$$

$$\frac{55}{62}$$

∴ The maximum power loss on the MOSFET is 0.89 W.

Power Dissipation caused by On-Resistance (Eq 3.12)

$$T_{J\,hot} = 110;\ R_{DS(on)\,25\,^\circ C} = \frac{V_{in_{\min}}}{V_{out}} \times \frac{1}{{I_{out_{max}}}^2 \times (1 + 0.005\,(T_{J\,hot} - 25))}\ P_{D_{TOT}} \times 0.6$$

0.0348428

∴ The on-resistance at 25 °C is 34.84 mΩ.

Power Dissipation caused by Hot On-Resistance (Eq 3.11)

$$R_{DS(on)\,HOT} = (1 + 0.005\,(T_{J\,hot} - 25))\ R_{DS(on)\,25\,^\circ C}$$

0.0496509

∴ The hot on-resistance is 49.65 mΩ.

Power Loss Due to On-Resistance MOSFET (Eq 3.10)

$$P_{D_{RDS}} = \frac{V_{out}}{V_{in_{\min}}} \times {I_{out_{max}}}^2 \times R_{DS(on)\,HOT}$$

0.532258

∴ The power loss due to on-resistance is 0.532 W.

Power Loss Due to Switching MOSFET (eq 3.13)

$$C_{RSS} = 120 \times 10^{-12};\ I_{Gate} = 1;\ f = 50 \times 10^3;\ P_{Dsw} = \frac{C_{RSS} \times {V_{in_{max}}}^2 \times f \times I_{out_{max}}}{I_{Gate}}$$

0.00381024

∴ The power loss due to switching MOSFET is 3.81 mW.

Net Power Dissipated by MOSFET (Eq 3.14)

$$P_{Dsw} + P_{D_{RDS}}$$

0.536068

∴ The net dissipated power is 0.536 W.

Calculated Efficiency of the Buck Converter

$\boldsymbol{P_{C_{in_{rms}}} = 0.1008;\ P_{DCR_{rms}} = 0.1298;\ P_{C_{o_{rms}}} = 0.1508;}$

$\boldsymbol{\eta = (V_{out} \times I_{out_{max}}) \Big/ \left((V_{out} \times I_{out_{max}}) + P_{C_{in_{rms}}} + P_{DCR_{rms}} + P_{C_{o_{rms}}} + P_{Dsw} + P_{D_{RDS}} + P_{diode} + 0.75\right)}$

0.89212

∴ The efficiency of the buck converter is estimated to be 89%.